**The Pennsylvania State University**

**The Graduate School**

# VIBRATION CONTROL OF DISTRIBUTED PARAMETER SYSTEMS AND FLUIDIC FLEXIBLE MATRIX COMPOSITES

A Dissertation in

Mechanical Engineering

by

Amir Lotfi Gaskarimahalle



Submitted in Partial Fulfillment

of the Requirements

for the Degree of

Doctor of Philosophy

December 2009

The dissertation of Amir Lotfi Gaskarimahalle was reviewed and approved* by the following:

Christopher D. Rahn

Professor of Mechanical Engineering

Dissertation Advisor, Chair of Committee

Alok Sinha

Professor of Mechanical Engineering

Qian Wang

Associate Professor of Mechanical Engineering

George A. Lesieutre

Professor of Aerospace Engineering

Karen A. Thole

Professor and Head of Mechanical Engineering

*Signatures are on file in the Graduate School.

# Abstract

Vibration degrades the performance of many mechanical systems, reducing the quality of manufactured products, producing noise, introducing fatigue in mechanical components, and generating an uncomfortable environment for passengers. Vibration control is categorized as: active, passive, semi-active or hybrid, based on the power consumption of the control system and feedback or feedforward based on whether sensing is used to control vibration. In this thesis, we study input shaping control of Distributed Parameter Systems (DPS) and passive and semi-active vibration control using Fluidic Flexible Matrix Composites ($F^2MC$).

First, we extend input shaping control to one dimensional continua. Unlike discrete systems where the input is shaped only in the temporal domain, temporal and spatial input shaping can produce zero residual vibration in setpoint position control of distributed strings and beams. For collocated and noncollocated boundary control of strings and domain control of strings and pinned beams, the response to step inputs is solved in closed form using delays. For a clamped beam model, a closed form infinite modal series is used. The boundary controlled string can be setpoint regulated using two-pulse Zero Vibration (ZV) and three-pulse Zero Vibration and Derivative (ZVD) shapers but ZVD is not more robust to parameter variations than ZV, a unique characteristic of second-order PDE systems. Noncollocated ZV and ZVD boundary control enables rigid body translation of a string with zero residual vibration. Domain controlled strings and pinned beams with spatial input distributions that satisfy certain orthogonality conditions (e.g. midspan point load or uniformly distributed load) can be setpoint regulated with shaped inputs. For the cantilevered beam, modal shaping of the input distribution and ZV or ZVD temporal shaping drives the tip to the desired position with zero residual vibration.

A command shaping approach in vibration control using $F^2MC$ tubes as variable stiffness structures is studied in the third chapter. The apparent stiffness of $F^2MC$ tubes

can be changed using a variable orifice valve. With fiber reinforcement, the volume inside the tube may change with external load. With an open valve, the liquid is free to move in or out of the tube, so the apparent stiffness does not change. When the valve is closed, the high bulk modulus liquid is confined, which resists the volume change and causes the apparent stiffness of the tube to increase. The equations of motion of an $F^2$MC-mass system is derived using a 3-D elasticity model and the energy method. A reduced order model is then developed for fully-open and fully-closed valves. A Skyhook control that cycles the valve between open and closed, asymptotically decays the vibration. A Zero Vibration (ZV) Stiffness Shaping technique is introduced to suppress the vibration in finite time. A sensitivity analysis of the ZV Stiffness Shaper studies the robustness to parametric uncertainties.

We also investigate passive and semi-active vibration control using $F^2$MC tubes. $F^2$MC tubes filled with fluid and connected to an accumulator through a fixed orifice can provide damping forces in response to axial strain. If the orifice is actively controlled, the stiffness of $F^2$MC tubes can be dynamically switched from soft to stiff. The stability of the unforced dynamic system is proven using a Lyapunov approach. The reduced-order model for operation with either a fully-open or fully-closed valve motivates the development of a ZV feedback control law, that suppresses vibration in finite time. Coupling of a fluid-filled $F^2$MC tube to a pressurized accumulator through a fixed orifice is shown to provide significant passive damping. The open valve orifice size is optimized for optimal passive, Skyhook, and ZV controllers by minimizing the ITAE cost function. Simulation results show that the optimal open valve orifice provides a damping ratio of 0.35 compared to no damping in closed valve case. The optimal ZV controller outperforms optimal passive and Skyhook controllers by 32.9% and 34.2% for impulse and 34.7% and 60% for step response, respectively. Theoretical results are confirmed by experiments that demonstrate the improved damping provided by optimal passive control $F^2$MC and fast transient response provided by semi-active ZV control.

Finally, we develop a novel Tuned Vibration Absorber (TVA) using $F^2$MC. Coupling of a fluid-filled $F^2$MC tube through a fluid port to a pressurized air accumulator can suppress primary mass forced vibration at the tuned absorber frequency. A 3-D elasticity model for the tube and a lumped fluid mass produces a $4^{th}$ order model of an $F^2$MC-mass system. The model provides a closed-form isolation frequency that depends mainly on the port inertance, orifice flow coefficient, and the tube parameters. A small viscous damping in the orifice increases the isolation bandwidth. With a fully closed orifice, the zero disappears, and the system has a single resonant peak. Variations in the primary mass do not change the isolation frequency, making the $F^2$MC TVA robust to mass variations. Experimental results validate the theoretical predictions in showing a tunable isolation frequency that is insensitive to primary mass variations, and a 94% reduction in forced vibration response relative to the closed valve case.

# Table of Contents

# List of Figures

# List of Tables

# Acknowledgments

Graduating with a Ph.D. degree has been a long journey for me, and I could never have done it without the support and encouragement of many people.

First, I would like to thank my advisor, Dr. Chris Rahn, who has been a real mentor to me. You have helped make my move across the world more than worth it. Your kindness and support always encouraged me to improve myself. My weekly research meetings with you guided me through all the difficulties. If I were to describe a great advisor, you would definitely be the first on my mind. I remember your patience at times when the research was not going well, and I also remember your enthusiasm when I had good results. I am sure that you will be my role model for my future career.

I owe a great debt to my parents who never doubted my capabilities and always supported my decisions. Your continuous love and support from childhood has helped me through all the difficulties in my life. You are the best parents one could ever have. I also acknowledge Meisam and Mahsa for your companionship and encouragement.

I would like to express my thanks to my committee members. I am honored to have Dr. George Lesieutre, Dr. Alok Sinha, and Dr. Qian Wang on my committee who have been my teachers as well. They provided me with invaluable advice and comments on my research. My thanks also go to Dr. Kon-Well Wang and Dr. Chuck Bakis for their great ideas in our MAST group.

I have been fortunate to have a great group of friends at Penn State. This includes my current and previous lab-mates. I would like to especially thank Lloyd Scarborough for helping me with my experiments. Deepak Trivedi, Hareesh Kommepalli, and Suyi Li have been there for me whenever I needed to discuss my research problems. My friends in ISA, especially Sahar Louyeh and Saed Roudsari, have been a great part of my life during these five years. We celebrated many great events, picnics, and parties together. I will always remember such fantastic friends.

Finally, I would like to dedicate this work to my wife, Mastaneh. Working hard as a full-time graduate student is never frustrating if you have a kind, lovely, and understanding wife to spend the rest of the day with. I appreciate all your support during these years. You have been there for me in good and bad times. You made it easy for

me. For all of this, I thank you.

# Dedication

To my wife, Mastaneh.

Chapter 1

# Introduction

Vibration degrades the performance of many mechanical systems. The accuracy of trajectory tracking and set-point regulation is often determined by structural vibration. Vibration can cause instability in controlled systems, if critical modes are neglected or frequencies vary over time. This chapter reviews methods of vibration control and their applications in distributed parameter systems (DPS) and variable stiffness structures.

## 1.1 Vibration control methods

Vibration control is categorized as: active [1], passive [2], semi-active [3, 4] or hybrid [5], based on the power consumption of the control system and feedback or feedforward based on whether sensing is used to control vibration.

Active vibration control systems provide the best performance in suppressing structural vibration. The supplied energy from the control input gives the designer the required power to meet the control objectives and constraints. The energy consumption, however, is a drawback of these methods because the control input is continuously ex-

pending power. In addition, sensor and actuator dynamics and system variability may introduce instability in these systems [6, 7].

Passive vibration isolators and absorbers are pre-configured structural elements that do not consume power. Tuned vibration absorbers, for example, have been widely used to reduce vibration for nearly one hundred years [8]. Winthrop *et al.* [9] describe the shortcomings of passive vibration control systems, including inability to achieve isolation at very low frequencies, trade-off between resonant peak and high-frequency attenuation, inability to adapt to variations in parameters and excitation frequencies. Hybrid vibration control utilizes both active and passive methods to reduce the energy consumption while improving the performance [5].

Semi-active or adaptive-passive control schemes substitute active force generators with structural elements that have adjustable parameters. Actively tuning the damping or stiffness can overcome the limitations of passive control and effectively manage the energy flow in the system. Tuning the damping coefficient of a fluid damper using a variable orifice is an approach that has been used for many years [10]. Electro/magneto-rheological (ER/MR) dampers, for example, are two semi-active elements in which the damping is controlled by electric/magnetic field. Many researchers have studied the performance of various control methods using MR fluid [11, 12, 13, 14]. Oh *et al.* [15] develop a variable stiffness liquid-crystal ER fluid for vibration isolation. They derive an equivalent mechanical system to model the ER isolator consisting of a parallel low stiffness spring and a variable damper in series with a high stiffness spring.

In a feedback control system, the control input is based on the sensed error. Feedforward control does not use a sensor but requires an actual model of the dynamic system.

The input shaping technique (IST), for example, uses a feedforward reference to regulate the position of flexible systems to a desired setpoint position

## 1.2 Tuned vibration absorbers

Tuned Vibration Absorbers (TVAs) are effective engineering devices for suppressing vibrations in mechanical systems. Passive vibration isolators and absorbers are pre-configured structural elements that do not require external power [8, 10]. TVAs without damping consist of mass and spring elements tuned to exactly cancel a certain disturbance frequency [16]. Tuned mass dampers (TMDs) are damped TVAs used to achieve damping over a narrow frequency range without the sharp peaks in the undamped absorber. Maximum amplitude reduction, however, is achieved if the absorber is lightly damped and accurately tuned to the excitation frequency.

Recently, smart materials and structures have been used to design novel vibration absorbers. Electro-mechanical coupling in piezoelectric materials makes them a candidate for suppressing vibration [17, 18]. Electrical boundary conditions of a piezoceramic patch can be changed using electrical shunting to achieve variable stiffness and damping. For example, the spring stiffness can be continuously adjusted from the piezoceramic open-circuit elastic modulus to its short-circuit modulus by shunting through a variable capacitor [19]. Rusovici *et al.* [20] design a TVA using a single-crystal piezoceramic that provides fast response time and variable frequency tuning.

Shape Memory Alloys (SMAs) are used in vibration suppression as well. Liang and Rogers [21] demonstrate variable stiffness SMA springs that can change stiffness by 2.5

times. Williams *et al.* [22] design an adaptive TVA that uses SMA variable stiffness properties to achieve on-line adaptation.

Fluid motion can also suppress vibration by providing inertial and damping forces [23]. A Tuned Liquid Column Damper (TLCD), proposed by Sakai *et al.* [24], eliminates vibration in tall buildings by dissipating the energy via fluid flow through an orifice connecting two containers. Active, semi-active, and passive TLCDs have been studied by many researchers [25, 26]. Recently, Shum [27] develops a closed form optimal solution for a TLCD that minimizes vibration.

Halwes [28] introduces the Liquid Inertia Vibration Eliminator (LIVE) in which the fluid inertia acts as the vibration absorber mass. du Plooy *et al.* [29] extend this idea to accomplish a tunable LIVE system where a pressure control valve adjusts the isolation frequency. Smith *et al.* [30] develop a lumped mass model to analytically calculate the isolation frequency of the Fluidlastic LIVE used in a pylon isolation system for the Bell Model 427 Helicopter.

## 1.3 Input shaping technique

Reference command is one of the essential parts of any control system. If the system model is accurately known, then a purely feedforward command can eliminate the need for measurement, reducing costs significantly. Input shaping is an open loop, feedforward technique for flexible systems that provides setpoint regulation [31, 32, 33, 34, 35, 36, 37]. The input to the system, typically a force, moment, or displacement, is shaped into a predefined command typically consisting of a series of pulses or steps that move the

output degree-of-freedom (dof) to a desired position without residual vibration. Figure (1.1) shows the concept of input shaping technique in a harmonic system *e.g.* a classical spring-mass system.

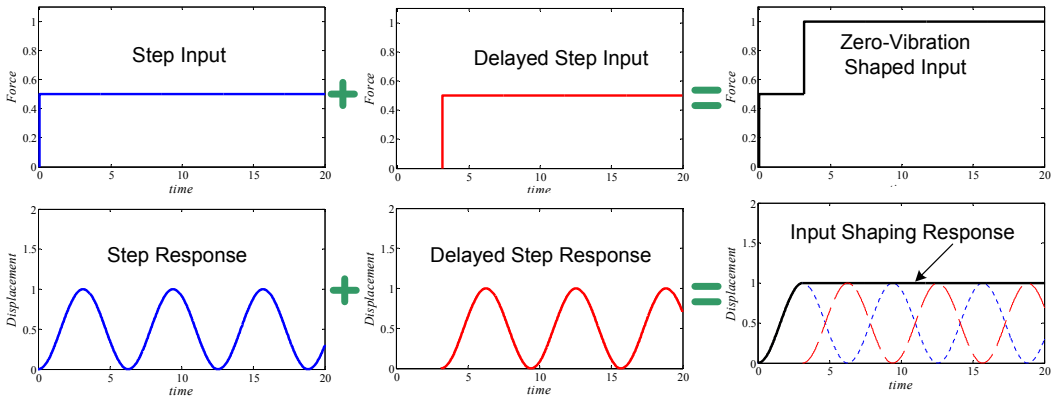


**Figure 1.1.** A typical ZV input shaper for a harmonic system. By superposing the delayed responses, ZV shaper regulates the position with zero residual vibration.

The idea of command filtering in feedforward control is introduced by Gimple *et al.* [38]. More than three decades later, Singer *et al.* [39] conduct a comprehensive study on various approaches to input shaping, robustness. Pao *et al.* [40] prove the equivalence of time-optimal zero vibration input shaping and the traditional time-optimal methods. Hyde *et al.* [31], Singh [32], and Pao [35] further extend input shaping to multi-mode systems. Shan *et al.* [37] modify the conventional representation of input shaping to generalize and improve the suppression procedure for multi-mode systems. They show that by using more steps in a modified zero-vibration (ZV) and zero-vibration-and-derivative (ZVD) shaper, better robustness is obtained.

Multi-mode input shaping design consists of simultaneously solving the equations of motion for all modes or convolving shapers designed for each mode. For an infinite dimensional system, the first method is not feasible. In addition, according to [34], con-

volution of designed shapers consists of a series of step inputs acting at all combinations of modal delay times. This implies that the last step acts at the summation of all time delays. In distributed parameter systems this summation does not converge, leading to an infinitely long settling time.

## 1.4 Vibration control of distributed parameter systems

The most common control approach in distributed parameter systems (DPSs) is discretizing the partial differential equations (PDEs), controlling the dominant modes of vibration, and neglecting the rest of the modes. Finite element analysis (FEA), modal analysis [41], Galerkin [42] and assumed mode [43] methods are the most seen discretization tools in literature. For instance, Kwak *et al.* [44] derive the state-space equations for a cantilevered structure using finite element method (FEM) and designs a full-state-derivative feedback control law, state estimator and linear quadratic regulator (LQR) optimal controller. Another example of using FEM is the work by Pereira *et al.* [45] where they compare the performance of negative-velocity feedback and Lyapunov method for a cantilevered beam. The order of the reduced dynamics in a discretized model should be chosen with caution. If the order is too small, there is a risk of instability in a feedback system due to controller spill-over (caused by sensing and actuating neglected higher modes) [46]. In feedforward control, there is no observation spill-over, but control spill-over can cause residual vibration and maybe instability. In addition, it may lead to inaccurate model prediction. On the other hand, choosing a large order, increases the complexity and computation cost [47].

Although, for most complex systems, discretization is the only feasible trend, continuous systems described by PDEs can be used to model a variety of geometrically simple industrial, military and consumer products from nano-scale switches to large space structures. The advantage of using the governing PDEs in control analysis rather than discretized models is that none of the modes are neglected. Many researchers develop control theory for distributed parameter models and demonstrate experimental performance [6, 48, 49, 50, 51]. Spatial shaping of distributed actuation and sensing can be used in the control of distributed systems [52, 53, 41]. Shaped piezoelectric laminates provide sensing/actuation for specified modes of distributed systems [54],[55]. Using finite number of actuators on the boundary and/or domain is another way of controlling these systems, seen in cables [51], strings [56], beams [57] and flexible arms [58]. Most of these researchers have used Lyapunov-based feedback methods, in which stability is guaranteed. However, the choice of Lyapunov functional is not a straightforward procedure and the control law is complicated. Rahn [59] summarizes distributed parameter model-based control, analysis and experimental implementation.

Command generation can be used in DPSs, if a proper knowledge of the system is available. Simplicity of the control law and straightforward procedure, makes this approach most suited for geometrically simple continuous systems like slender structures. Unlike other vibration control methods, the input shaping technique in DPSs represented by PDEs is not studied in more than a handful of publications. Singh and Alli [60] use an optimization technique to develop a time-delay (bang-bang) controller to cancel the residual vibration in the wave equation. Fortgang et al. [53] use a command shaping method to suppress the vibration of a longitudinal beam under axial load. They do not

discuss, however, cases with non-commensurate modes and higher order (e.g. bending beam) PDEs.

The most commonly used and easiest to implement shapers use step and impulse inputs. Multi-mode input shaping design consists of simultaneously solving the equations of motion for all modes or convolving shapers designed for each mode. For an infinite dimensional system the first method is not feasible. In addition, according to [34], convolution of designed shapers consists of a series of step inputs acting at all combinations of modal delay times. This implies that the last step acts at the summation of all time delays. In distributed parameter systems this summation does not converge leading to an infinitely long settling time. This problem and its solutions will be addressed in details in Chapter 2.

## 1.5 Variable stiffness structures

Command shaping in vibration control, using smart materials is investigated in the second phase of this research. To revolutionize smart structures applications requires the development of materials with widely ranging mechanical properties (*e.g.* elasticity and viscosity) [61]. Smart structures can then be tuned adaptively to adjust to varying magnitude, type, and frequency of loading during operation. Some missions require a morphing structure that is rigid in desired shapes and compliant during shape changes.

Piezoelectrics are the smart materials that elongate due to electric field (actuation) and generate voltage under tension (sensing). They are widely used in structural applications because of their high frequency actuation, high stiffness and accurate sensing

[62]. Piezoelectrics, however, suffer from limited strain capabilities, a critical requirement in morphing structures. In addition, their stiffness variation is not sufficient for many applications.

Shape memory alloys (SMAs) can achieve larger displacements up to 10% (~2% in the elastic range) [61]. These materials undergo a phase transformation in response to temperature changes. The modulus variation of SMAs is about 2-4 times [63], however, because of thermal actuation, their frequency response is usually slow (less than 1 Hz) depending on surface area over volume ratio.

Other common types of smart materials are shape memory polymers (SMPs), magnetorheological (MR) fluids, electrorheological (ER) fluids, electro/magneto-strictive materials, ionic gels and so on. The Young's modulus of SMPs is on the order of MPa and it varies up to 1000 times [64]. MR and ER fluids are widely used in variable damping structures. Oh *et al.* [15] develop a variable stiffness liquid-crystal type ER fluid for vibration isolation. They derive an equivalent mechanical system to model the ER isolator as a combination of high and low stiffness springs and a variable damper.

Smart materials are excellent candidates for semi-active control methods because one can tune their mechanical properties with minimal energy. Switching between different mechanical properties is called state-switching [65]. Clark [66] develops a state-switching vibration controller using a piezoelectric actuator that stores energy in the high-stiffness state and dissipates the stored energy in the low-stiffness state. This method, also called the Skyhook control method, has better performance than traditional tuned damping approaches. Cunefare *et al.* [67] propose a substitute for state-switching that avoids instantaneous changes in potential energy by switching at zero strain.

## 1.6 Fluidic flexible matrix composites

Fluidic Flexible Matrix Composites ($F^2MC$) are variable stiffness structures consisting of Flexible Matrix Composite (FMC) tube with two families of fibers wound at $\pm\alpha$ with respect to the longitudinal axis (See Fig. 1.2), an inner liner, and working fluid. Philen *et al.* [68] show that FMC tubes can elongate or contract in response to internal pressure. Tubes with fiber angles greater than 54° extend due to pressurization, while smaller fiber angles result in contractor tubes (*e.g.* Mckibben actuators [69, 70, 71]). Due to the differences in the elastic properties of the fibers and resin, FMC tubes have cylindrical anisotropy. Figure (1.2) shows an FMC laminate and its fiber orientation.

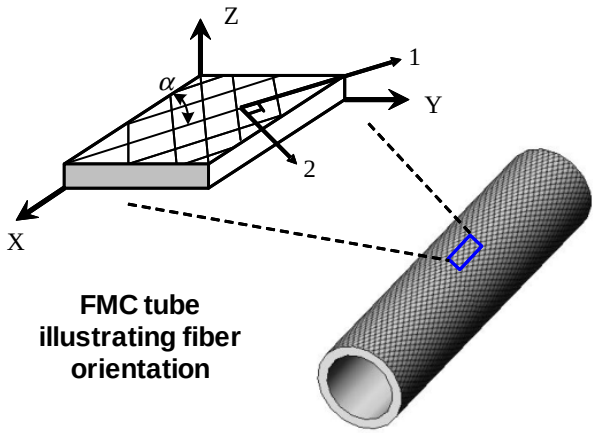


**Figure 1.2.** Schematic plot of FMC laminate with two-directional fiber angles. The axis 1 shows the positive fiber orientation and XYZ axes are the global coordinate system.

Shan *et al.* [72] study the nonlinear-elastic axisymmetric deformation of FMC tubes using large deformation theory. This model accounts for the end-fitting effects that are neglected in models with infinitely-long tube assumptions. Philen *et al.* [73] develop a variable stiffness adaptive structure using $F^2MC$ tubes with valve control. This shell theory is used to derive the effective elastic modulus of the tube for open (soft) and

closed (stiff) cases. Shan *et al.* [74] add the effect of wall compliance by using a 3D elasticity model of the laminate. The analytical model predicts that $F^2MC$ structures are capable of changing stiffness by more than 3 orders of magnitude. By tailoring material properties such as the Young's modulus of the fibers and resin and fiber angle, one can generate $F^2MC$ structures that outperform currently available variable stiffness materials, including shape memory polymers and PZT. Other advantages of the $F^2MC$ tubes are inexpensive and available materials, ease of integration into a structure, and tunability of open-valve and closed-valve stiffnesses.

## 1.7 Overview of the present work

This research investigates novel ideas in structural vibration control. Distributed parameter systems are the focus of the first part of this thesis. A two dimensional input shaper is designed for vibration suppression of one dimensional continua. The second part of the work introduces a ZV Stiffness Shaping controller, optimal passive controller, ZV semi-active controller, and tuned vibration absorber using $F^2MC$ tubes.

Chapter 2 studies the position regulation of 2nd and 4th-order DPSs such as strings, rods, acoustic waves, and beams with zero residual vibration. The effects of different boundary conditions including free, clamped and inertial boundary conditions are investigated. An input shaper is designed that temporally suppresses all the admissible modes and spatially cancels out the remaining modes of vibration. This study proves that the sensitivity of the input shapers in DPSs is different than discrete systems which can only be observed by solving the PDE system.

Dynamics analysis of $F^2MC$ tubes as variable stiffness structures are studied in chapter 3. A 3-D elasticity model develops the closed-form equations of motion of an $F^2MC$ tube. Then, a reduced order dynamic model based on the fully-open and fully-closed valve motivates a ZV stiffness shaping technique that suppresses vibration in finite time. Chapter 4 extends this technique to a ZV feedback control law. A Lyapunov approach proves the stability of the $F^2MC$-mass system regardless of the valve condition. In this chapter, a novel optimal passive controller is demonstrated that uses a fluid-filled $F^2MC$ tube coupled to a pressurized accumulator through a fixed orifice. The impulse and step responses of the $F^2MC$-mass system is simulated for optimal passive, ZV, and Skyhook controllers. An experimental setup is designed and fabricated to validate the theory.

Chapter 5 introduces a new fluidic composite TVA. Coupling of a fluid-filled $F^2MC$ tube through a fluid port to a pressurized air accumulator can suppress primary mass forced vibration at the tuned absorber frequency. 3-D elasticity model for the tube and a lumped fluid mass develops a 4th-order model of an $F^2MC$-mass system. Experimental results validate the theoretical predictions showing tunable isolation frequency, insensitivity to primary mass variations, and a great reduction in forced vibration relative to the closed valve case.

Chapter 2

# Input Shaping Technique for Distributed Parameter Systems

## 2.1 Introduction

This chapter extends input shaping technique to vibration suppression of one-dimensional continuous systems. It is shown that temporally-shaped boundary and distributed inputs can provide setpoint regulation of second order (string) systems. For fourth order systems (beams), temporal and spatial (or 2-D) input shaping is introduced. The robustness of the input shaping controllers to uncertainties in system parameters is quantified. A unique characteristic of continuous systems is demonstrated in which the sensitivity curve does not match that of finite dof systems.

The most commonly used and easiest to implement shapers use step and impulse inputs. Multi-mode input shaping design consists of simultaneously solving the equations of motion for all modes or convolving shapers designed for each mode. For an infinite dimensional system the first method is not feasible. In addition, according to [34], convolution of designed shapers consists of a series of step inputs acting at all com-

binations of modal delay times. This implies that the last step acts at the summation of all time delays. In distributed parameter systems this summation does not converge leading to an infinitely long settling time. In order to avoid this problem, researchers design the shapers based on dominant modes of vibration and neglect higher mode excitation. Therefore, this research designs an input shaper that temporally suppresses all the admissible modes and spatially cancels out the remaining modes.

## 2.2 Strings

Figure (2.1) shows four example string models for which input shaping controllers are developed. These examples can be used to model micro-switches, pneumatic servos, flexible cable cranes, and fiber handling machinery [59]. Figure 2.1(a) shows a boundary controlled string where the input force $P(t)$ is used to move the end to a desired position with no residual vibration. In Fig. 2.1(b), the left boundary displacement is shaped to provide a desired right boundary displacement. The distributed force input $P(x,t)$ applied to the pinned string in Fig. 2.1(c) can be shaped in both space and time to drive the mid-span displacement to a desired value. A string with a mass at the lower boundary in Fig. 2.1(d) is controlled by a shaped input force at the upper end.

One can assume that the string is homogeneous and has constant tension in a small deformation range. The field equation is simplified to a standard wave equation form:

$$Tu_{xx} + p(x,t) = \rho u_{tt} \tag{2.1}$$

where, $T$ and $\rho$ are the tension and mass/length respectively, the transverse displacement

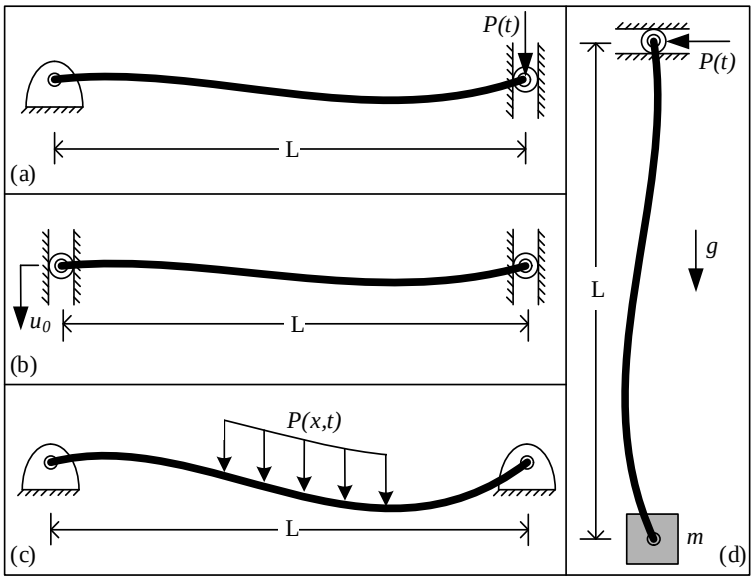


**Figure 2.1.** Four typical string applications: (a) Boundary controlled string, (b) Noncollocated boundary controlled string, (c) Domain controlled string, (d) Noncollocated boundary controlled string with mass.

$u(x,t)$ depends on position $x$ and time $t$, $p(x,t)$ is the distributed transverse force and subscripts indicate partial differentiation. The nondimensional parameters are defined as follows:

$$u = u^* L \ ; \quad x = x^* L \ ; \quad t = t^* L \sqrt{\frac{\rho}{T}} \ ; \quad p^*(x,t) = \frac{L}{T} P(x,t) \tag{2.2}$$

to produce

$$u_{tt} - u_{xx} = P(x,t), \tag{2.3}$$

where the superscript stars are eliminated for convenience. Note that the displacements are assumed small and the response characteristics are independent of amplitude for this linear model.

### 2.2.1 Boundary controlled string

The right boundary solution to Eq. (2.3) with the boundary conditions shown in Fig. 2.1(a),

$$u(0,t) = 0 \ , \quad u_x(1,t) = P(t) \ , \tag{2.4}$$

and for the step input $P(t) = P_0 H(t-\tau)$, is

$$u(1,t) = \sum_{n=1}^{\infty} \frac{8P_0 H(t-\tau)}{(2n-1)^2 \pi^2} \left[1 - \cos\left((2n-1)\frac{\pi}{2}(t-\tau)\right)\right], \tag{2.5}$$

where $P_0$ is a constant, $H(t)$ is the heaviside step function, and $\tau$ is the delay time. The detailed solution is in [41].

The infinite series (2.5) can be simplified by Fourier series analysis to the periodic sawtooth function with period 4,

$$\begin{aligned} u(1,t) = P_0(-1)^{floor\left(\frac{t-\tau}{2}\right)} \Bigg[(t-\tau) - 2floor\left(\frac{t-\tau}{2}\right) \\ +(-1)^{floor\left(\frac{t-\tau}{2}\right)} - 1\Bigg] H(t-\tau), \end{aligned} \tag{2.6}$$

shown in Fig. 2.2.

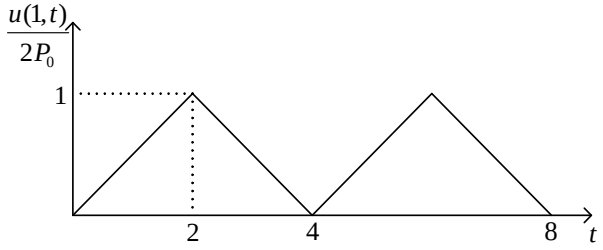


**Figure 2.2.** Sawtooth function in Eq. (2.6) with $\tau = 0$.

### 2.2.2 Input shaping design

The response of the string at a desired location $l$, to multiple step inputs

$$P = \sum_{i=1}^{m} P_i H(t - \tau_i), \tag{2.7}$$

is

$$\begin{aligned} u(l,t) = A_0(l) \sum_{i=1}^{m} P_i H(t - \tau_i) + \\ \sum_{i=1}^{m} \sum_{n=1}^{\infty} A_n(l) P_i \cos\left[n\alpha(t - \tau_i)\right] H(t - \tau_i), \end{aligned} \tag{2.8}$$

where $0 < l < 1$ and $A_i(l)$ are constants. For a pinned-forced string, $\alpha = \frac{\pi}{2}$, and from Eq. (2.5) only odd ($n = 1, 3, ...$) mode numbers appear in the response.

The purpose of input shaping is to suppress the vibration after the last step has been applied. For sufficiently large times, a zero residual vibrations is desired.

$$V(l,t) = \sum_{i=1}^{m} \sum_{n=1}^{\infty} A_n P_i \cos\left((2n-1)\alpha(t - \tau_i)\right) \equiv 0. \tag{2.9}$$

To enforce the condition (2.9), one can design $\mathrm{P}_i$ and $\tau_i$ to suppress the vibration of all the modes as follows:

$$\begin{aligned} 0 \equiv \cos(2n-1)\,\alpha t \sum_{i=1}^{m} \left[P_i \cos(2n-1)\,\alpha\tau_i\right] \\ + \sin(2n-1)\,\alpha t \sum_{i=1}^{m} \left[P_i \sin(2n-1)\,\alpha\tau_i\right]. \end{aligned} \tag{2.10}$$

The coefficients of the time-varying terms in Eq. (2.10) are

$$\sum_{i=1}^{m} P_i \cos(2n-1)\,\alpha\tau_i \equiv 0 \qquad \forall n \in \mathbb{N},$$
$$\sum_{i=1}^{m} P_i \sin(2n-1)\,\alpha\tau_i \equiv 0 \qquad \forall n \in \mathbb{N}. \tag{2.11}$$

The number of equations in (2.11) is infinite but there are finite number of unknowns to be determined (*e.g.* for a two-step input shaper $P_1$, $P_2$ and $\tau_2$ are the unknowns and $\tau_1 = 0$). So the equations for $n > 1$, should be dependent on the first set of Eqs. (2.11). If $\tau$ is constructed so that

$$\begin{aligned} \cos\alpha\tau_i &= \cos(2n-1)\,\alpha\tau_i \qquad \forall n \in \mathbb{N}, \\ \sin\alpha\tau_i &= \sin(2n-1)\,\alpha\tau_i \qquad \forall n \in \mathbb{N}, \end{aligned} \tag{2.12}$$

Eqs. (2.11) are satisfied. So, the admissible time delays are

$$\tau = k\frac{\pi}{\alpha} \qquad k \in \{0, 1, 2, ...\}, \tag{2.13}$$

Substituting Eq. (2.13) into Eqs. (2.11) one obtains

$$\sum_{i=1}^{m} P_i(-1)^{k_i} = 0 \tag{2.14}$$

where $k_i$ is a nonnegative integer corresponding to the delays.

Finally, normalization of the pulse train ensures that

$$\sum_{i=1}^{m} P_i = 1 \ . \tag{2.15}$$

Solving Eqs. (2.14) and (2.15) one takes $\tau_1 = 0$ and $\tau_2 = \frac{\pi}{\alpha} = 2$ for the pinned-forced string. The ZV input shaper is

$$P(t) = 0.5H(t) + 0.5H(t-2) \tag{2.16}$$

Figure (2.3) shows the ZV input $F(t)$ and output response $u(1,t)$. The output grows linearly with time in response to the step inputs at $t = 0$ and 2. At $t = 2$, the output stops with no residual vibration. The inset shows the time evolution of the spatial wave propagating from right to left.

### 2.2.3 Robustness

Input shaping is sensitive to parameter uncertainties due to the lack of feedback. To increase robustness a ZVD shaper [31] ensures that

$$\frac{\partial V}{\partial \omega} = 0. \tag{2.17}$$

This results in two equations, one of which is trivial and the other

$$\sum_{i=1}^{m} P_i \tau_i (-1)^{k_i} = 0. \tag{2.18}$$

By choosing the delay times to be the first three admissible times from Eq. (2.13), the ZVD input shaper is obtained

$$P(t) = 0.25H(t) + 0.5H(t-2) + 0.25H(t-4) \tag{2.19}$$

Figure 2.3 shows that the ZVD shaper also produces zero residual vibration for the distributed boundary controlled string model. The spatial response is different, however, settling out in twice the time of ZV.

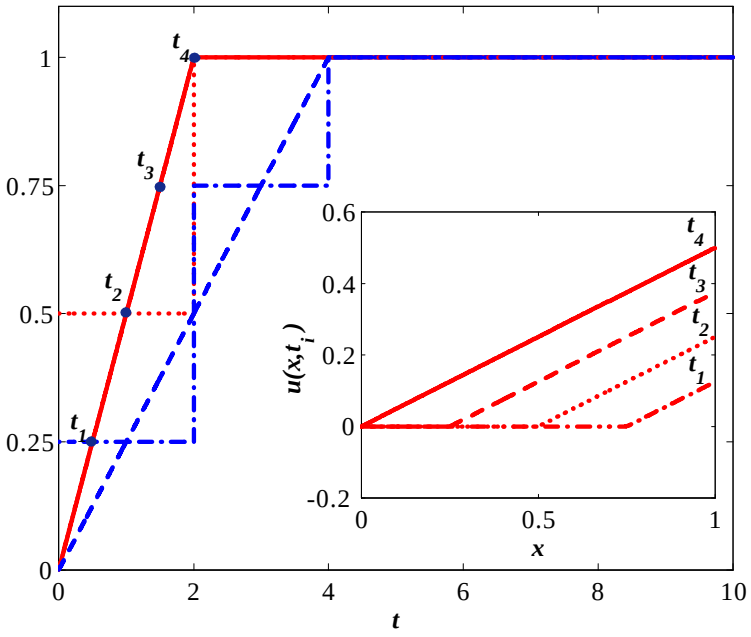


**Figure 2.3.** Boundary controlled string response to ZV ($p(t)$ = dotted and $u(1,t)$ = solid) and ZVD ($p(t)$ = dash-dotted and $u(1,t)$ = dashed) shapers. Inset shows displacement distribution response $u(x,t_i)$ to the ZV input at times $t_i = \frac{i}{2}$.

As has been shown in the literature for discrete systems [39, 33, 34], the ZV shaper is relatively sensitive to frequency error and the ZVD shaper adds robustness. In single or multi-DOF systems, the ZVD shaper has always shown improved robustness. One criteria for robust performance is the sensitivity curve [75] or plot of the percentage resid-

ual vibration ($\%V$ = vibration amplitude with shaping divided by vibration amplitude without shaping) versus the normalized frequency ($\omega_r$ = the actual frequency divided by the modeling frequency). For instance, by introducing a frequency error in the vibration term in Eq. (2.9), for a boundary controlled string,

$$V(l,t) = \sum_{i=1}^{m} \sum_{n=1}^{\infty} \frac{2}{\left(\omega_r(2n-1)\frac{\pi}{2}\right)^2} P_i \cos\left(\omega_r(2n-1)\frac{\pi}{2}(t-\tau_i)\right). \tag{2.20}$$

Fourier series analysis shows that the amplitude of vibration for an unshaped input is

$$|V(l)| = \frac{1}{\omega_r^2} \quad \text{for } 0 < \omega_r < 2, \tag{2.21}$$

and the normalized vibration amplitude is obtained as

$$\%V = |1 - \omega_r| \qquad \text{for } 0 < \omega_r < 2 \tag{2.22}$$

for both the ZV and ZVD shapers, a result that appears to be unique to distributed parameter systems. Figure 2.4(a) shows the response to an input shaper designed with a 10% error in natural frequencies or $\sqrt{\frac{\rho L^2}{T}}$. The ZV and ZVD shapers produce different responses but have the same amplitude of residual vibration. Figure 2.4(b) shows the sensitivity curves for the first and second modes of vibration under ZV and ZVD shapers. These curves show the characteristic ZV and ZVD shapes. The ZV sensitivity curve has a slope discontinuity at $\omega_r = 1$, resulting in a V-shaped curve. The constraint 2.17 ensures that the sensitivity curves have zero slope at $\omega_r = 1$, resulting in a parabolic shape. These curves repeat the shape from $\omega_r \in [0, 2)$ with increasing $\omega_r$. Fig. 2.4(c) shows the

normalized vibration of the distributed system (all modes). The ZV and ZVD curves lie on top of each other, predicting the same sensitivity for ZV and ZVD shapers. The ZVD shaper does not appear to have a zero slope at $\omega_r = 1$, an apparent contradiction. The individual modes of vibration in Fig. 2.4(b), however, clarifies that each has zero-slope so the summation of all modes must also have zero slope. Figure 2.4(c) also shows that the sensitivity is maximum at the even multiples of the first mode and zero at the odd multiples.

### 2.2.4 Noncollocated boundary controlled string

In Fig. 2.1(b) the right boundary is controled using the noncollocated left boundary displacement input. Thus, the entire string can translate vertically. The field Eq. (2.3) applies with pinned boundary conditions $u^*(0,t) = u^*(1,t) = 0$ and

$$u = Lu_0^* - Lu^* \ , \quad P^*(x,t) = -(u_0^*)_{tt} \tag{2.23}$$

where

$$u_0^* = \frac{u_0}{L} \ . \tag{2.24}$$

Thus, the left boundary input acceleration acts as a uniformly distributed input force to a pinned string. The shape of the acceleration is designed to ensure bounded displacement. Therefore, the acceleration and velocity of the left boundary should vanish after the settling time leading to

$$\sum_{i=1}^{m} P_i = 0 \tag{2.25}$$

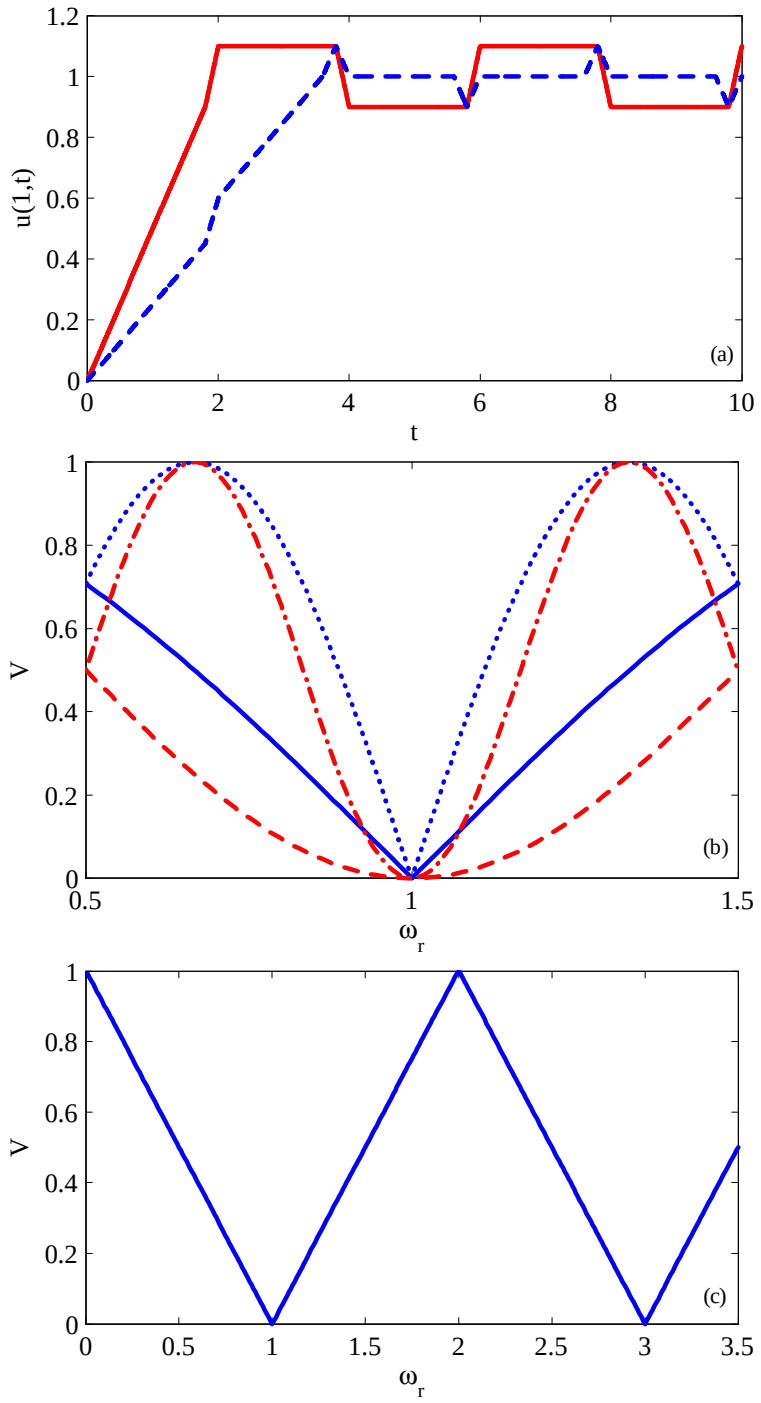


**Figure 2.4.** Boundary controlled string robustness (a) Response to ZV (solid) and ZVD (dotted) shapers with a 10% error in the natural frequencies and (b) Sensitivity curve for the first mode under ZV (solid) and ZVD (dashed) and the second mode under ZV (dotted) and ZVD (dash-dotted) shapers. (c) Sensitivity curve for the string under ZV and ZVD shapers (same curve).

and Eq. (2.18) which are solved simultaneously with Eq. (2.14) to produce the ZVD acceleration input

$$P(t) = \frac{1}{8}H(t) - \frac{1}{8}H(t-2) - \frac{1}{8}H(t-4) + \frac{1}{8}H(t-6). \tag{2.26}$$

Equation (2.26) and the corresponding system response are shown in Fig. 2.5. The boundary displacement is smooth and the corresponding output shows an S-shaped curve. The spatial response shows the left boundary displacement initially leading the right and then lagging as the vibration wave moves right, bounces off the right boundary, and returns.

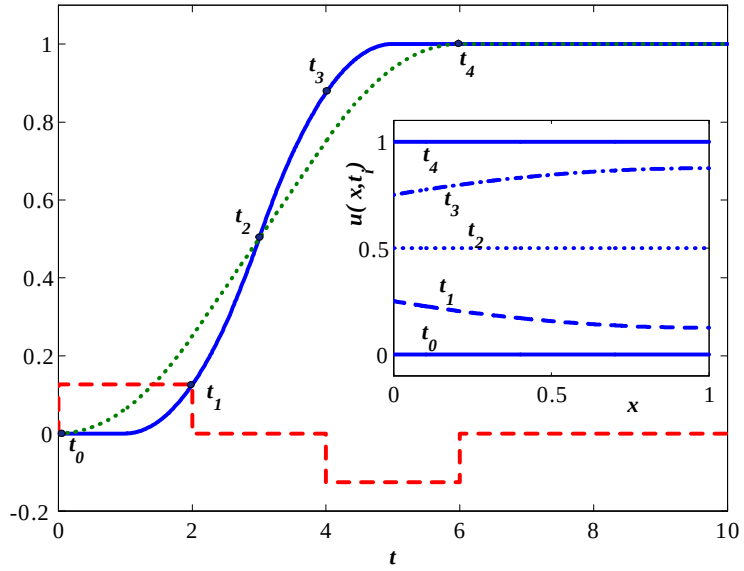


**Figure 2.5.** Noncollocated boundary controlled string: Input $u_0(t)$ (dotted), acceleration $(u_0)_{tt}$ (dashed) and response $u(1,t)$ (solid). Inset shows displacement distribution $u(x,t_i)$ in response to the ZVD input at times $t_i = 0, 2, 3, 4, 6$.

### 2.2.5 String with boundary dynamics

In Fig. 2.1(d) the lower boundary mass displacement is controled using the noncollocated upper boundary force input. This model represents applications in distributed parameter systems such as gantry cranes that include boundary dynamics. For simplicity, it is assume that the string weight is negligible, so the tension is constant and the load swing angle is small.

The characteristic equation is obtained considering the unforced system with mass $m$ at the boundary.

$$m\omega_n \cos(\omega_n) + \sin(\omega_n) = 0, \tag{2.27}$$

which shows that the first modal frequency is zero and the modes are not commensurate. The response of this system to a force at the left boundary is

$$u(x,t) = \int_0^t \int_0^t F(\tau)d\tau + \sum_{n=2}^{\infty} \frac{1}{\omega_n m_{nn}^2} \cos(\omega_n x) \int_0^t F(\tau) \sin \omega_n (t-\tau) d\tau. \tag{2.28}$$

where, $m_{nn}$ is the mode normalization factor.

In Eq. (2.28), the first term corresponds to the rigid body motion and the remaining terms deal with the modal vibration. In order to suppress the vibration after some time $t_0$, one needs to find $F(t)$ such that

$$\int_0^t F(\tau) \sin \omega_n (t-\tau) d\tau \equiv 0 \qquad \forall t > t_0. \tag{2.29}$$

As discussed in section (2.4), a series of step input forces can control the position and suppress the vibration of a noncollocated boundary controlled string. On the other hand,

to control the mass, a series of impulses is required. Using this intuition, one seeks an input force in the form of

$$F(t) = m\left[p_1\delta(t) + p_2\delta(t-\tau) + p_3\delta(t-2\tau)\right] + \left[q_1 H(t) + q_2 H(t-\tau) + q_3 H(t-2\tau)\right], \tag{2.30}$$

where $\tau = 2$ is twice the time delay required for a wave to travel between the boundaries. Since the trajectory involves a rigid body motion, the input force should vanish after $t_0$ for bounded displacement. This implies

$$p_1 + p_2 + p_3 = 0 \quad \text{and} \quad q_1 + q_2 + q_3 = 0. \tag{2.31}$$

Substituting Eqs. (2.30-2.31) to Eq. (2.29) and simplifying, for $t > t_0$

$$0 \equiv m\omega_n\left[p_1\cos\omega_n(t-1) - p_3\cos\omega_n(t-3)\right] + \left[q_1\sin\omega_n(t-1) - q_3\sin\omega_n(t-3)\right]. \tag{2.32}$$

Equation (2.32) can be converted to the characteristic equation, Eq. (2.27), by choosing $p_1 = -p_3 = \frac{1}{4}$ and $q_1 = q_3 = \frac{1}{4}$ (consequently $p_2 = 0$ and $q_2 = \text{-}\frac{1}{2}$), or

$$0 \equiv (m\omega_n\cos(\omega_n) + \sin(\omega_n))\cos\omega_n(t-2) \quad \forall t > t_0. \tag{2.33}$$

Hence, the input shaper for this system is

$$F(t) = \frac{m}{4}\left[\delta(t) - \delta(t-4)\right] + \frac{1}{4}\left[H(t) - 2H(t-2) + H(t-4)\right].$$

Figure (2.6) shows the shaped response of the noncollocated boundary controlled string with mass. After a delay of one, the output grows linearly and stops at $t = 3$. The spatial response is complex, showing multiple waves reflecting off the mass.

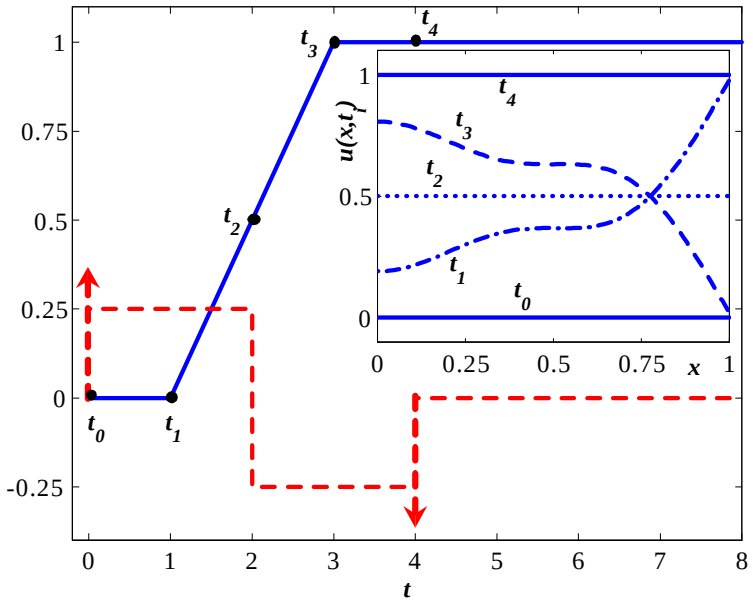


**Figure 2.6.** Noncollocated boundary controlled string with mass: Input $F(t)$ (dotted) and response $u(1,t)$ (solid). Inset shows displacement distribution $u(x,t_i)$ at times $t_i = i$.

### 2.2.6 Domain controlled string

The response of the pinned-pinned string in Fig. 2.1(c) to a set of distributed step loads $p(x,t) = \sum_{i=1}^{m} P_i\ q(x) H_i(t-\tau_i)$ is

$$u(x,t) = \sum_{i=1}^{m}\sum_{n=1}^{\infty}\left\{\left(\frac{2}{n^2\pi^2}\right)\sin(n\pi x)\left[1-\cos(n\pi(t-\tau_i))\right] P_i H(t-\tau_i)\int_0^1 \sin(n\pi x)\, p(x)dx\right\}. \quad (2.34)$$

In Eq. (2.34) one can shape the spatial input distribution $p(x)$. This spatial shaping

can be achieved by patterning a variable-width electrode under an electrostatic bridge, for example. The residual vibration is

$$V(x,t) = \sum_{i=1}^{m} \sum_{n=1}^{\infty} A_n \left( \int_0^1 \sin(n\pi x)\, p(x) dx \right) \cos(n\pi(t-\tau_i)) \equiv 0. \tag{2.35}$$

Expanding the time dependent terms results in

$$\begin{aligned} \sum_{i=1}^{m} \left( \int_0^1 \sin(n\pi x)\, p(x) dx \right) P_i \cos(n\pi\tau_i) &\equiv 0 \quad \forall n \in \mathbb{N}, \\ \sum_{i=1}^{m} \left( \int_0^1 \sin(n\pi x)\, p(x) dx \right) P_i \sin(n\pi\tau_i) &\equiv 0 \quad \forall n \in \mathbb{N}. \end{aligned} \tag{2.36}$$

These equations hold for all the modes, so

$$\cos\pi\tau_i = \cos n\pi\tau_i \ , \quad \sin\pi\tau_i = \sin n\pi\tau_i \qquad \forall n \in \mathbb{N}, \tag{2.37}$$

which can be satisfied if $\tau = k$. One can choose the step amplitudes $P_i$ and distribution $p(x)$ such that the odd terms ($n = 1, 3, 5, ...$) cancel and for the even terms

$$\int_0^1 \sin(n\pi x) \left( \sum_{i=1}^{m} p_i(x) \right) dx = 0 \qquad n = 2, 4, 6, ... \tag{2.38}$$

Thus, the distribution must be orthogonal to the even modes. Example of distributions that satisfy Eq. (2.38) are a uniform load and a point force at $x = \frac{1}{2}$.

The ZV and ZVD input shaper for these cases are:

$$P(t) = 0.5H(t) + 0.5H(t-1),$$

$$P(t) \quad = \quad 0.25H(t) + 0.5H(t-1) + 0.25H(t-2), \tag{2.39}$$

respectively. Figure 2.7 shows the response of the pinned string to a point force at $x = \frac{1}{2}$ (Fig. 2.7(a)) and a uniformly distributed force (Fig. 2.7(b)) under ZV and ZVD control. The point force produces linear spatial and time distributions that correspond to wave propagation and boundary reflection. The uniformly distributed forced response shows smooth time and space trajectories. In both cases, there is no residual vibration. The ZV and ZVD shaped responses come to steady-state at $t = 1$ and 2, respectively.

## 2.3 Beams

The equation of motion for an Euler-Bernoulli beam (Fig. 2.8) is:

$$\rho u_{tt} + EIu_{xxxx} = p(x,t) \ , \tag{2.40}$$

where $EI$ and $\rho$ are the bending stiffness and mass/length, respectively, and $p(x,t)$ is the distributed force acting transversely on the beam. Introducing the nondimensional

$$u^* = \frac{u}{L}, \ x^* = \frac{x}{L}, \ t^* = \frac{t}{L^2\sqrt{\frac{\rho}{EI}}}, \ p^*(x,t) = \frac{L^3}{EI}p(x,t) \ , \tag{2.41}$$

the following is obtained

$$u_{tt} + u_{xxxx} = p(x,t) \tag{2.42}$$

where the stars are omitted for convenience.

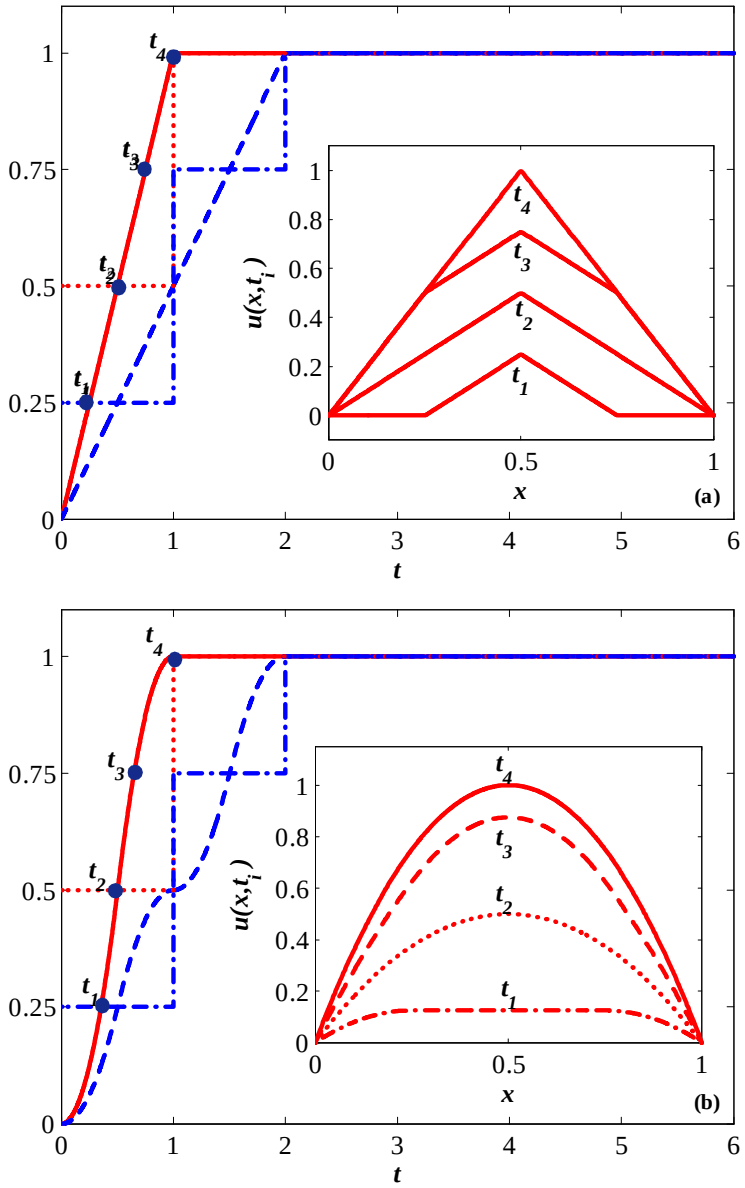


**Figure 2.7.** ZV ($p(t)$ = dotted and $u(\frac{1}{2},t)$ = solid) and ZVD ($p(t)$ = dash-dotted and $u(\frac{1}{2},t)$ = dashed) shaped domain controlled string responses to (a) Point force at $x = \frac{1}{2}$ and (b) Distributed force. Insets show displacement distribution $u(x,t_i)$ at times $t_i = \frac{i}{4}$.

### 2.3.1 Pinned-pinned beam

The response of a pinned-pinned beam to a set of distributed step loads $p(x,t) = \sum_{i=1}^{m} P_i$ $p(x)H_i(t-\tau)$ is

$$u(x,t) = \sum_{i=1}^{m}\sum_{n=1}^{\infty}\left\{\left(\frac{2}{n^4\pi^4}\right)\left[1-\cos\left(n^2\pi^2(t-\tau_i)\right)\right]\sin\left(n\pi x\right)\right.$$

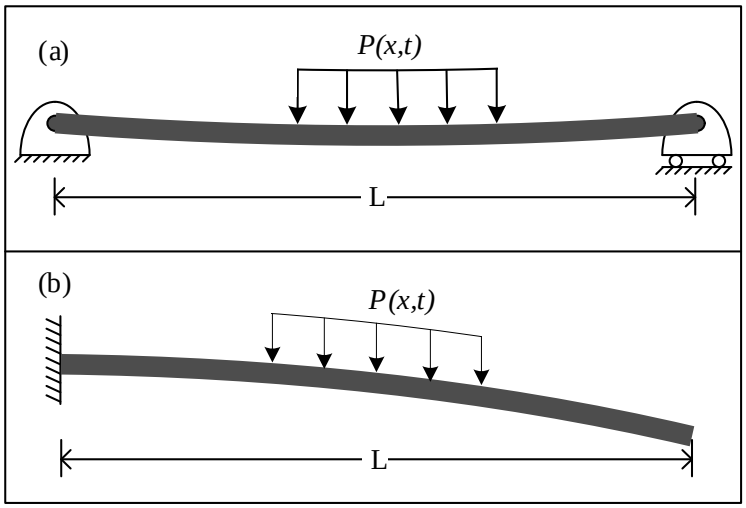


**Figure 2.8.** Two typical beam applications: (a) Pinned-pinned beam, (b) Cantilevered beam.

$$H(t-\tau_i)\int_0^1 \sin(n\pi x)\, p_i(x)dx\Bigg\}. \tag{2.43}$$

As with the pinned string, the odd terms ($n = 1, 3, 5, ...$) are cancelled in the residual vibration through proper selection of the step amplitudes and the even terms are cancelled by ensuring

$$\int_0^1 \sin(n\pi x)\, p(x)dx = 0 \qquad \forall n = 2, 4, ... \tag{2.44}$$

Midspan point loads and uniformly distributed forces, for example, satisfy the orthogonality condition (2.44).

Thus, the ZV and ZVD input shapers are

$$\begin{aligned} P(t) &= 0.5H(t) + 0.5H(t-\frac{1}{\pi}), \\ P(t) &= 0.25H(t) + 0.5H(t-\frac{1}{\pi}) + 0.25H(t-\frac{2}{\pi}), \end{aligned} \tag{2.45}$$

respectively with orthogonal input distributions satisfying Eq. (2.44). Figure 2.9 shows

the response of the pinned beam to ZV and ZVD midspan inputs. The spatial response in the inset of Fig. 2.9 looks similar to the pinned string under uniform load. The midspan displacement converges smoothly to the desired position without residual vibration for both the ZV and ZVD shapers.

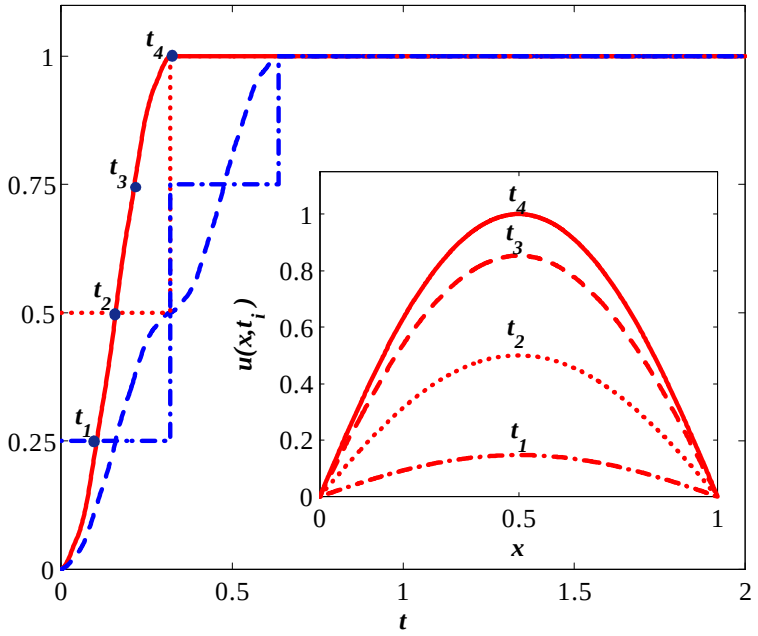


**Figure 2.9.** ZV ($p(t)$ = dotted and $u(\frac{1}{2},t)$ = solid) and ZVD ($p(t)$ = dash-dotted and $u(\frac{1}{2},t)$ = dashed) domain control pinned beam response to a midspan point load. Inset shows displacement response to ZV inputs $u(x,t_i)$ at times $t_i = \frac{i}{4\pi}$.

Figure 2.10(a) shows the time response of the ZV and ZVD shaped responses with 10% error. Unlike the pinned string case, however, the pinned beam has less residual vibration with the ZVD shaper. The sensitivity curve in Fig. 2.10(b) shows the residual vibration as a function of error for the ZV and ZVD shapers.

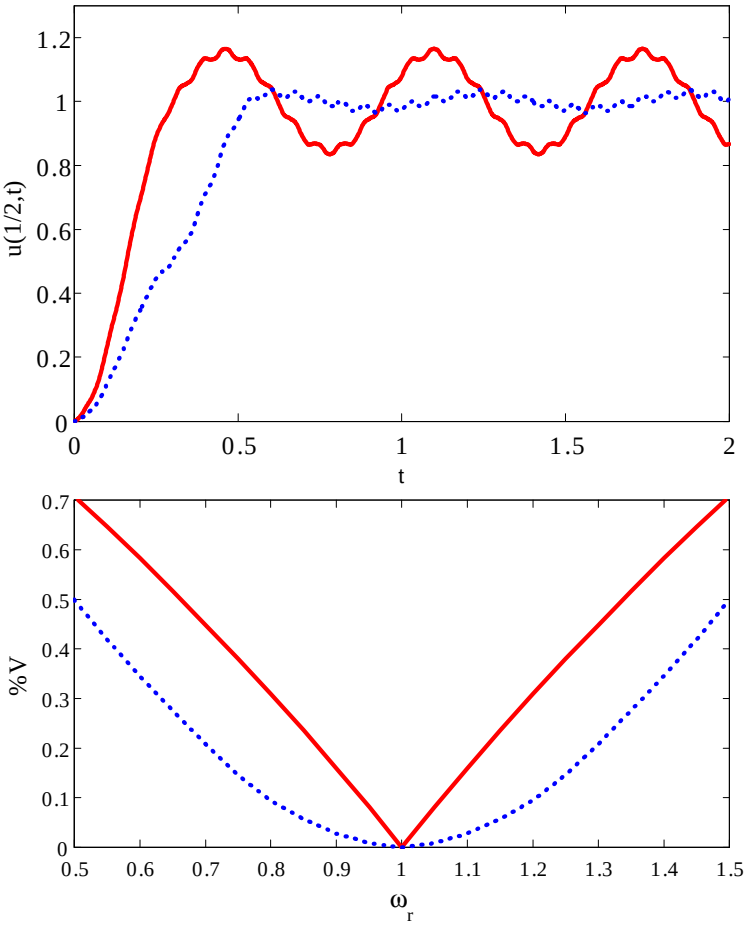


**Figure 2.10.** Pinned-pinned beam robustness (a) Response to ZV (solid) and ZVD (dotted) shapers with 10% error in the first natural frequency and (b) Sensitivity curves for ZV (solid) and ZVD (dotted) shapers.

### 2.3.2 Cantilevered beam

For most continuous systems there are no closed form solutions. In many cases, the response can be expressed in an infinite modal series

$$u(x,t) = \sum_{n=1}^{\infty} \eta_n(t) U_n(x) \ , \tag{2.46}$$

where $\eta_n(t)$ are the modal coordinates and $U_n(x)$ are the mode shapes. The modal response to a step input is

$$\ddot{\eta}_n(t) + \omega_n^2 \eta_n(t) = H(t-\tau) \int_0^1 p(x) U_n(x) dx \tag{2.47}$$

where $\omega_n$ are the natural frequencies [41]. If one chooses to shape the time response to cancel residual vibration in the first mode, then one can spatially shape the input to cancel all the other modes.

$$\int_0^1 p(x) U_n(x) dx = 0 \qquad n \in \mathbb{N} \quad , \quad n \neq 1. \tag{2.48}$$

From the orthogonality of mode shapes,

$$\int_0^1 U_1(x) U_n(x) dx = 0 \qquad n \in \mathbb{N} \quad , \quad n \neq 1. \tag{2.49}$$

Therefore, if the input force is spatially shaped according to the first mode shape, then only this mode will be excited. For the cantilevered beam, one can choose

$$p(x,t) = P_0 U_1(x) \sum_{i=1}^{m} P_i H(t-\tau_i) \tag{2.50}$$

where $P_0$ is the orthonormality constant and

$$\begin{aligned} U_1(x) \;=\; & \sin(\beta_1 x) + \frac{\cos(\beta_1) + \cosh(\beta_1)}{\sin(\beta_1) - \sinh(\beta_1)} \cos(\beta_1 x) \\ & - \sinh(\beta_1 x) - \frac{\cos(\beta_1) + \cosh(\beta_1)}{\sin(\beta_1) - \sinh(\beta_1)} \cosh(\beta_1 x) \end{aligned} \tag{2.51}$$

with $\beta_1 = \sqrt{\omega_1}$.

The input shaper design follows that of a second order system with the natural frequency equal to $\omega_1$. Thus, the ZV and ZVD shapers are

$$\begin{aligned} ZV : P(t) &= 0.5\left(H(t) + H(t - \frac{\pi}{\omega_1})\right), \\ ZVD : P(t) &= 0.25\left(H(t) + 2H(t - \frac{\pi}{\omega_1}) + H(t - \frac{2\pi}{\omega_1})\right), \end{aligned} \tag{2.52}$$

respectively. Figure 2.11 shows the spatial and temporal response of the cantilevered beam to the spatially and ZV and ZVD temporally shaped inputs. The endpoint position smoothly converges to the desired setpoint.

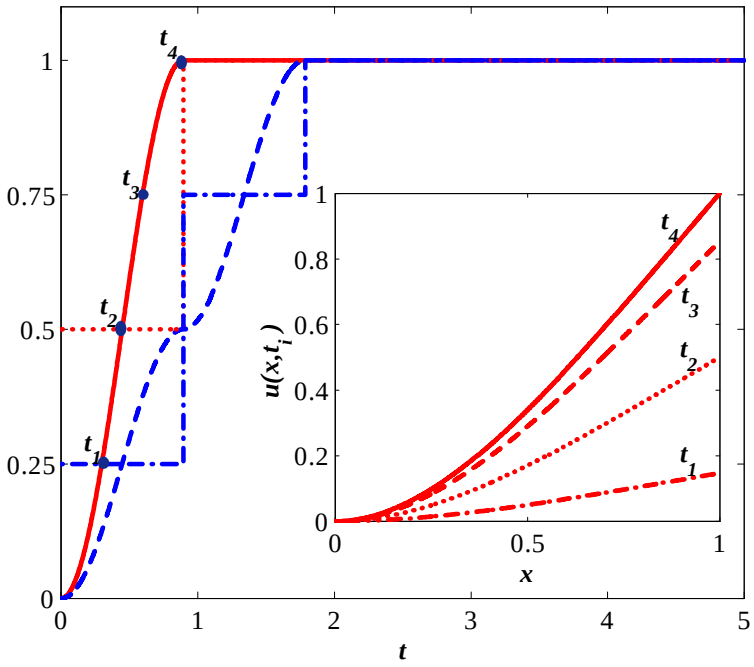


**Figure 2.11.** Cantilevered beam response to ZV ($p(t)$ = dotted and $u(1,t)$ = solid) and ZVD ($p(t)$ = dash-dotted and $u(1,t)$ = dashed) shapers. Inset shows the displacement distribution $u(x,t_i)$ at times $t_i = \frac{i}{4}$.

## 2.4 Conclusion

Spatial and temporal input shaping can produce zero residual vibration in setpoint position control of one dimensional continua. For strings and pinned beam models, the response to step inputs is solved in closed form using delays. For more complicated (*e.g.* clamped beam) models, a closed form infinite modal series is the solution. The boundary controlled string can be setpoint regulated using two-pulse ZV and three-pulse ZVD shapers but, unlike discrete systems, ZVD is not more robust than ZV. Noncollocated ZV and ZVD boundary control enables translation of a string with zero residual vibration. Domain controlled strings and beams with spatial input distributions that satisfy certain orthogonality conditions (*e.g.* midspan point load and uniformly distributed load) can be setpoint regulated with shaped inputs. The pinned beam with ZVD shaped inputs is shown to have less sensitivity to parameter variations than with ZV. For systems with known eigenfunctions, modal shaping of the input distribution and ZV or ZVD temporal shaping drives the output to the desired position with zero residual vibration. Using a force distribution shaped according to the first mode, the tip position of a cantilevered beam, for example, is driven to the desired setpoint without residual vibration.

Chapter 3

# Feedforward Vibration Control of Fluidic Flexible Matrix Composites

This chapter extends the static analysis of F$^2$MC tubes by Shan *et al.* [74] and derive the closed form equations of motion of an F$^2$MC tube attached to a mass. Then, the order of the dynamic system is reduced. A Skyhook feedback control scheme [66] is then developed. Finally, a novel stiffness shaping technique is introduced to suppress the residual vibration in finite time and is compared with Skyhook method.

## 3.1 Elasticity model of the F$^2$MC tubes

F$^2$MCs are FMC tubes consisting of high elastic modulus fibers embedded in a flexible resin and filled with high bulk modulus fluid (*e.g.* water). Due to the differences in the elastic properties of the fibers and resin, the composite tube is anisotropic. The composite structure is formed by winding the fibers around a cylindrical mandrel. A soft resin layer between the fluid and the FMC laminate prevents leakage. A valve controls the fluid flow in and out of the tube. When the tube is axially loaded, the volume inside the tube changes based on the orthotropic properties of the composite. If

the valve is open, then fluid flows in or out freely. If the valve is closed, then the inside fluid is constrained by the composite wall and generates pressure. As a consequence, the apparent stiffness of the tube increases relative to the open-valve case.

The F$^2$MC tube elasticity model consists of three interacting components: the FMC laminate, inner liner and fluid (See Fig. (3.1)). For simplicity, the end-fitting effects are neglected and the FMC tube is assumed to be infinitely long.

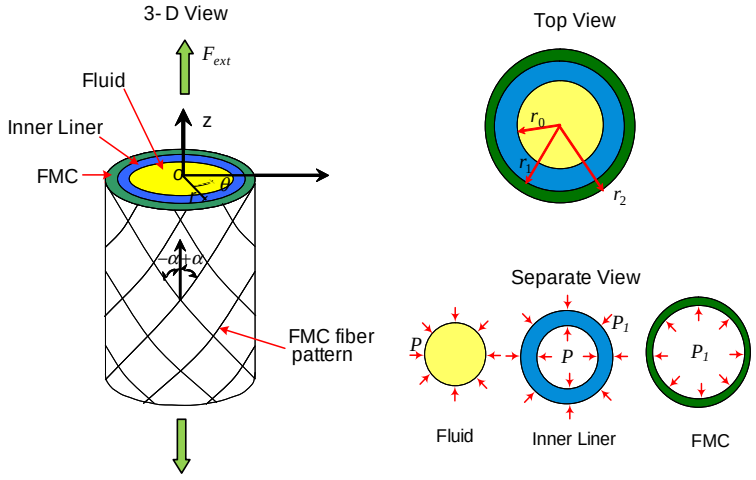


**Figure 3.1.** Schematic plot of F2MC tube with the associated dimensions and loadings on the layers.

**Inner Liner** - The inner liner is an isotropic material under external pressure $P_1$and internal pressure $P$ carrying part of the axial force $F_1$. The stress field in the radial, circumfrential, and axial directions is

$$\begin{aligned}
\sigma_r^i &= \frac{Pr_0^2 - P_1 r_1^2}{r_1^2 - r_0^2} - \frac{r_0^2 r_1^2}{r\left(r_1^2 - r_0^2\right)}\left(P - P_1\right), \\
\sigma_\theta^i &= \frac{Pr_0^2 - P_1 r_1^2}{r_1^2 - r_0^2} + \frac{r_0^2 r_1^2}{r\left(r_1^2 - r_0^2\right)}\left(P - P_1\right), \\
\sigma_z^i &= \frac{F_1}{\pi\left(r_1^2 - r_0^2\right)},
\end{aligned} \tag{3.1}$$

where, $r_0$ and $r_1$ are the inner and outer radii of the liner, respectively and $r$ is the radial position. Using Hooke's law, $\{\varepsilon^i\} = [A^i]\{\sigma^i\}$, one can find the strains $\varepsilon_r^i, \varepsilon_\theta^i$ and $\varepsilon_z^i$. Compliance matrix $[A^i]$ is a $3 \times 3$ diagonal matrix.

**FMC Laminate** - To obtain the stress and strain in the FMC layer, Lekhnitskii's solution is used for tubes with cylindrical anisotropy under axial loads and internal end external pressures [76]. The fibers in the FMC tube are wound in both directions. So it has orthotropic properties. Thus, the compliance matrix $A^F = [a_{ij}]_{6\times6}$ consists of 12 non-zero elements $\{a_{ij} : i = 1..3, j = 1..3\}, a_{44}, a_{55}, a_{66}$ and 24 zeros [76]. The matlab code for calculating the compliance matrix is in Appendix A. The FMC is stressed by the internal pressure $P_1$ and the axial force $F_2$ as follows

$$\begin{aligned}
\sigma_r^F &= S_1 P_1 r^{k-1} - S_2 P_1 r^{-k-1} + CX(1 + C_1 r^{k-1} + C_2 r^{-k-1}), \\
\sigma_\theta^F &= S_1 P_1 k r^{k-1} + S_2 P_1 k r^{-k-1} + CX(1 + C_1 k r^{k-1} - C_2 k r^{-k-1}), \\
\sigma_z^F &= C - \frac{1}{a_{33}} \left( a_{13}\sigma_r^F + a_{23}\sigma_\theta^F \right), \qquad (3.2)
\end{aligned}$$

where

$$\begin{aligned}
X &= \frac{(a_{13} - a_{23})\beta_{44}}{\beta_{22}\beta_{44} - \beta_{24}^2 - \beta_{11}\beta_{44} + \beta_{14}^2}, \\
S_1 &= \frac{r_1^{k+1}}{r_2^{2k} - r_1^{2k}},\ S_2 = S_1 r_2^{k+1} r_1^{k+1}, \\
C_1 &= -\frac{r_2^{k+1} - r_1^{k+1}}{r_2^{2k} - r_1^{2k}},\ C_2 = C_1 r_2^{k+1} r_1^{k+1}, \\
k &= \sqrt{\frac{\beta_{11}}{\beta_{22}}},\ \text{where, } \beta_{ij} = a_{ij} - \frac{a_{i3}^2}{a_{33}}
\end{aligned}$$

with, $r_1$ and $r_2$ equal to the inner and outer radii of the laminate, respectively. The

variable $C$ is obtained from the force balance in the axial direction,

$$\int_{r_1}^{r_2} \left(r\sigma_z^F\right) dr = F_2. \tag{3.3}$$

The strains $\varepsilon_r^F, \varepsilon_\theta^F$ and $\varepsilon_z^F$ are again determined using the compliance matrix of Hooke's law, $\{\varepsilon^F\} = [A^F]\{\sigma^F\}$.

**FMC Laminate + Inner Liner** - From the total axial force balance, the stresses and strains are found in terms of the external force $F$ and fluid pressure $P$. Therefore, the total strain energy of the FMC laminate and inner liner is derived by integration over the volume of both sections.

$$\begin{aligned} U_{FMC} &= \iiint \left( \sum_{j=r,\theta,z} \sigma_j^i \varepsilon_j^i \right) dV^i + \iiint \left(\sigma_j^F \varepsilon_j^F\right) dV^F \\ &= a_1 P^2 + a_2 PF + a_3 F^2, \end{aligned} \tag{3.4}$$

where, $a_1, a_2$ and $a_3$ are complicated and lengthy constants in terms of the material properties, fiber angle, and tube geometry. The matlab code for calculating these constants is in Appendix B. Castigliano's second theorem [77] produces the relationships between the axial displacement, $x$, and volume change, $V$, and the loads, $P$ and $F$,

$$\frac{\partial U_{FMC}}{\partial F} = x, \ \frac{\partial U_{FMC}}{\partial P} = V. \tag{3.5}$$

Solution of Eq. (3.5) for the loads and substitution in Eq. (3.4) yields the structural strain energy

$$U_{FMC} = \frac{1}{\Delta}\left(a_1 x^2 - a_2 xV + a_3 V^2\right). \tag{3.6}$$

where,

$$\Delta = 4a_1a_3 - a_2^2.$$

**Fluid -** For the open valve case, the fluid is assumed not to contribute to the strain energy of the system. Pressure waves and fluid dynamics are neglected so the pressure is zero. Using Eqs. (3.4) and (3.5) the F$^2$MC acts as a spring with stiffness $K_o = \frac{1}{2a_3}$. When the valves are closed, however, the fluid volume remains fixed. Under axial loads the FMC wall tries to expand or contract but the fluid resists this volume change. Assuming a linearly compressible fluid results

$$V = -\frac{\pi r_0^2}{B}P. \tag{3.7}$$

where, $B$ is the bulk modulus. The higher the bulk modulus, the more the fluid resists volume change. The stored potential energy of the fluid is

$$U_w = \frac{BV_w^2}{2\pi r_0^2} = \frac{\pi r_0^2 P^2}{2B}. \tag{3.8}$$

Substitution of Eq. (3.7) into Eqs. (3.5), one finds the equivalent axial stiffness of the F$^2$MC tube in the closed-valve condition,

$$K_c = \frac{2a_1B + \pi r_0^2}{B\Delta + 2a_3\pi r_0^2}. \tag{3.9}$$

The stiffness ratio is derived as

$$R = \frac{K_c}{K_o} = \frac{4a_1a_3B + 2a_3\pi r_0^2}{B\Delta + 2a_3\pi r_0^2}. \tag{3.10}$$

## 3.2 Dynamic model of the F$^2$MC - mass system

### 3.2.1 Equations of motion

F$^2$MC tubes can be used as variable stiffness elements of many smart structures. Figure (3.2) shows the schematic diagram of a simple structure where the tube is connected to a mass, $m$. The variable orifice valve at the end of the F$^2$MC tube controls the fluid flow. The FMC wall is assumed to have negligible mass relative to the lumped mass at the end and that the fluid pressure is constant inside the tube. Thus, both the F$^2$MC structure and fluid dynamics are neglected.

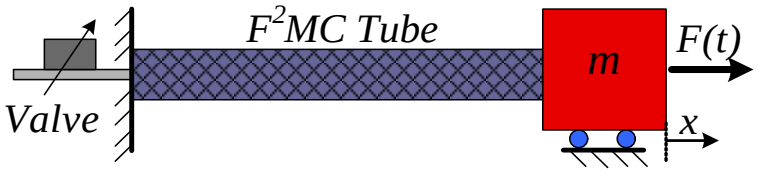


**Figure 3.2.** The schematic plot of the dynamic system. $F(t)$ is the external force and $x$ is the displacement of the mass.

Based on these assumptions, the kinetic energy

$$T = \frac{1}{2}m\dot{x}^2. \tag{3.11}$$

Substitution of Eqs. (3.6), (3.8) and (3.11) into Hamilton's principle yields.

$$m\ddot{x} + \frac{2a_1}{\Delta}x - \frac{a_2}{\Delta}V = F(t). \tag{3.12}$$

The volume dynamics come from conservation of mass over the fluid control volume,

$$\dot{V} = \dot{V_w} - Q. \tag{3.13}$$

where$V_w$ is the fluid volume change, and $Q$ is the fluid flow through the valve. Various models are available for the fluid flow through a valve or an orifice. The most common model in the literature, $Q = hC_d\sqrt{P}$, gives a good approximation for most applications [78]. $C_d$ is the valve constant and $h$ is the percentage of valve opening. This model, however, is not valid for small pressures, because the derivative of the flow with respect to pressure goes to infinity. Using a linear model avoids this problem. It will be shown that the pressure remains small during the operation justifying the use of the linear model,

$$Q = hC_dP. \tag{3.14}$$

Substitution of the Eqs. (3.7) and (3.14) into Eq. (3.13) yields

$$\dot{V} = \frac{1}{B\Delta + 2a_3\pi r_0^2}\left(a_2\pi r_0^2\dot{x} + hC_dB\left(a_2x - 2a_3V\right)\right). \tag{3.15}$$

Equations (3.12) and (3.15) are a 3rd order state space model of the $F^2MC$ with valve control, where the axial displacement, velocity and volume change are the states.

The control input for this system is the valve flow parameter $h$ which goes from 0 in closed-valve to 1 in open-valve.

### 3.2.2 Reduced-order dynamics

Figure (3.3) shows the root-locus plot of the system as $h$ varies from 0 to 1 for two stiffness ratios. The stiffness ratio $R$ can be observed from this plot by dividing the square of the branches crossing the imaginary axis. In addition, it provides an understanding about the dynamic behavior of the system due to valve variations. In the closed-valve case, 2 poles lie on the imaginary axis and one pole appears on the origin which means the system can be reduced to second-order. On the other hand, there are 2 poles on the imaginary and one pole on the negative real axis in the open-valve scenario. The negative real pole introduces damping which translates as the energy dissipation in the valve. When the valve is gradually opened, this pole moves away from the origin reducing its effects on the dynamics. Table 3.1 shows the parameters used in the root-locus analysis with fiber angles of 42 and 52 degrees corresponding to stiffness ratios of 15 and 4, respectively.

**Table 3.1.** $F^2MC$ parameters used in the model analysis.

| | Property | Value |
|---|---|---|
| FMC Lamina | $E_1$ | $115GPa$ |
| | $E_2$ | $1.5MPa$ |
| | $G_{12}$ | $1.5GPa$ |
| | $\nu_{12}, \nu_{13}$ | 0.33 |
| | $\nu_{23}$ | 0.93 |
| Inner Liner | $E$ | $0.1GPa$ |
| | $\nu$ | 0.497 |
| Fluid | $B$ | $2.0GPa$ |
| Geometry | $r_0$ | $4.5mm$ |
| | $r_1$ | $5mm$ |
| | $r_2$ | $5.5mm$ |

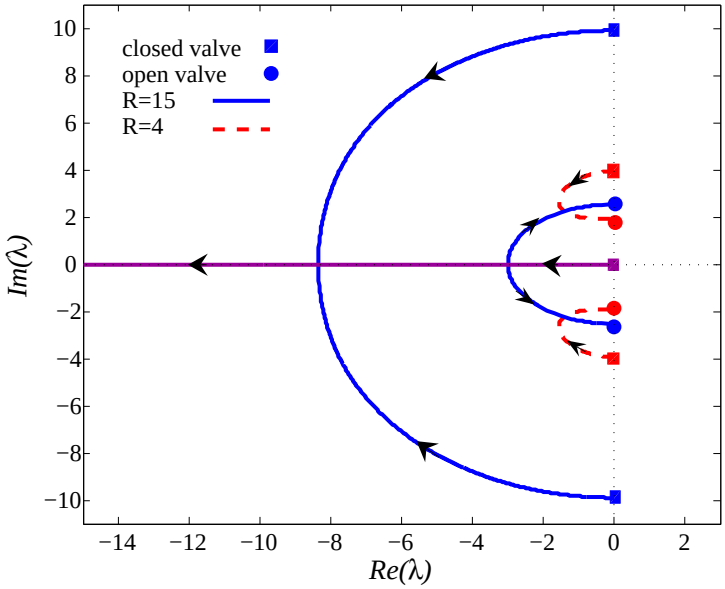


**Figure 3.3.** Root locus plot of the dynamic system for changes in valve position. The arrows show the direction of the poles movement when the valve is gradually opened. $\lambda$ respresents the eigenvalues of the system.

The root-locus analysis shows that if $C_d$ is sufficiently large, the volume dynamics in open-valve can be neglected. With a fast acting on/off valve (at least 10 times faster than the closed-valve dynamics), the dynamics can be switched between two states: fully open and fully closed valve.

**Open-valve Model -** In this case, the fluid is free to move in or out of the tube and the pressure is zero. A quasistatic solution in Eqs. (3.15) ($\dot{V} = \dot{x} = 0$) obtains

$$V = \frac{a_2}{2a_3}x \tag{3.16}$$

**Closed-valve Model -** In this case, $h = 0$ in Eq. (3.15) and

$$V = \frac{a_2\pi r_0^2}{B\Delta + 2a_3\pi r_0^2}(x - x_c) + \frac{a_2}{2a_3}x_c \tag{3.17}$$

where $x_c$ is the position at the time of switching from open to closed valve, simplified using Eq. (3.16).

Combining the equations obtained from the two cases, an equivalent second order equation is derived as

$$m\ddot{x} + K_c\left(1 - h\alpha\right)x = F(t) + K_c\alpha\left(1 - h\right)x_c, \tag{3.18}$$

where, parameter $\alpha$ is defined as

$$\alpha = 1 - \frac{1}{R}. \tag{3.19}$$

## 3.3 Switched stiffness for vibration control

Stiffness shaping involves the specification of the stiffness switching time history to ensure that system response decays to zero in minimum time. The stiffness is switched using an on-off valve that cycles between open and closed at predetermined times based on the assumed known initial condition, and model parameters. If the initial condition is not known, then the response must be sensed to determine a rate or position crossing to initialize the feedforward control sequence. If the model parameters are not known, then the performance will be degraded.

One way to shape the on-off stiffness trajectory is to switch between on-off using the Skyhook scheme [66] as follows

$$\begin{cases} \text{if } x.\dot{x} > 0 & \text{then } \ h = 0 \\ \text{if } x.\dot{x} \leq 0 & \text{then } \ h = 1 \end{cases}. \tag{3.20}$$

The phase portrait in Fig. (3.4) shows that valve opens when the mass is approaching zero and closes when it is moving away from the origin. As implemented in Eq. (4.13), this method requires position and velocity sensing. If the initial velocity is zero, the stiffness is simply cycled between low for $\tau = \frac{\pi}{2}\sqrt{\frac{m}{K_o}}$ and high for $\tau = \frac{\pi}{2}\sqrt{\frac{m}{K_c}}$. The rate of approach to the origin increases for higher stiffness ratios. Figure (3.4) shows that the response decays asymptotically as $t \to \infty$.

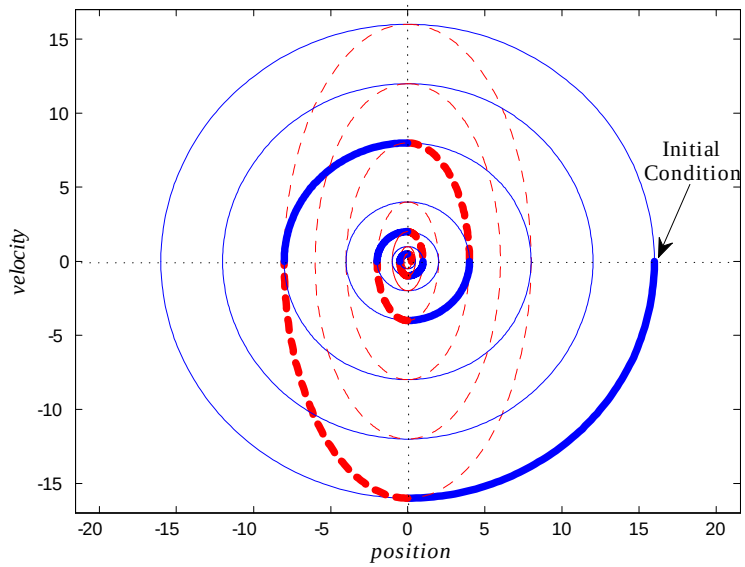


**Figure 3.4.** The phase portrait of a typical skyhook control method. The solid and dashed lines are open-valve and closed-valve trajectories, respectivly.

In $F^2MC$ tubes, the energy is conserved between any two consecutive switches and the energy drops during the switch to open. With a closed valve, the pressure increases as the mass moves away from the origin. The FMC wall is squeezed in response to this pressure and stores strain energy. When the valve opens, this stored energy dissipates suddenly in the form of fluid flow through the orifice.

One of the characteristics of $F^2MC$ structures is the ability to shift the equilibrium state using the second term on the right hand side of Eq. (3.18). For the open-valve

case, $h = 1$, and this term vanishes, so open-valve trajectories oscillate around the origin. Closed-valve trajectories, on the other hand, can be shifted by switching at nonzero positions.

By combining the input shaping concept and shifting properties of $F^2MC$ structures, the switching times is shaped in a way that a closed-valve trajectory passes through the origin. This has the potential to bring the response to zero in finite time. Based on the reduced-order Eq. (3.18), closed-valve trajectories that pass through the origin have the following homoclinic orbits

$$\left(\frac{\dot{x}}{\omega_c}\right)^2 + (x - \alpha x_c)^2 = (\alpha x_c)^2 , \tag{3.21}$$

where, $\omega_c = \sqrt{K/m}$ and $\omega_o = \sqrt{K(1-\alpha)/m}$ are defined as closed and open-valve frequencies, respectively. If the valve is switched to closed at

$$\dot{x}_c = \pm \omega_c x_c \sqrt{2\alpha - 1}, \tag{3.22}$$

then the orbits in Eq. (3.21) intersects the origin. Switching to an open valve when $x = 0$ brings the system to rest with zero residual vibration.

Figure (3.5) clarifies this control method. The initial condition is not necessarily on the desired closed-valve trajectories in (3.21). However, if the initial velocity is zero, an open valve trajectory brings the states to the crossing point of a branch of Eq. (3.22). Since this point lies on trajectories (3.21), switching to a closed valve at this point guarantees vibration suppression in finite time. To stop the motion at the origin, the

valve is switched back to open. This controller suppresses the vibration in finite time and is called Zero-Vibration (ZV) Stiffness Shaper to follow the convention used in IST.

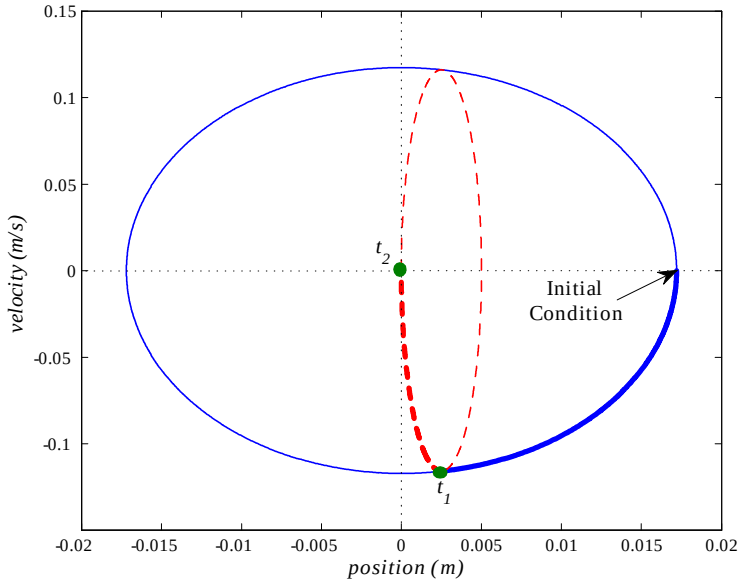


**Figure 3.5.** Phase plane plot of zero-vibration stiffness shaping technique. $t_1$ and $t_2$ are the times to close and open the valve, respectively. Bold lines are the controlled trajectories and normal lines are trjectories without swithings.

As with IST, Stiffness Shaping requires precalculation of the time delays. The first switching time is derived using the solution to Eq. (3.18) with $h = 1$ and initial and final conditions of $(x_0, 0)$ and $(x_c, \dot{x}_c)$, respectively. The second time delay is obtained by solving Eq. (3.18) with $h = 0$ and initial and final conditions of $(x_c, \dot{x}_c)$ and $(0, 0)$, respectively. Consequently, the control law is

$$\begin{cases} t_0 = 0 & \text{Start with open-valve} \\ t_1 = \frac{1}{\omega_0} \arccos\left(\sqrt{\frac{1}{\alpha} - 1}\right) & \text{Switch to closed-valve} \\ t_2 = t_1 + \frac{1}{\omega_c} \arccos\left(1 - \frac{1}{\alpha}\right) & \text{Switch to open-valve} \end{cases} \tag{3.23}$$

The time delays in Eq. (3.23) are independent of initial position but require zero initial velocity.

Figure (3.6) compares the results of Skyhook method with the new ZV Stiffness Shaping technique using the full order model Eqs. (3.12) and (3.15). The stiffness shaping trajectory stops at zero in finite time with less than 0.81% residual vibration.

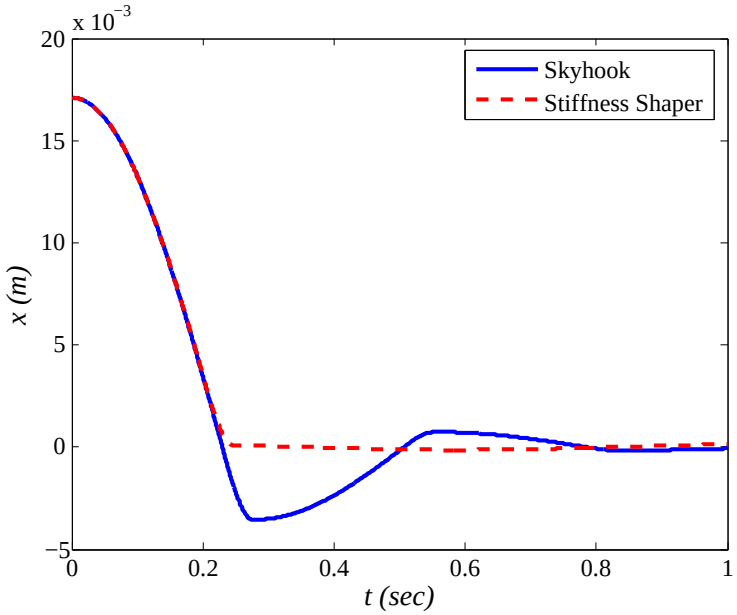


**Figure 3.6.** Comparison of skyhook (solid) and ZV stiffness shaping (dashed) techniques.

Note that the time delays exist if the argument of the square root function inside the inverse cosine in Eq. (3.23) is positive and less than 1. Therefore, the existence criteria for ZV Stiffness Shapers is:

$$\frac{1}{2} \leq \alpha < 1 \qquad \text{or} \qquad 2 \leq R. \tag{3.24}$$

and the solution exists for all the variable stiffness systems with stiffness ratios greater than or equal to 2.

Chapter 4

# Passive and Switched Stiffness Vibration Controllers Using Fluidic Flexible Matrix Composites

In the previous chapter, a feedforward ZV stiffness shaper is developed for an F$^2$MC-mass system. This chapter extends this work by introducing a novel ZV feedback control law. The optimal valve flow coefficient for passive, ZV, and Skyhook control is calculated based on the ITAE performance index. The performance of these controllers are compared for impulse and step loads. Finally, the experimental results validate the theory.

## 4.1 F$^2$MC equations of motion

Following the dynamics modeling section in chapter 3, the equations of motion for the F$^2$MC-mass system is derived using Hamilton's principle and conservation of mass.

$$m\ddot{x} + \frac{2a_1}{\Delta}x - \frac{a_2}{\Delta}V = F(t), \tag{4.1}$$

$$\dot{V} = \frac{1}{B\Delta + 2a_3\pi r_0^2 L}\left(a_2\pi r_0^2 L\dot{x} + hc_d B\left(a_2 x - 2a_3 V\right)\right). \tag{4.2}$$

where $F(t)$ is the applied load and $a_1, a_2$, and $a_3$ are complicated and lengthy constants in terms of the material properties, fiber angle, and tube geometry. $B$ is the bulk modulus of the fluid, and $r_0$ and $L$ are the inner radius and length of the tube and $\Delta = 4a_1a_3 - a_2^2$.

Equations (4.1) and (5.4) are a 3rd-order model of the F$^2$MC-mass system with valve control. The control input for this system is the valve flow parameter $h$ which goes from 0 for a closed valve to 1 for an open valve.

## 4.2 Stability analysis

Before introducing the control laws for the F$^2$MC-mass system, the stability of the unforced dynamic system is studied. The Lyapunov functional is defined as the total energy of the system.

$$E = T + U_{F+L} + U_w > 0. \tag{4.3}$$

Substituting the equations of motion (3.8), (4.1), and (5.4) into the time derivative of the Lyapunov functional results

$$\begin{aligned}\dot{E} &= \dot{x}\left(\frac{2a_1}{\Delta}x + \frac{a_2}{\Delta}V\right) + \frac{\pi r_0^2 LP\dot{P}}{B} + \\ &\quad \frac{1}{\Delta}\left(2a_1 x\dot{x} - a_2\dot{x}V + \dot{V}\left(2a_3V - a_2x\right)\right) \\ &= -hc_d\left(\frac{2a_3V - a_2x}{\Delta}\right)^2 \leq 0.\end{aligned} \tag{4.4}$$

which guarantees the stability of the unforced system for any time-varying valve opening ($h > 0$).

## 4.3 Nondimensionalized equations of motion

In order to reduce the number of variables involved in the F$^2$MC-mass analysis, the nondimensional variables are defined as

$$y = 2\sqrt{-\frac{a_3}{a_2}}x, \quad w = \sqrt{-\frac{a_2 a_3}{a_1^2}}V, \quad \tau = t\sqrt{\frac{2a_1}{m\Delta}}, \quad \widetilde{F} = \frac{F\Delta}{a_1}\sqrt{-\frac{a_3}{a_2}}. \tag{4.5}$$

Substitution in Eqs. (4.1) and (5.4) produces

$$\begin{aligned} \ddot{y} &= -y + w + \widetilde{F}(\tau), \\ \dot{w} &= (1 - K_c)\dot{y} + hC_d\left((1 - K_o)y - w\right), \end{aligned} \tag{4.6}$$

where the nondimensional closed-valve and open-valve stiffnesses and equivalent flow coefficient of the valve are

$$\begin{aligned} K_c &= 1 - \frac{a_2^2 \pi r_0^2 L}{2a_1\left(B\Delta + 2a_3\pi r_0^2 L\right)}, \\ K_o &= \frac{\Delta}{4a_1 a_3}, \\ C_d &= \frac{2a_3 B c_d}{\left(B\Delta + 2a_3\pi r_0^2 L\right)\sqrt{2a_1/m\Delta}}, \end{aligned} \tag{4.7}$$

respectively.

## 4.4 Reduced-order dynamics

In the nondimensional equations of motion (4.6), the fluid dynamics appear in the second equation with the time constant $hC_d$. The third-order model can be reduced to a second order model if the fluid and valve dynamics are sufficiently fast.

**Open-Valve Model -** In this case, the fluid is free to move in or out of the tube, and no pressure is generated if the valve opening is sufficiently large. For $C_d \to \infty$, Eq. (4.6) reduces to

$$w = -(1 - K_o)y. \tag{4.8}$$

**Closed-Valve Model -** In this case, $h = 0$ and the nondimensional volume change is found by integration of Eq. (4.6) to be

$$w = (K_c - 1)y + C. \tag{4.9}$$

The volume and displacement are continuous at the switching time, so the constant $C$ can be determined from

$$w^- = -(1 - K_o)y_c = w^+ = (K_c - 1)y_c + C, \tag{4.10}$$

where $w^-$ and $w^+$ are the volumes before and after the switch, $y_c$ is the position at the switch, and $C$ is an integration constant. Solving Eq. (4.10) for $C$ and substituting into (4.9) gives the closed valve volume change

$$w = (K_c - 1)(y - y_c) - (1 - K_o)y_c. \tag{4.11}$$

Combining Eqs. (4.6), (4.8), and (4.11), results an equivalent second order equation,

$$\ddot{y} + (K_c\,(1-h) + K_o h)\,y = (K_c - K_o)(1-h)y_c + \widetilde{F}(\tau). \tag{4.12}$$

Equation (4.12) is a second-order dynamic system that switches between high and low frequency when the valve opening, $h$, switches 0 and 1.

## 4.5 Passive and semi-active vibration control

### 4.5.1 Optimal passive control

For passive damping, one can use root-locus analysis to find the optimal fixed orifice opening. Figure 4.1 shows the location of the poles for an example $F^2$MC-mass system described by Eqs. (4.6) with nondimensional parameters $K_c = 1$ and $K_o = 0.35$ as the orifice varies from closed to fully open. The closed valve system has 2 poles on the imaginary axis and one at the origin as expected from the reduced order model in Eq. (4.12). As the valve opens more, damping increases. The minimum settling time (ST) occurs where the imeginary part of the complex poles is minimum, corresponding to an optimal orifice with $C_d = 1.1$. With a large orifice, one of the poles moves away from the origin and the 2 other poles approach the imaginary axis.

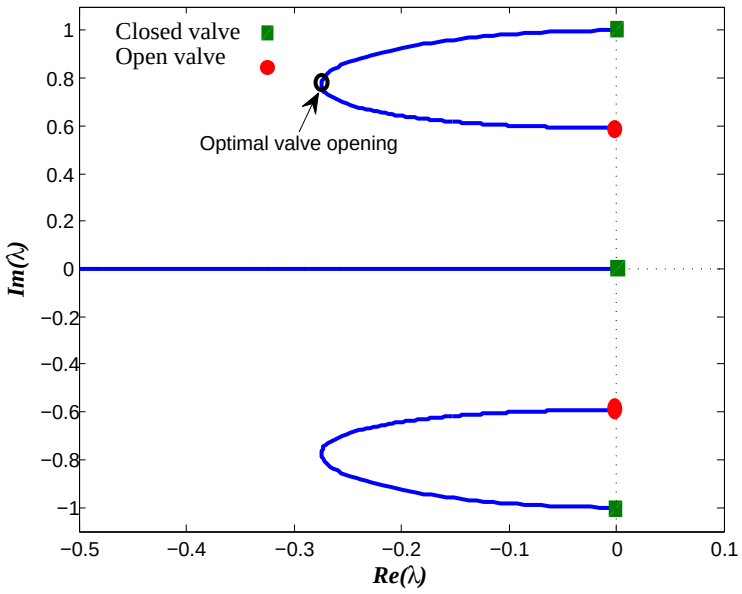


**Figure 4.1.** Root Locus analysis of an example F$^2$MC-mass system for changes in valve opening.

### 4.5.2 Skyhook control approach

The Skyhook scheme [66] is

$$\begin{cases} \text{if } y\dot{y} > 0 & \text{then } \ h = 0. \\ \text{if } y\dot{y} \leq 0 & \text{then } \ h = 1. \end{cases} \tag{4.13}$$

The phase portrait in Fig. 4.2 shows that the valve opens when the position moves toward zero and closes when the position moves away from zero. With a closed valve, the pressure increases as the mass moves away from zero. The FMC wall is squeezed in response to this pressure and stores strain energy. When the valve opens, this stored energy dissipates suddenly in the form of fluid flow through the orifice.

Due to the fully open and closed valve assumption in the reduced order model (4.12), the energy is conserved between any two consecutive switches and drops only during the

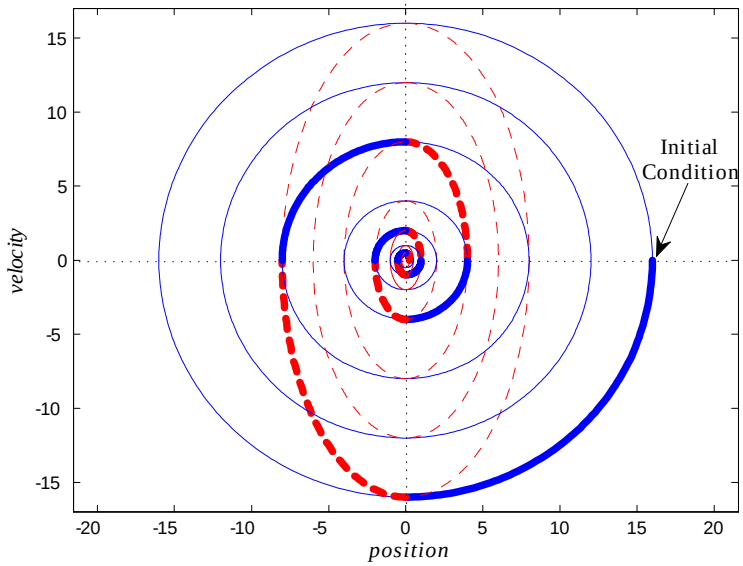


**Figure 4.2.** Phase portrait of the example F$^2$MC-mass system under Skyhook control: Open valve (solid) and closed valve (dashed) trajectories. Solid circles are the switching points. The thin lines indicate continuously open or closed valve trajectories and the heavy lines are the response under skyhook control.

switch opening. In order to optimize the performance of the Skyhook controller, the ITAE performance index is defined as

$$J = \int_0^{\tau} |y - y_{desired}| \, \tau d\tau \tag{4.14}$$

to find the optimal, open valve flow coefficient $C_d$.

### 4.5.3 Zero vibration (ZV) control approach

One of the characteristics of F$^2$MC structures and other switched stiffness systems is their ability to shift the equilibrium state using the first term on the right hand side of Eq. (4.12). For the open-valve case, $h = 1$, this term vanishes, so open-valve trajectories oscillate around the origin. Closed-valve trajectories, on the other hand, can be shifted

by switching at non-zero positions. This characteristic has the potential to bring the response to zero in a finite time. Based on the reduced-order Eq. (4.12), closed-valve trajectories that pass through the origin have the following homoclinic orbits

$$\frac{\dot{y}^2}{K_c} + \left( y - \left( 1 - \frac{K_o}{K_c} \right) y_c \right)^2 = \left( 1 - \frac{K_o}{K_c} \right)^2 y_c^2, \tag{4.15}$$

Eq. (4.15) is used to define the closed valve condition

$$\dot{y}_c = \pm y_c \sqrt{K_c - 2K_o}, \tag{4.16}$$

The switching line defined by Eq. (4.16) determines when to close the valve. Opening the valve when the closed valve trajectory intersects the origin brings the system to rest with zero residual vibration. Therefore, the ZV controller is defined

$$\begin{cases} \left| \dot{y} \right| > |y| \sqrt{K_c - 2K_o} & \text{then} \quad h = 0 \\ \\ \left| \dot{y} \right| \leq |y| \sqrt{K_c - 2K_o} & \text{then} \quad h = 1 \end{cases} \tag{4.17}$$

The control law (4.17) is realizable if the argument of the square root in Eq. (4.16) is positive. Therefore, the existence criteria for ZV control is

$$\frac{K_c}{K_o} \geq 2, \tag{4.18}$$

meaning that the $F^2MC$ tube should have a stiffness ratio greater than or equal to 2.

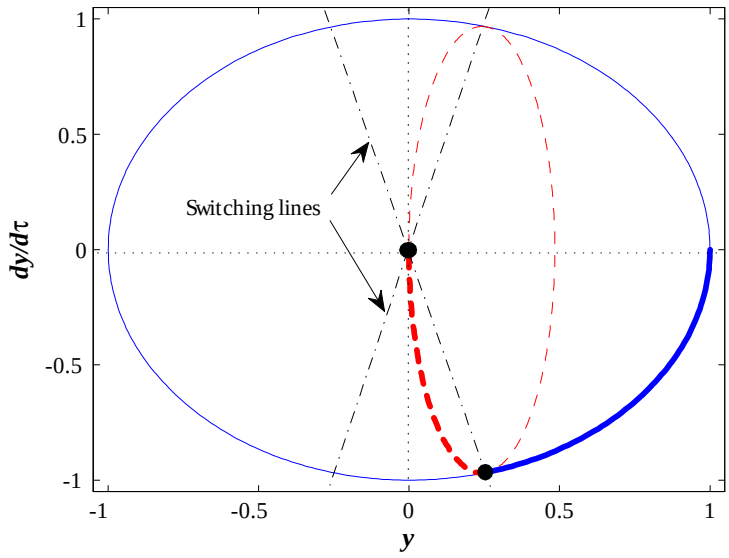


**Figure 4.3.** Phase portrait of the example F$^2$MC-mass system under ZV control: Open valve (solid) and closed valve (dashed) trajectories. Solid circles are the switching points. The thin lines indicate continuously open or closed valve trajectories and the heavy lines are the response under ZV control.

Figure 4.3 shows the ZV controlled response from an initial condition $y(0) = 1$, $\dot{y}(0) = 0$. The system starts out with an open valve that closes when the trajectory crosses the switching line (4.16). The valve then opens again at the origin, bringing the system to rest with zero vibration. As with Skyhook control, the flow coefficient, $C_d$, is optimized using the performance index (4.14).

### 4.5.4 Simulations and discussion

Simulation of the impulse and step responses for an example F$^2$MC-mass system with the nondimensional parameters $K_c = 1$ and $K_o = 0.35$ compares the performance of the passive, Skyhook, and ZV controllers. Under state-switch control the linear Eqs. (4.6) become nonlinear, so the optimal flow coefficients cannot be derived using root locus as with the passive case. Therefore, the performance index is calculated using the

simulation of the system for a range of flow coefficients .

Figure 4.4 shows the performance indices for impulse and step responses using Skyhook, ZV, and passive controllers. The ITAE index is calculated based on nondimensional time of $\tau = 30$. The figures show that $F^2MC$ tubes with a fixed orifice (passive case) can provide significant damping. As predicted by root locus analysis, the optimal $C_d = 1.1$ provides a damping ratio of 0.35. The state switch controllers perform better under impulse inputs than step inputs, with the Skyhook yielding a minimum $J = 15.8$ at $C_d = 2.2$ and the ZV controller approaching to the minimum value of 10.4 asymptotically as $C_d$ increases. The impulse response of the ZV controller with $C_d = 10$ outperforms Skyhook and optimal passive controllers by 34.2% and 32.9%, respectively. The step input changes the equilibrium by an unknown amount but the switching lines for both semi-active controllers are based at the origin. Thus, switches may not occur because the response orbits around the non-zero equilibrium. The open valve orifice opening ($C_d$) can be optimized, however, to improve the step response. Figure 4.4(b) shows that the Skyhook technique is not as good at suppressing the step response. The ZV controller has a minimum value of $J = 11.5$ at $C_d = 1.2$, 60% and 34.7% lower than the optimal Skyhook and passive controllers, respectively.

The optimal time response of the controllers for impulse and step inputs are shown in Figs. 4.5 and 4.6. The settling time for impulse loads is defined as the time when the response becomes less than 2% of the maximum uncontrolled closed valve response. The settling time for a step input is defined as the time elapsed when the response remains within 2% of the equilibrium position. Table 4.1 summarizes the simulation results for the three controllers under impulse and step inputs. Figure 4.5 shows that

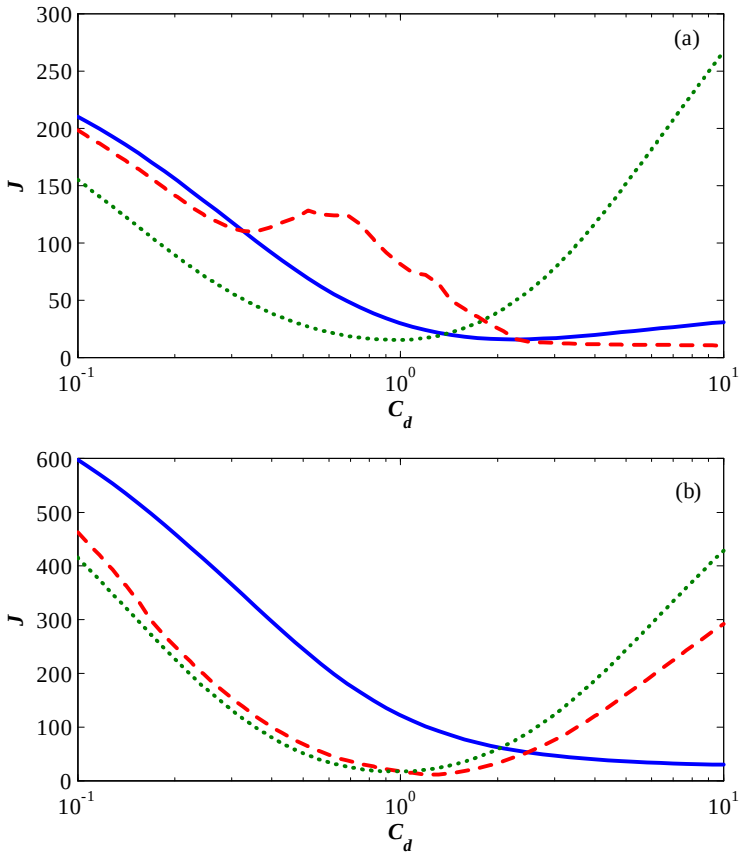


**Figure 4.4.** The ITAE performance index versus flow coefficient: impulse (a) and Step (b) responses using Skyhook (solid), ZV (dashed), and optimal passive (dotted) controllers.

the ZV controller achieves 3.3 and 2.8 times faster settling time in response to an impulse input than Skyhook and optimal passive controllers, respectively. Moreover, for a step input (Fig. 4.6), the ZV controller settling time is 2.5 times faster than the Skyhook technique. The optimal passive controller, however, is only slightly slower than the ZV controller.

**Sensitivity Analysis** - The stability analysis in section 2 proves that the transient response is stable regardless of the control law, so stability robustness is not an issue. The optimal ZV, Skyhook, and passive controllers, however, have a tuned valve coefficient that minimizes the ITAE as shown in Fig. 4.4. This figure can be used to assess

**Table 4.1.** Theoretical results.

| | Controller | ITAE | 2% settling time |
|---|---|---|---|
| Impulse | Optimal passive | 15.5 | 14.9 |
| | Skyhook | 15.8 | 17.9 |
| | ZV | 10.4 | 5.4 |
| Step | Optimal passive | 17.6 | 9.9 |
| | Skyhook | 28.8 | 10.9 |
| | ZV | 11.5 | 6.3 |

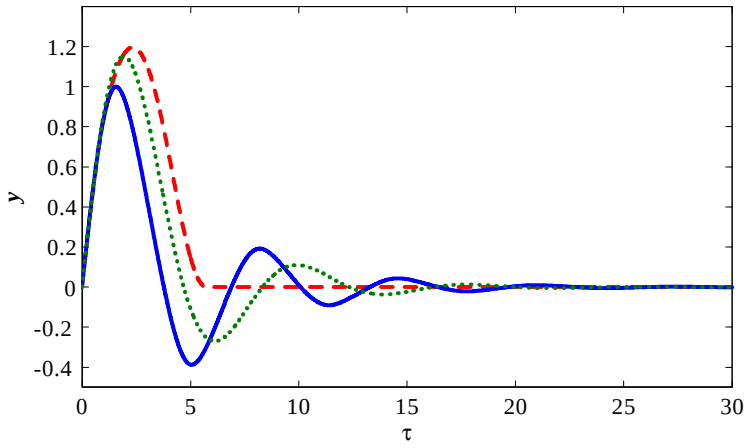


**Figure 4.5.** Impulse response of the example F$^2$MC-mass system with optimal Skyhook (solid), ZV (dashed), and passive (dotted) controllers.

the performance sensitivity of these three methods to changes in flow coefficient. The nondimensional model (4.6) also has the parameters $K_c$ and $K_o$, so it is instructive to analyze the performance sensitivity to variations in these parameters as well. For high bulk modulus fluids, $K_c \approx 1$, so only the response sensitivity to variations in $K_o$ is of interest. Figure 4.7 compares the performance robustness of the three controllers to changes in the nondimensional open valve stiffness for impulse and step responses. Neither the Skyhook nor passive controller are explicitly based on $K_o$. The performance of these systems does depend on the model parameters, specifically because $C_d$ is tuned for a specific $K_o$. The ZV controller explicitly depends on $K_o$ in Eq. (4.17), so we

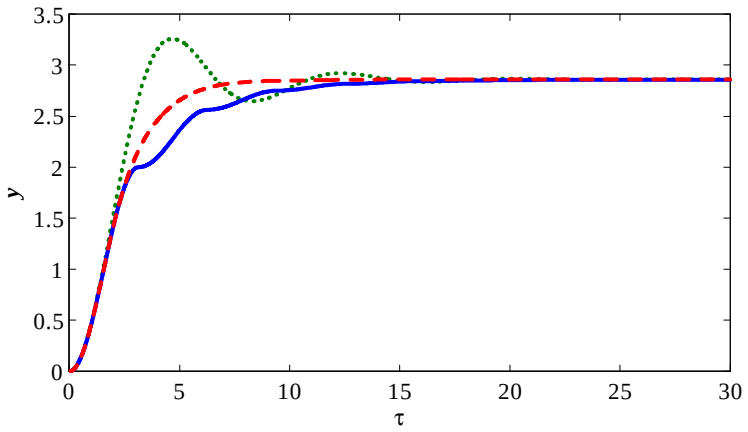


**Figure 4.6.** Step response of the example F$^2$MC-mass system with optimal Skyhook (solid), ZV (dashed), and passive (dotted) controllers.

expect more performance sensitivity to variations in $K_o$. The sensitivity curves in Fig. 4.7, however, show that the ZV controller has more and sometimes less performance sensitivity than passive and Skyhook controllers. For small positive changes in $K_o$, the ZV impulse response is the least sensitive. For negative changes in $K_o$, Skyhook and passive performance improves while ZV degrades. For step inputs, ZV sensitivity outperforms passive and Skyhook for small positive changes in $K_o$. For small negative changes in $K_o$, passive control is lease sensitive (performance improves) but ZV is better than Skyhook. The ZV controller remains a better approach than Skyhook technique for up to 17% and 19% stiffness changes under impulse and step forces, respectively.

## 4.6 Experimental validation

Figure 4.8 shows the test setup used to validate the theoretical results. The F$^2$MC tube consists of a 7.6$mm$ diameter and 1.6$mm$ thick soft rubber inner liner inside a Flexo 9.5$mm$ diameter $PET$ braided mesh sleeve. Pre-pressurization of the tube to

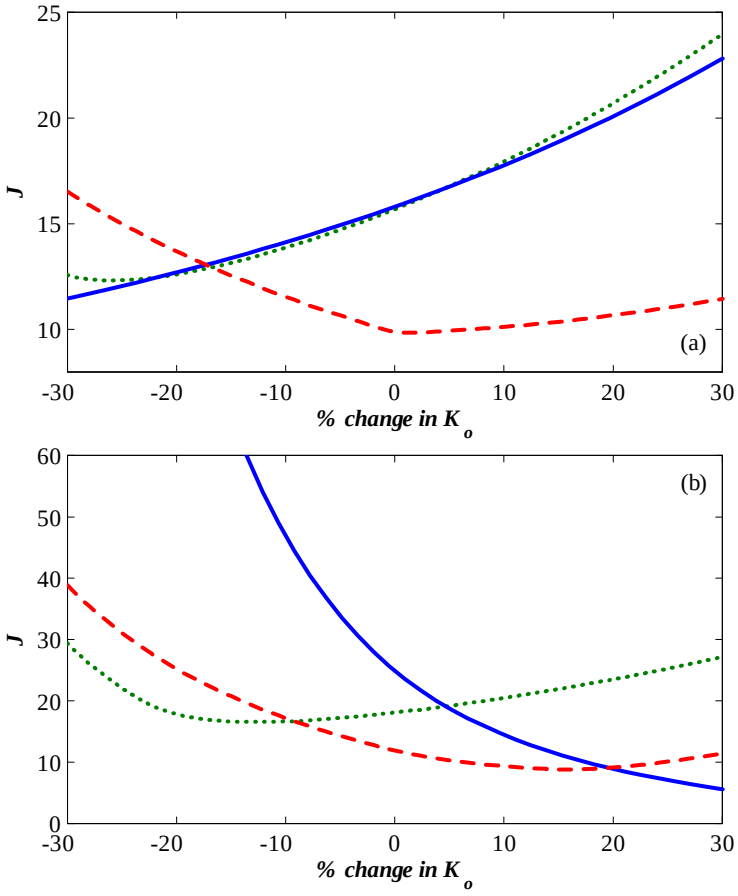


**Figure 4.7.** ITAE performance indices for Skyhook (solid), ZV (dashed), and optimal passive (dotted) controllers versus changes in $K_o$ : (a) impulse and (b) Step responses.

$27psi$ ensures that the fluid (water) does not experience negative pressures during the tests, guarantees tight coupling between the mesh and tube, and minimizes the effects of trapped air. Table 4.2 lists the material properties and other relevant parameters of the F$^2$MC-mass system.

One end of the F$^2$MC tube is attached to a solid frame. The other end is connected to a mass that is excited by a Ling LMT100 shaker. A high-speed Omega SV126 solenoid valve with a $5 - 14ms$ response time permits fluid to flow back and forth between the F$^2$MC tube and a $12.7mm$ diameter solid, clear tube that acts as pressurized air over wa-

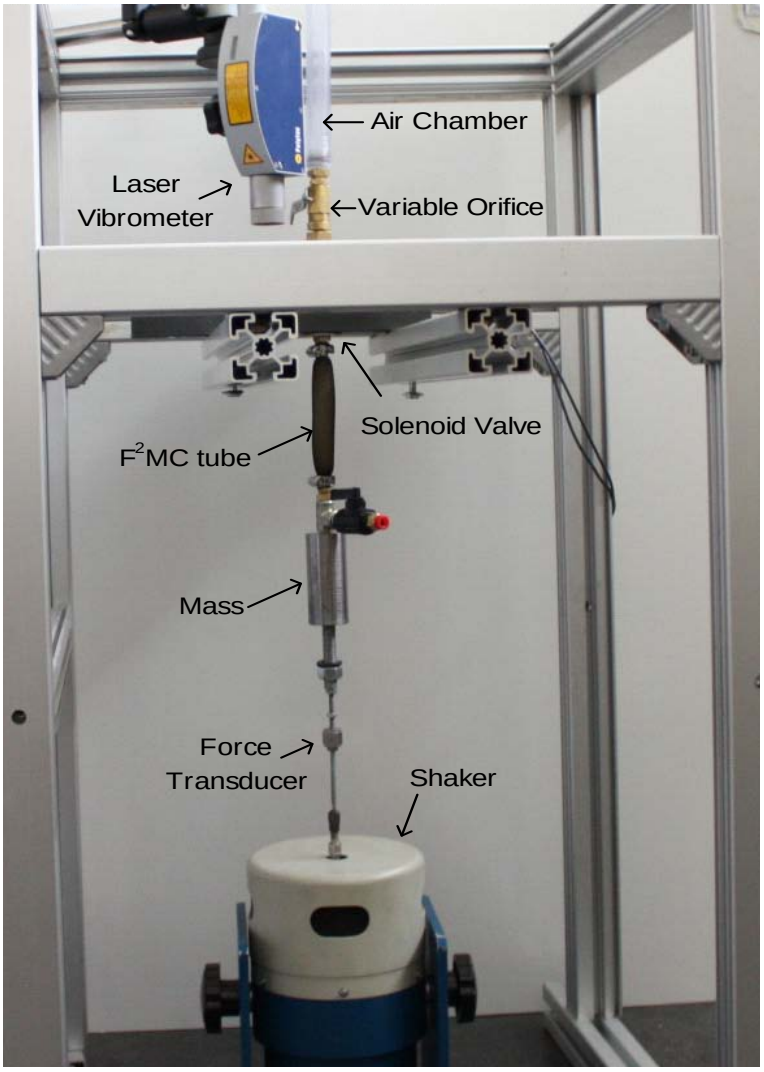


**Figure 4.8.** Experimental setup

ter accumulator. A PCB-208C02 PZT force transducer, with a sensitivity of $100mV/Kg$, inserted on the stinger that connects the mass and the shaker, measures the input force. A Polytec OFV5000 laser vibrometer measures the velocity and displacement of the mass with $125mm/s/V$ and $1.280mm/V$ sensitivities, respectively. A low-pass filter cleans the signals and a fast-tracking filter stabilizes the displacement signal. In addition, a second order low-pass filter with cut-off frequency of $300Hz$ is incorporated to avoid excessive

**Table 4.2.** Parameters of the experimental F$^2$MC-mass system.

| | Parameters | Values |
|---|---|---|
| FMC | $a_1$ | $9.0 \times 10^{-12} \frac{m^5}{N}$ |
| | $a_2$ | $-2.6 \times 10^{-8} \frac{m^3}{N}$ |
| | $a_3$ | $2.1 \times 10^{-5} \frac{m}{N}$ |
| | $L$ | $0.101m$ |
| | $r_0$ | $3.8mm$ |
| Fluid | $B$ | $2 \times 10^9 GPa$ |
| Valve | $c_d$ | $0.011 \frac{m^3}{hr.bar}$ |
| Mass | $m$ | $11.8kg$ |
| Nondimensional parameters | $K_c$ | 0.991 |
| | $K_o$ | 0.275 |
| | $C_d$ | $3.1 \times 10^8$ |

valve chatter. A dSpace data acquisition system generates control signals for the valve and the shaker in addition to capturing the signals from the force transducer and laser vibrometer.

To obtain the frequency response of the system, a chirp signal is sent to the shaker, ranging from $0 - 25Hz$, and then measure the response. As seen in Fig.4.9, the closed-valve frequency response has a single peak at $13Hz$. Since the effect of fluid dynamics is assumed to be negligible, the F$^2$MC tube is only partially filled with water. Thus, air, not water, flows through the valve. With this configuration, a single peak at $8Hz$ is observed for the open-valve frequency response. Figure 4.9 shows that the theoretical frequency responses for the open and closed-valve cases match the experimental peaks but the model lacks the structural damping. The small peak around $17Hz$ corresponds to a support structure mode.

**Optimal passive control -** The experimental results show that F$^2$MC tubes with a fixed orifice can provide substantial structural damping. The variable orifice is manually

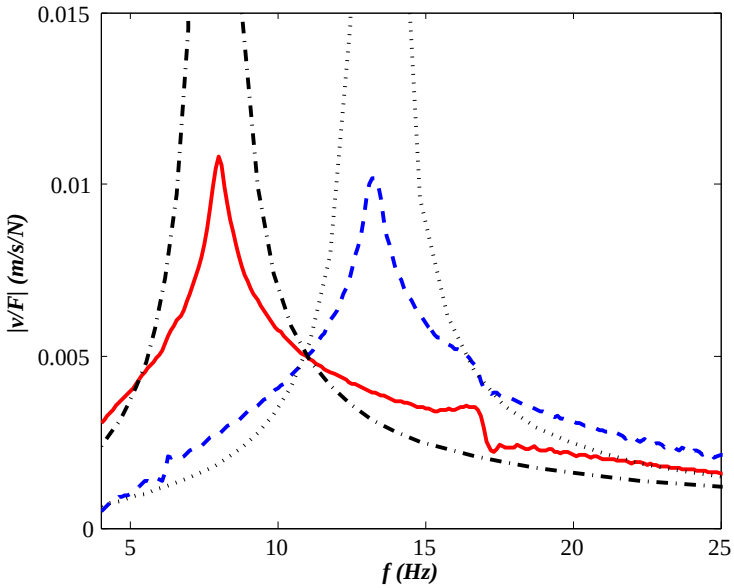


**Figure 4.9.** Frequency response of the velocity to the force for experimental open (solid) and closed (dashed) valve and theoretical open (dash-dotted) and closed (dotted) valve.

adjusted to maximize damping. Compared to the closed valve $\zeta = 0.09$, Figs. 4.10 and 4.11 show that optimal passive control increases damping to $\zeta = 0.20$ for step and impulse responses as measured by the log decrement method, an increase of 122%. Figures 4.10 and 4.11 show the improved impulse and step responses provided by passive F2MC damping relative to the closed valve case.

**Semi-Active Control -** Skyhook and ZV controllers provide semi-active vibration reduction using $F^2$MC tubes and an on/off valve. The ITAE and 8% settling time results for closed valve, passive, and semi-active control are tabulated in Table 4.3. The settling time criteria is increased to 8% (compared to 2% in the simulations) due to noise and unmodeled dynamics that cause residual oscillations in the response. Figures 4.10 and 4.11 show the experimental impulse and step responses for the four cases. The experiments corroborate the simulation results showing better performance for impulse

response than step response. For step response, the semi-active controllers do not significantly outperform the optimal passive control. ZV control does perform better than Skyhook or closed valve, settling almost twice as fast as Skyhook and three times faster than the closed valve case. The ZV impulse response settles twice as fast as optimal passive and Skyhook.

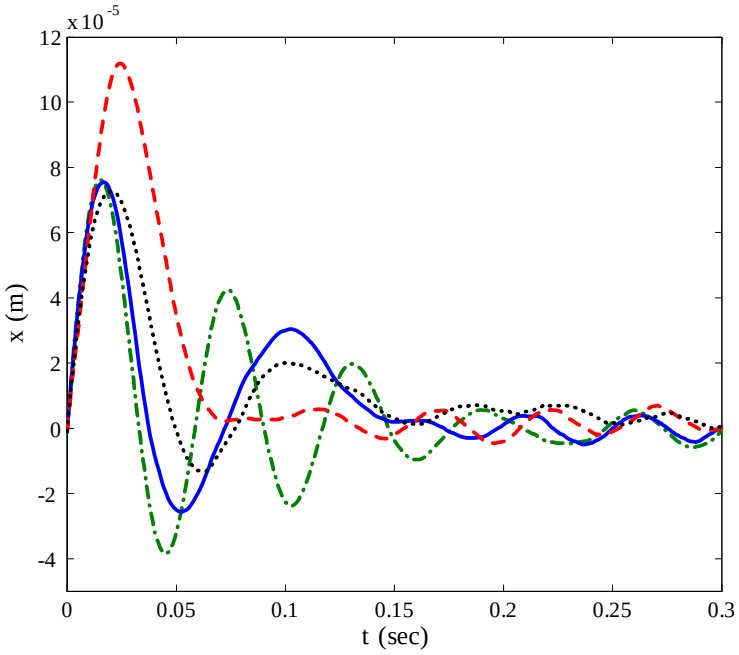


**Figure 4.10.** Experimental impulse response of the F$^2$MC-mass system for optimal passive (dotted), skyhook (solid), and ZV (dashed) controllers and the closed valve case (dash-dotted).

**Table 4.3.** Experimental results.

| | Controller | ITAE ($m.s$) | 8% ST ($s$) | ND ITAE | ND 8% ST |
|---|---|---|---|---|---|
| Impulse | Closed valve | $3.35 \times 10^{-7}$ | 165 | 0.26 | 19.25 |
| | Opt passive | $3.02 \times 10^{-7}$ | 139 | 0.24 | 16.21 |
| | Skyhook | $2.78 \times 10^{-7}$ | 133 | 0.22 | 15.51 |
| | ZV | $2.37 \times 10^{-7}$ | 62 | 0.19 | 7.23 |
| Step | Closed valve | $1.70 \times 10^{-6}$ | 346 | 1.33 | 40.36 |
| | Opt passive | $7.27 \times 10^{-7}$ | 119 | 0.57 | 13.88 |
| | Skyhook | $1.18 \times 10^{-6}$ | 191 | 0.93 | 22.28 |
| | ZV | $5.57 \times 10^{-7}$ | 111 | 0.44 | 12.95 |

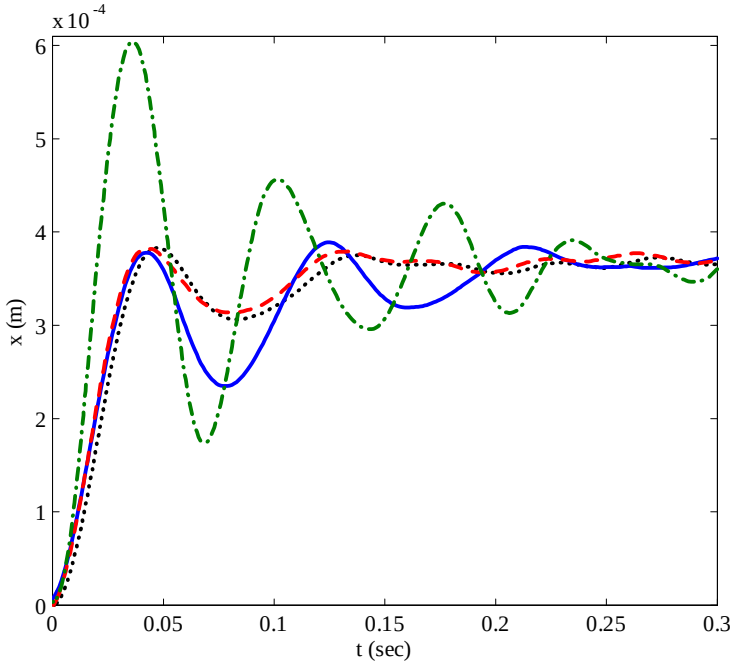


**Figure 4.11.** Experimental step response of the F$^2$MC-mass system for optimal passive (dotted), skyhook (solid), and ZV (dashed) controllers and the closed valve case (dash-dotted).

Chapter 5

# Fluidic Composite Tuned Vibration Absorbers

This Chapter investigates the application of $F^2MC$ tubes as TVAs by coupling them to a fluid port and a pressurized air chamber. A 3-D elasticity model for the tube and a lumped-mass model for the fluid results a $4^{th}$ order system with two poles and one zero. The vibration absorber frequency depends on the fluid port inertance, orifice flow coefficient and the material properties of the $F^2MC$ tube. The effects of these parameters on the isolation frequency are studied by simulating the frequency response and experimentally validating the performance.

## 5.1 $F^2MC$ modeling

$F^2MC$ tubes can be used as a TVA element in many structures. Figure 5.1 shows the schematic diagram of a simple structure where the tube is connected to a mass, $m$. The

tunable orifice at the end of the F$^2$MC tube controls the fluid flow into an air over water accumulator. A classic mechanical system analogy of the F$^2$MC TVA is shown in Fig. 5.1. The mass $m$ corresponds to the primary mass and the mass $m_f$ is related to the inertance of the fluid. The orifice effect appears as a damper, $c$, and the tube and air equivalent stiffnesses appear in $k_1, k_2$, and $k_3$. The objective of the F$^2$MC TVA is to reduce the response $x(t)$ to the applied force $F(t)$ at a specific frequency.

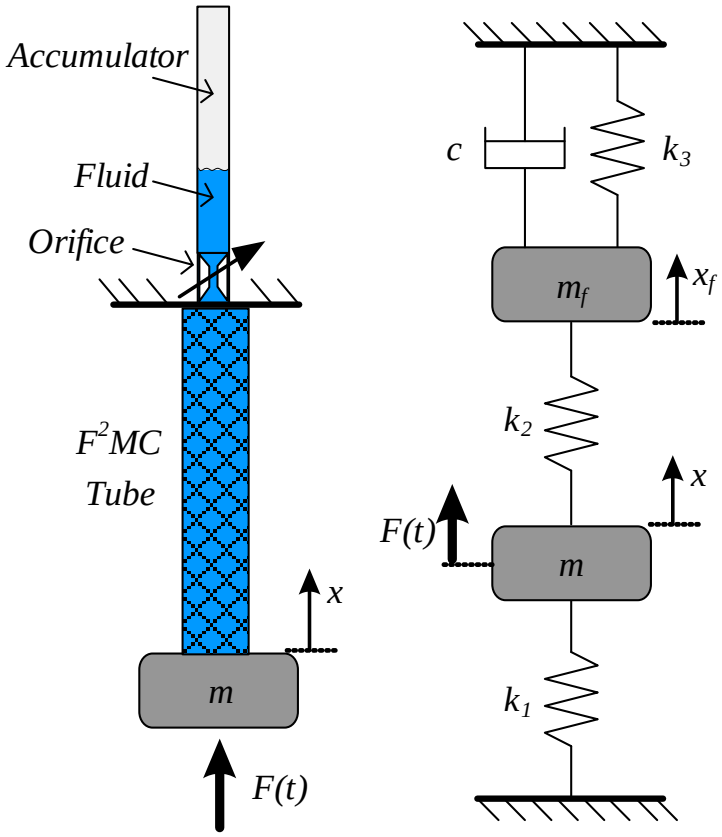


**Figure 5.1.** Schematic (left) and equivalent mechanical model (right) of the F$^2$MC-mass dynamic system.

Using Hamilton's principle, the equations of motion for mass, $m$, is obtained.

$$m\ddot{x} + \frac{2a_1}{\Delta}x - \frac{a_2}{\Delta}V = F(t). \tag{5.1}$$

where $F(t)$ is the applied load.

**Fluid Dynamics -** the fluid is assumed to be incompressible, so the tube volume change, $\dot{V} = -Q$, is equal to the fluid flow, $Q$, with positive flow from the F$^2$MC tube to the port. The pressure difference between the tube inner liner and the air chamber accelerates the fluid in the port. The flow resistance in the tube can be modeled assuming a laminar flow,

$$P - P_{air} = I\dot{Q} + \frac{Q}{c_d} = -I\ddot{V} - \frac{\dot{V}}{c_d}, \tag{5.2}$$

where, $I$ is the port inertance. For a circular tube, the inertance is $I = \frac{\rho l}{A}$ with $\rho, l$, and $A$ equal to the density, fluid length, and tube cross-sectional area, respectively. The pressure in the air chamber is assumed to be uniform and equal to the gauge pressure, $P_{air}$. $c_d$ is the flow coefficient of the orifice. The equivalent air stiffness is calculated using the ideal gas model $\widetilde{P}_{air}\widetilde{V}_{air} = nRT$. Superscripts $\tilde{}$ represent the absolute values. For small volume changes, this model is linearized to find the equivalent air stiffness.

$$k_{air} = \frac{P_{air}}{V_{air}} = -\frac{nRT}{V_i^2}, \tag{5.3}$$

where $V_{air}$ is the volume change of the air ($\dot{V_{air}} = -Q$) and $V_i$ is the initial air volume. The negative sign in Eq. (5.3) shows that increasing pressure contracts the air volume. By substituting Eq. (5.3) into Eq. (5.2), the fluid governing equation is derived,

$$I\ddot{V} + \frac{\dot{V}}{c_d} + (\frac{2a_3}{\Delta} - k_{air})V - \frac{a_2}{\Delta}x = 0. \tag{5.4}$$

The $4^{th}$ order F$^2$MC TVA Eqs. (5.1) and (5.4) are analogous to the classic mechanical

system in Fig. 5.1. If one defines $x_f = \hat{A}V$, where $\hat{A}$ is the accumulator cross-sectional area, the parameters in the mechanical system in Fig. 5.1 can be defined as

$$\begin{aligned} m_f &= I\hat{A}^2, c = \frac{\hat{A}}{c_d}, \\ k_1 &= \frac{2a_1 - \hat{A}a_2}{\Delta}, k_2 = \frac{\hat{A}a_2}{\Delta}, k_3 = \hat{A}\left(\frac{2a_3\hat{A} - a_2}{\Delta} - \hat{A}k_{air}\right). \end{aligned}$$

## 5.2 Tuned vibration absorption

The F$^2$MC-mass system represented by Eqs. (5.1) and (5.4) can be used as a TVA element. The transfer function of the velocity, $v$, to the external force, $F$ is derived as

$$\left|\frac{v(s)}{F(s)}\right| = \frac{s\left(Is^2 + \frac{1}{c_d}s + \frac{2a_3}{\Delta} - k_{air}\right)}{\left(Is^2 + \frac{1}{c_d}s + \frac{2a_3}{\Delta} - k_{air}\right)\left(ms^2 + \frac{2a_1}{\Delta}\right) - \frac{a_2^2}{\Delta^2}}. \tag{5.5}$$

The transfer function in Eq. (5.5) has four poles and two zeros. Vibration suppression occurs at the frequency where the numerator is zero or the zero frequency. This frequency depends on the port inertance, orifice flow coefficient, air equivalent stiffness, and tube parameters. For a sufficiently large air reservoir or small pressures, the effect of air stiffness is negligible.

Figure 5.2 shows the frequency response of the F$^2$MC-mass system for several port inertances. The baseline parameters used for simulation are in Table 5.1. Without fluid in the tube ($I = 0$), the frequency response has only one peak corresponding to the tube open-valve stiffness $K_o = \frac{1}{2a_3}$ [79]. As the port inertance is increased by either decreasing the port diameter or increasing the fluid level in the port, the second peak and a zero appear in the frequency response. As $I \to \infty$, the fluid inertia is much greater than

**Table 5.1.** Baseline parameters of the F$^2$MC-mass system.

| | Parameters | Values |
|---|---|---|
| FMC | $a_1$ | $9.0 \times 10^{-12} \frac{m^5}{N}$ |
| | $a_2$ | $-2.6 \times 10^{-8} \frac{m^3}{N}$ |
| | $a_3$ | $2.1 \times 10^{-5} \frac{m}{N}$ |
| | $L$ | $0.101m$ |
| | $r_0$ | $3.8mm$ |
| Orifice | $c_d$ | $0.011 \frac{m^3}{hr.bar}$ |
| Mass | $m$ | $11.8kg$ |
| Fluid Port | $\rho$ | $1000 \frac{kg}{m^3}$ |
| | $l$ | $17.8cm$ |
| | $A$ | $3.17 \times 10^{-6} m^2$ |
| Air | $V_i$ | $9.6 \times 10^{-5} m^3$ |
| | $k_{air}$ | $3 \times 10^9 \frac{N}{m^5}$ |
| | $\hat{A}$ | $1.2 \times 10^{-5} m^2$ |

the primary mass inertia and the response is similar to the closed-valve case. Figure 5.2 also shows the minimum amplitude envelope that can be obtained by varying the port inertance.

The flow coefficient $c_d$ introduces damping into the system. Figure 5.3 shows the frequency response of Eqs. (5.1) and (5.4) for different flow coefficients. When the resistance is very small ($Resistance = \frac{1}{c_d} \propto \frac{1}{orifice\ size}$), due to a large orifice with $c_d \rightarrow \infty$, there are two undamped peaks and one zero. As $c_d$ decreases (smaller orifice), the frequency response becomes more damped until the poles and zero disappear. Further decrease in the orifice size ($c_d \rightarrow 0$) prevents the fluid from flowing. In this case, Eqs. (5.1) and (5.4) reduce to a 2nd order system with closed-valve stiffness $K_c = \frac{2a_1}{\Delta}$, yielding the single peak in Fig. 5.3.

The frequency of isolation in a TVA is independent of the primary mass, making it robust to mass variations. Figure 5.4 shows the frequency response of the system

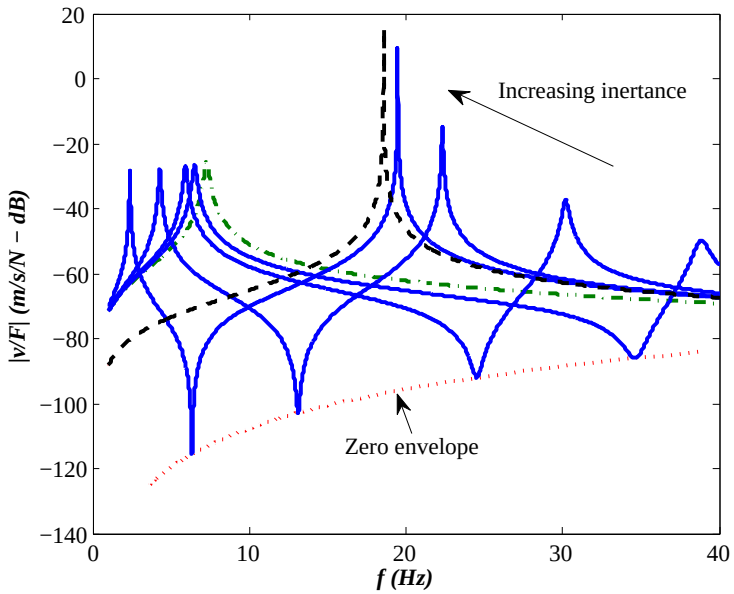


**Figure 5.2.** Magnitude of the velocity over force transfer function for parameters in Tab. 5.1 and $I = 0$ (dash-dotted), $8 \times 10^6, 1.6 \times 10^7, 5.6 \times 10^7, 2.4 \times 10^8$, and $\infty \frac{kg}{m^4}$ (dashed).

for variations in the primary mass. The frequency of the second peak decreases as the mass is increased, but the first peak and the zero do not shift. Thus, the F$^2$MC TVA is insensitive to the primary mass.

## 5.3 Experimental validation

Figure 5.5 shows the test setup used to validate the theoretical results. The F$^2$MC tube consists of a 7.6$mm$ diameter and 1.6$mm$ thick soft rubber liner inside a Flexo 9.5$mm$ diameter $PET$ braided mesh sleeve. Pre-pressurization of the tube to 28$psi$ ensures that the fluid (water) does not experience negative pressures during the tests, guarantees tight coupling between the mesh and the tube, and minimizes the effects of trapped air.

One end of the F$^2$MC tube is attached to a solid frame. The other end is connected to a mass that is excited by a Ling LMT100 shaker. A manual valve permits fluid to flow

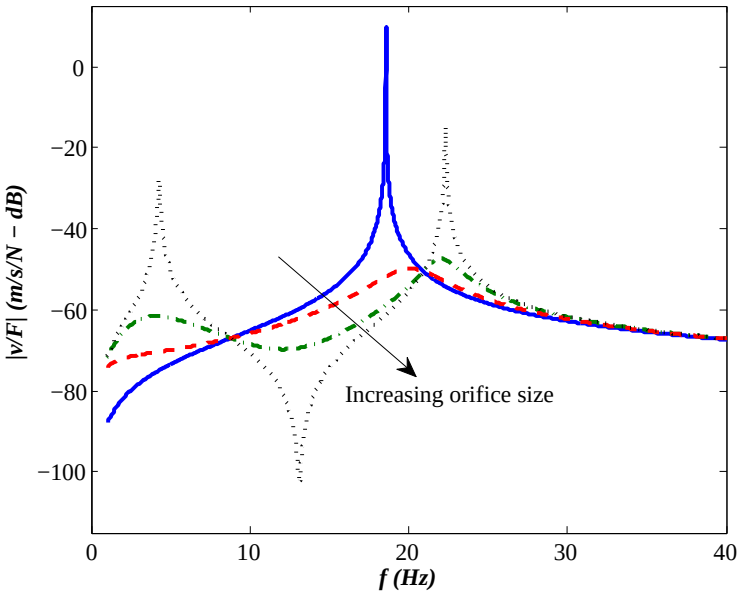


**Figure 5.3.** Magnitude of the velocity over force transfer function for $c_d = 0$ (solid), 0.040 (dashed), 0.132 (dash-dotted), and $6.588 \frac{m^3}{bar.hr}$ (dotted), and other parameters in Tab. 5.1.

back and forth between the F$^2$MC tube and a $4.3mm$ diameter clear tube that provides both inertance and a pressurized air over water accumulator. A PCB-208C02 PZT force transducer, with a sensitivity of $10mV/N$, inserted on the stinger that connects the mass and the shaker, measures the input force. A Polytec OFV5000 laser vibrometer measures the velocity of the mass with $25mm/s/V$ sensitivity. A low-pass filter reduces high frequency noise. A LabView data acquisition system generates control signals for the shaker in addition to capturing the signals from the force transducer and laser vibrometer.

To obtain the frequency response of the system, a chirp signal is sent to the shaker, ranging from $0-40Hz$, and then measure the response. To demonstrate the capability of the F$^2$MC TVA in shifting the isolation frequency by changing the port inertance, a small diameter clear tube is chosen so that a small change in the amount of water results in a noticeable shift in the water level and the port inertance. The boundary layer effects

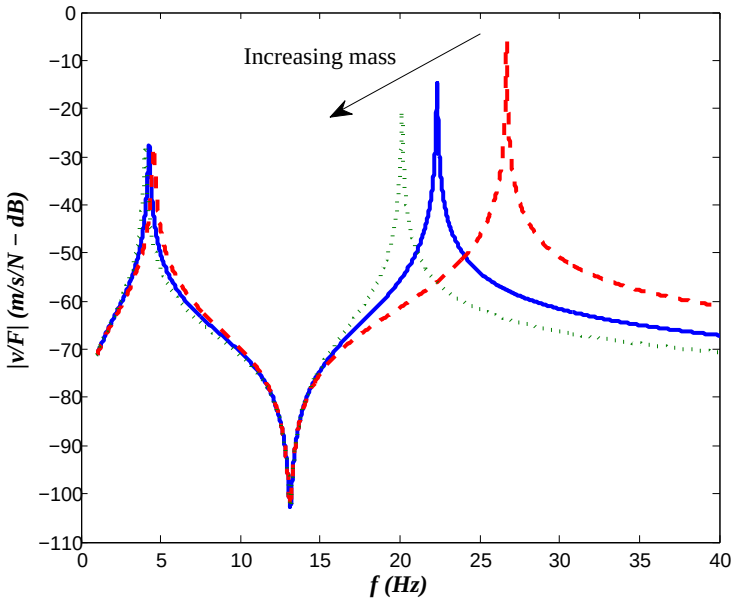


**Figure 5.4.** Magnitude of the velocity over force transfer function for $m = 7.2kg$ (dashed), $11.8kg$ (solid), and $16.3kg$ (dotted).

of the small diameter tube, however, reduce the effective cross-sectional area for the fluid flow. To calibrate the effective port cross-sectional area in the model, two tests are performed by setting the water level in the clear tube to $7.6cm$ and $11.4cm$. Then, the inertances are calculated in the model that match the experiment. Since the inertance depends linearly on the water level, the slope of the fitted line to these two points determines the effective cross-sectional area $A = 3.17 \times 10^{-6}m^2$. In addition, the zero crossing of the fitted line is very small, meaning that the inertance of the F$^2$MC tube is negligible compared to the port inertance. Figure 5.6 shows the frequency response of the F$^2$MC TVA with water levels of $7.6cm$, $17.8cm$, and $38.1cm$. The theoretical responses, shown by dotted lines, agree well with the experiment, except for the structural damping that has been neglected in the modeling. The experiment shows that by adding only $4.5g$ of water to the clear tube, the isolation frequency decreases from $20Hz$ to $9Hz$.

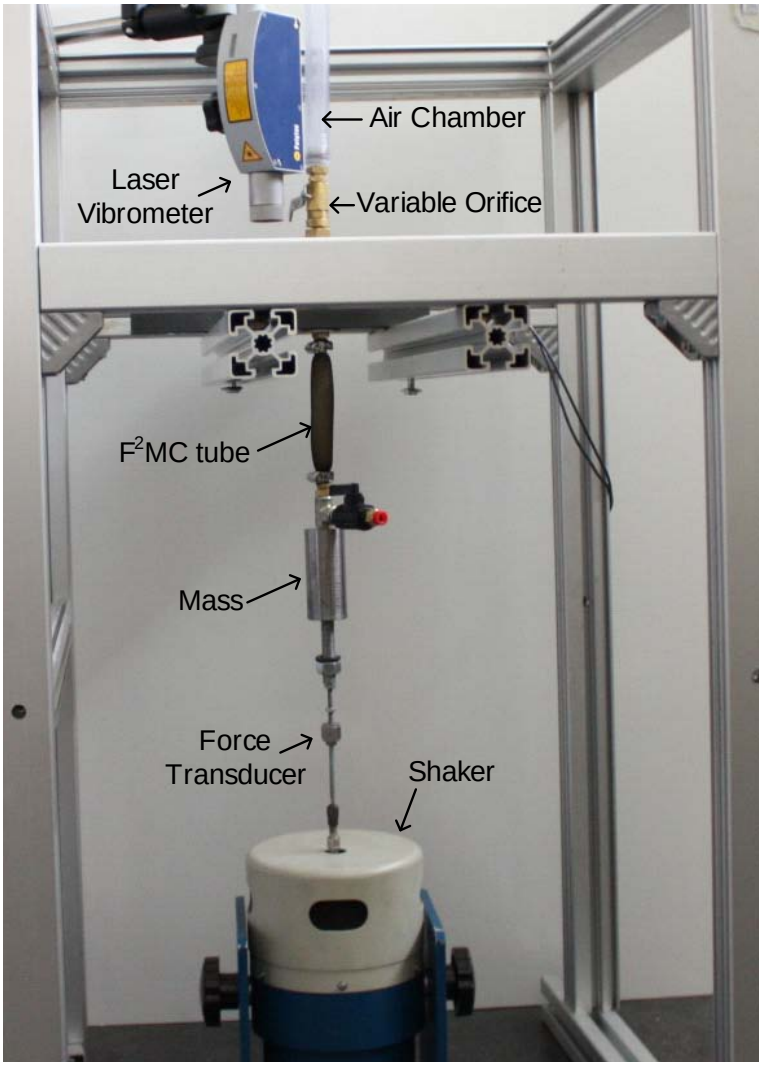


**Figure 5.5.** Experimental setup.

The effect of orifice size on the frequency response is studied in Fig. 5.7. A manual ball-valve is used to control the flow coefficient of the orifice. The four solid curves in Fig. 5.7 show how the peaks and zero shift as the valve closes. The model predictions for the fully open and closed valve cases agree well with the experimental frequency responses. The experimental results show that the vibration amplitude can be reduced by 94% from the closed valve case to the open valve case at the isolation frequency of $13.4Hz$.

The weight of the mass is equal to the pre-tension in the tube. By changing the

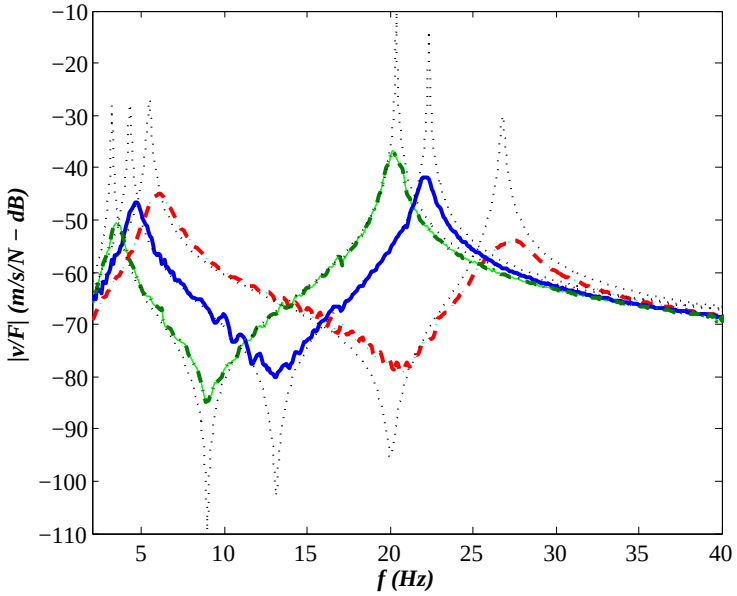


**Figure 5.6.** Experimental frequency response of the F$^2$MC-mass system $\left|\frac{v}{F}\right|$ with water levels of 7.6$cm$ (dashed), 17.8$cm$ (solid), and 38.1$cm$ (dash-dotted). The dotted curves are the corresponding theoretical responses.

mass, the tube length and fiber angle changes. The tube parameters $a_1, a_2$, and $a_3$ are functions of the fiber angle so the frequency response is somewhat sensitive to changes in weight. To study only the effect of mass changes, the tube length is kept constant by adjusting the pressure for each mass case. The frequency response of the system to variations in the primary mass is shown in Fig. 5.8. The baseline mass of 11.8$kg$ is reduced by 40% and the experiment shows the same isolation frequency, agreeing with theory. The theory over estimates the second peak for the smaller mass by 1.3$Hz$. This difference is due to nonlinear effects associated with re-pressurizing the tube.

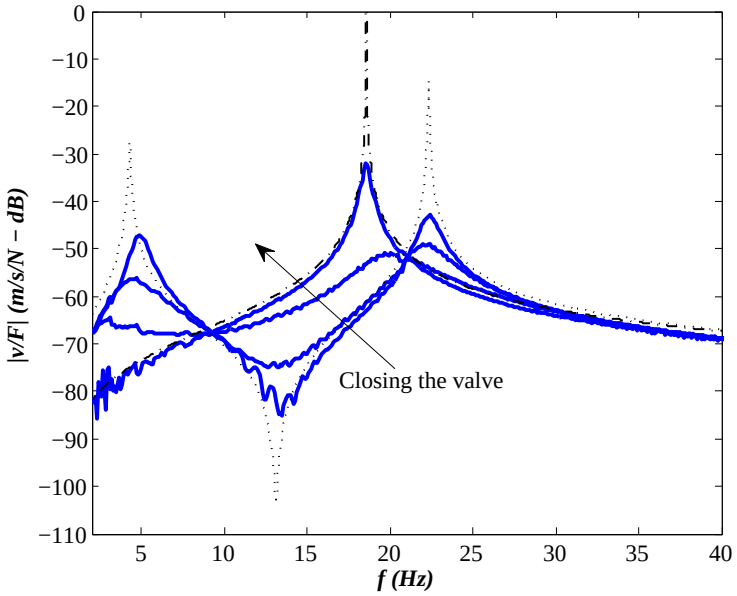


**Figure 5.7.** Experimental frequency response of the F$^2$MC-mass system $\left|\frac{v}{F}\right|$ with 17.8$cm$ water level for open, 1/3 closed, 2/3 closed, and fully-closed valve. The theoretical responses for open-valve and closed-valve cases are shown by dotted and dash-dotted curves, respectively.

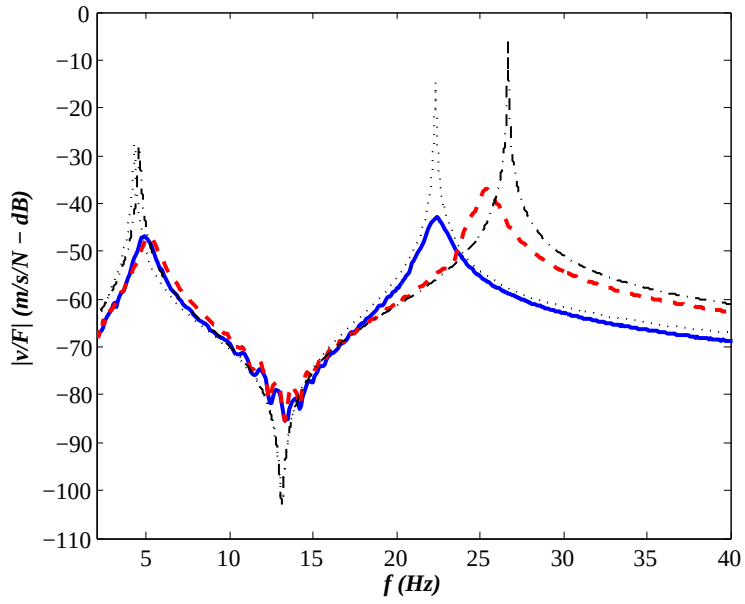


**Figure 5.8.** Experimental frequency response of the F$^2$MC-mass system $\left|\frac{v}{F}\right|$ with 17.8$cm$ water level for 7.2$kg$ (dashed) and 11.8$kg$ (solid) primary mass. The corresponding theoretical responses are shown by dash-dotted and dotted lines, respectively.

Chapter 6

# Conclusions and Future Work

## 6.1 Conclusions

This study shows that spatial and temporal input shaping can produce zero residual vibration in setpoint position control of one dimensional continua. For strings and pinned beam models, the response to step inputs is solved in closed form using delays. For more complicated (*e.g.* clamped beam) models, a closed form infinite modal series is the solution. The boundary controlled string can be setpoint regulated using two-pulse ZV and three-pulse ZVD shapers but, unlike discrete systems, ZVD is not more robust than ZV. Noncollocated ZV and ZVD boundary control enables translation of a string with zero residual vibration. Domain controlled strings and beams with spatial input distributions that satisfy certain orthogonality conditions (*e.g.* midspan point load and uniformly distributed load) can be setpoint regulated with shaped inputs. The pinned beam with ZVD shaped inputs is shown to have less sensitivity to parameter variations than with ZV. For systems with known eigenfunctions, modal shaping of the input distri-

bution and ZV or ZVD temporal shaping drives the output to the desired position with zero residual vibration. Using a force distribution shaped according to the first mode, the tip position of a cantilevered beam, for example, is driven to the desired setpoint without residual vibration.

Chapter 3 demonstrates that $F^2MC$ tubes can be used as variable stiffness structures for vibration suppression. A closed form $3^{rd}$-order equations of motion is derived using 3-D elasticity model and energy method. A reduced order model is developed based on operating in fully-open and fully-closed valve cases. A conventional Skyhook control method is applied which settles the vibration asymptotically. Then, a Zero Vibration Stiffness Shaping technique is introduced that suppresses the vibration in finite time and outperforms the Skyhook method.

In addition, $F^2MC$ tubes can be used for passive and semi-active vibration control. Based on a $3^{rd}$-order model, Lyapunov theory proves the stability of the unforced dynamic system for any valve control law. A reduced-order model for operation with either a fully-open or fully-closed valve motivates the development of a ZV controller that suppresses vibration in finite time. Optimization of the valve flow coefficient for passive, Skyhook, and ZV control minimizes the ITAE performance index. Coupling of a fluid-filled $F^2MC$ tube to a pressurized accumulator through a fixed orifice with optimal orifice size is experimentally shown to increase damping by 122% compared to the closed valve case. The performance of semi-active control is substantially better for impulse inputs than step inputs. The experimental ZV controller brings the impulse response to zero twice as fast as passive and Skyhook control. With optimal valve flow coefficient, ZV control performs as well as passive control (and almost twice as fast as optimal Skyhook

control) in response to step inputs.

Finally, this study shows that $F^2MC$ tubes coupled with a fluid port and an air accumulator can be used as tuned vibration absorbers. Using a 3-D elasticity for the tube and a lumped mass for the fluid, a $4^{th}$-order model is developed. The transfer function of this system contains four poles and two zeros. The isolation (zero) frequency depends mainly on the port inertance, orifice flow coefficient, and tube parameters. The port inertance is the most effective way of tuning the isolation frequency. Decreasing the orifice flow coefficient dampens the frequency response as long as the orifice is not too small. A fully-closed-valve results in an undamped $2^{nd}$-order system with no fluid dynamics. Variations in the primary mass do not appreciably change the isolation frequency. Experimental results validate the theoretical predictions, showing tunable isolation frequency, insensitivity to primary mass variations, and 94% reduction in forced vibration response relative to the closed valve case.

## 6.2 Future work

### 6.2.1 Semi-active position regulation

The equilibrium position in $F^2MC$ tubes can shift by switching from open to closed valve at nonzero positions. The trapped fluid in the tube in this case determines the new equilibrium. Hence, a semi-active position regulator can be proposed that follows a setpoint or a trajectory using the ambient disturbances. Figure (6.1) shows an example of such a performance. The solid and dashed lines are the open and closed valve trajectories, respectively. With no controller, the system oscillates around zero in response to a

harmonic excitation. If the switching law is defined as

$$\begin{cases} \dot{V} > 0, \text{ switch to closed valve} \\ \dot{V} \geq 0, \quad \text{switch to open valve} \end{cases} \tag{6.1}$$

the volume gradually increases, moving the output degree-of-freedom to a new setpoint (the dotted line in Fig. 6.1). This control technique has potentials to improve.

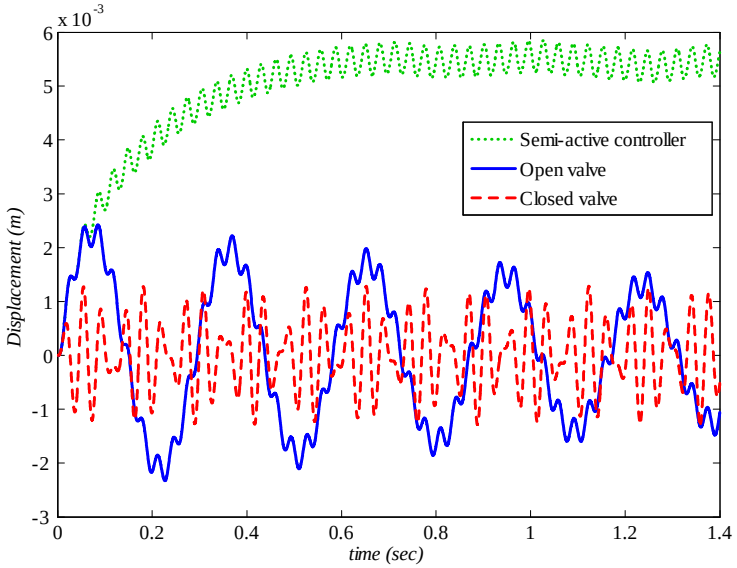


**Figure 6.1.** Mass displacement in open valve (solid), closed valve (dashed) and semi-active position regulator (dotted) cases. The disturbance frequency is 200 rad/s, 1.3 times more than the closed-valve frequency.

### 6.2.2 Semi-active vibration isolation

Variable stiffness structures have been used in forced vibration isolation. Cunefare *et al.* [67] develop a state-switch technique that outperforms tuned vibration absorbers for variable forcing frequencies. In this method, switching is done at zero positions to avoid instantaneous change in potential energy and transient response. Richard *et al.*

[80] introduce the Synchronized Switch Damping (SSD) technique using a piezoelectric insert and a small inductor that creates a phase shift between strain and voltage. They show that SSD can achieve a high vibration dissipation under harmonic excitation, as well as transient vibration.

$F^2MC$ tubes are potential candidates for semi-active vibration isolation. The ZV control law (4.17) can be investigated for forced vibration. In addition, by maximizing the dissipated energy in a cycle, one can develop an optimal vibration isolator with possible applications in engine mounts, helicopter seats, and so on. The dissipated energy in $F^2MC$ tubes appears in the fluid flow that can also be harvested as a fluid pump in a hydraulic system. The preliminary study on the new $F^2MC$ semi-active vibration isolator shows promising results compared to available control methods.

# Bibliography


[1] Alkhatib, R. and M. F. Golnaraghi (2003) "Active structural vibration control: A review," *The Shock and Vibration Digest*, **35**, pp. 367–383.

[2] Sun, J., M. Jolly, and M. Norris (1995) "Passive, adaptive and active tuned vibration absorbers - a survey," *Journal of Mechanical Design, Transactions of the ASME*, **117B**, pp. 234–242.

[3] Jalili, N. (2002) "A comparative study and analysis of semi-active vibration-control systems," *Journal of Vibration and Acoustics, Transactions of the ASME*, **124**(4), pp. 593–605.

[4] Franchek, M., M. Ryan, and R. Bernhard (1996) "Adaptive-passive vibration control," *Journal of Sound and Vibration*, **189**(5), pp. 565–585.

[5] Kemp, J. and R. Clark (2002) "Optimal hybrid active/passive vibration control design," *Proceedings of SPIE*, **4693**, pp. 440–450.

[6] Dadfarnia, M., N. Jalili, B. Xian, and D. Dawson (2004) "A Lyapunov-based piezoelectric controller for flexible cartesian robot manipulators," *Journal of Dynamic Systems, Measurement and Control*, **126**(2), pp. 347–358.

[7] Ramaratnam, A. and N. Jalili (2006) "A switched stiffness approach for structural vibration control: Theory and real-time implementation," *Journal of Sound and Vibration*, **291**(1), pp. 258–274.

[8] Frahm, H. (1911) "Device for Damping Vibrations of Bodies," *US Patent 989,958*.

[9] Winthrop, M. F. and C. R. G. (2003) "Survey of state-of-the-art vibration isolation research and technology for space applications," in *Smart Structures and Materials - Damping and Isolation*, vol. 5052, pp. 13–56.

[10] Ormondroyd, J. and J. Den Hartog (1928) "The theory of the dynamic vibration absorber," *ASME Transactions - Applied Mechanics*, **50**(17).

[11] Lee, J. K. and W. W. Clark (1999) "Semi-active control of flexural vibrations with an MR fluid actuator," in *Proceedings of SPIE*, vol. 3672, pp. 167–174.

[12] Dyke, S., B. Spencer, M. Sain, and J. Carlson (1996) "Modeling and control of magnetorheological dampers for seismic response reduction," *Journal of Sound and Vibration*, **5**(5), pp. 565–575.

[13] Shen, Y., M. Golnaraghi, and G. Heppler (2006) "Semi-active vibration control schemes for suspension systems using magnetorheological dampers," *Journal of Vibration and Control*, **12**(1), pp. 3–24.

[14] Choi, Y., N. Wereley, and Y. Jeon (2002) "Semi-active isolators using electrorheological/magnetorheological fluids," *Noise and vibration worldwide*, **33**(11), pp. 16–19.

[15] Oh, H. U., J. Onoda, and K. Minesugi (2004) "Semiactive isolator with liquid-crystal type ER fluid for momentum-wheel vibration isolation," *Journal of Vibration and Acoustics-Transactions of the ASME*, **126**(2), pp. 272–277.

[16] Den Hartog, J. P. (1985) "Mechanical vibrations," *Dover Publication, Mineola, NY*.

[17] Hagood, N. W. and A. Von Flotow (1991) "Damping of structural vibrations with piezoelectric materials and passive electrical networks," *Journal of Sound and Vibration*, **146**(2).

[18] Korenev, B. G. and L. M. Reznikov (1993) "Dynamic vibration absorbers," in *Wiley & Sons, New York:*, pp. 237–242.

[19] Davis, C. L. and L. G. A. (2000) "Actively tuned solid-state vibration absorber using capacitive shunting of piezoelectric stiffness," *Journal of Sound and Vibration*, **232**(3), pp. 601–617.

[20] Rusovici, R., J. J. Dosch, and G. A. Lesieutre (2002) "Design of a single-crystal piezoceramic vibration absorber," *Journal of Intelligent Material Systems and Structures*, **13**.

[21] Liang, C. and C. A. Rogers (1997) "Design of shape memory alloy springs with applications in vibration control," *Journal of Intelligent Material Systems and Structures*, **8**.

[22] Williams, K., G. Chiu, and R. Bernhard (2002) "Adaptive passive absorbers using shape memory alloys," *Journal of Sound and Vibration*, **249**(5).

[23] Noji, T. (1988) "Study on vibration control damper utilizing sloshing of water," *J. Wind Engineering*, (37).

[24] Sakai, F., S. Takaeda, and T. Tamaki (1989) "Tuned liquid column damper - new type device for suppression of building vibrations," in *Proc. Int. Conf. on Highrise BuiMings, Nanjing, China*, pp. 926–931.

[25] Fujino, Y., L. Sun, B. M. Pacheco, and P. Chaiseri (1992) "Tuned liquid damper (TLD) for suppressing horizontal motion of structures," *ASCE Journal ofEngineering Mechanics*, **118**.

[26] Abe', M., Y. Fujino, and S. Kimura (1998) "Active tuned liquid damper (TLD) with magnetic fluid," in *Proceedings of SPIE - Smart Structures and Materials - Smart Structures and Integrated Systems*, pp. 620–623.

[27] Shum, K. M. (2009) "Closed form optimal solution of a tuned liquid column damper for suppressing harmonic vibration of structures," *Engineering Structures*, **31**(1).

[28] Halwes, D. R. (1980) "LIVE – liquid inertia vibration eliminator," in *American Helicopter Society 36th Annual Forum, Washington, D.C.*

[29] du Plooy, N. F., P. S. Heyns, and M. J. Brennan (2005) "The development of a tunable vibration absorbing isolator," *International Journal of Mechanical Sciences*, **47**(7).

[30] Smith, M. R. and W. S. Redinger (1999) "The model 427 pylon isolation system," in *American Helicopter Society 55th Annual Forum, Montreal, Quebec, Canada*.

[31] Hyde, J. M. and W. P. Seering (1991) "Using input command pre-shaping to suppress multiple mode vibration," in *IEEE Int Conf on Robotics and Automation*, Sacramento, CA, pp. 2604–9.

[32] Singh, T. and G. R. Heppler (1993) "Shaped input control of a system with multiple modes," *ASME Journal of Dynamic Systems, Measurement, and Control*, **115**, pp. 341–7.

[33] Singhose, W. E., W. P. Seering, and N. Singer (1990) "Shaping inputs to reduce vibration: A vector diagram approach," in *Proc 1990 IEEE Int Conf Rob and Autom*, pp. 922–927.

[34] Singhose, W. E. (1997) "Command generation for flexible systems," *PhD. Thesis, Department of Mechanical Engineering, MIT*.

[35] Pao, L. Y. (1999) "Multi-input shaping design for vibration reduction," *Automatica*, **35**, pp. 81–89.

[36] Singhose, W. E., W. P. Seering, and N. C. Singer (1997) "Time-optimal negative input shapes," *ASME Journal of Dynamic System, Measurement and Control*, **119**, pp. 198–205.

[37] Shan, J., H. T. Liu, and D. Sun (2005) "Modified input shaping for a rotating single-link flexible manipulator," *Journal of Sound and Vibration*, **285**, pp. 187–207.

[38] Gimpel, D. J. and J. F. Calvert (1952) "Signal Component Control," *AIEE Transactions*, **339**(43).

[39] Singer, N. C. and W. P. Seering (1989) "Design and comparison of command shaping methods for controlling residual vibration," in *IEEE Int. Conf. Rob. and Autom.*, pp. 888–893.

[40] Pao, L. Y. and W. E. Singhose (1995) "On the equivalence of minimum time input shaping with traditional time-optimal control," in *Proc. 4th IEEE Conf*, Albany, NY, pp. 1120–1125.

[41] Meirovitch, L. and H. Baruh (1985) "Implementation of modal filters for control," *Journal of Guidance, Control and Dynamics*, **8**(6).

[42] Zhang, Q. and M. Sainsbury (2000) "Galerkin element method applied to the vibration of rectangular damped sandwich plates," *Computers and Structures*, **74**(6), pp. 717–730.

[43] Itik, M., M. U. Salamci, F. Demet U., and Y. Yaman (2005) "Active vibration suppression of a flexible beam via sliding mode and H infinity control," in

*Proceedings of the 44th IEEE Conference on Decision and Control, and the European Control Conference*, pp. 1240–1245.

[44] Kwak, S., G. Washington, and R. Yedavalli (2002) "Acceleration-based vibration control of distributed parameter systems using the "reciprocal state-space framework"," *Journal of Sound and Vibration*, **251**(3), pp. 543–557.

[45] Pereira, D., V. Shankar, S. Sathiyanaarayan, C. Lakshmana Rao, and S. Sivakumar (2002) "Vibration control of a cantilever beam using distributed PVDF actuator," in *Proceedings of SPIE*, vol. 5062, pp. 598–604.

[46] Balas, M. J. (1978) "Active control of flexible systems," *Journal of Optimization Theory and Applications*, **25**(3).

[47] De Queiroz, C. D., M. S.and Rahn (2002) "Boundary control of vibration and noise in distributed parameter systems: An overview," *Mechanical Systems and Signal Processing*, **16**(1), pp. 19–38.

[48] Qu, Z. (2002) "An iterative learning algorithm for boundary control of a stretched moving string," *Automatica*, **38**, pp. 821–827.

[49] Zhao, H. and C. D. Rahn (2005) "Iterative learning velocity and tension control for axially moving materials," in *Proc. of ASME DETC2005*, Long Beach, CA.

[50] Zhao, H., C. D. Rahn, and H. Canbolat (2005) "Repetitive control for an electrostatic microbridge," in *Proc. of ASME IMECE2005*, Orlando, FL.

[51] Baicu, C. F., C. D. Rahn, and N. B. D. (1996) "Active boundary control of elastic cables: theory and experiment," *Journal of Sound and Vibration*, **198**, pp. 17–26.

[52] Biswas, S. and N. Ahmed (1986) "Stabilization of a class of hybrid systems arising in flexible spacecraft," *Journal of Optimization Theory and Applications*, **50**, pp. 83–108.

[53] Fortgang, J. and W. Singhose (2005) "Input shaping for continuum beams under longitudinal vibration," in *IEEE/ASME International Conference on Advanced Intelligent Mechatronics*, Monterey, CA, pp. 1599–1604.

[54] Iwamoto, H. and N. Tanaka (2005) "Adaptive feed-forward control of flexural waves propagating in a beam using smart sensors," *Smart Materials and Structures*, **14**, pp. 1369–1376.

[55] dell'Isola, F., C. Maurini, and M. Porfiri (2004) "Passive damping of beam vibrations through distributed electric networks and piezoelectric transducers: Prototype design and experimental validation," *Smart Materials and Structures*, **13**, pp. 299–308.

[56] Fung, R. F., J. W. Wu, and S. L. Wu (1999) "Exponential stabilization of an axially moving string by linear boundary feedback," *Automatica*, **35**, pp. 177–181.

[57] Baz, A. (1997) "Boundary control of beams using active constrained layer damping," *Journal of Vibration and Acoustics*, **119**(2), pp. 166–172.

[58] Dawson, D. M., M. Agarwal, and F. Zhang (1999) "Adaptive nonlinear boundary control of a flexible link robot arm," *IEEE Transactions of Robotics and Automation*, **15**, pp. 779–787.

[59] Rahn, C. D. (2001) "Mechatronic control of distributed vibration and noise," *Berlin*.

[60] Singh, T. and H. Alli (1996) "Exact time-optimal control of the wave equation," *Journal of Guidance, Control and Dynamics*, **19**(1), pp. 130–134.

[61] Kornbluh, R., H. Prahlad, R. Pelrine, S. Stanford, M. Rosenthal, and P. Von Guggenberg (2004) "Rubber to rigid, clamped to undamped: Toward composite materials with wide-range controllable stiffness and damping," in *Proceedings of SPIE - Smart Structures and Materials - Industrial and Commercial Applications of Smart Structures Technologies*, pp. 372–386.

[62] Yang, S. and C. Jeng (1996) "Structural vibration suppression by concurrent piezoelectric sensor and actuator," *Smart materials and structures*, **5**(6).

[63] Hodgson, D., M. H. Wu, and R. Biermann "Shape memory alloys," *Metals Handbook, 10th Edition*, **2**.

[64] Liu, C., I. Rousseau, H. Qin, and P. Mather (2002) "Tailored shape memory polymers: not all SMPs are created equal," in *Proc. of The First World Congress on Biomimetics*, Albuquerque, New Mexico.

[65] Larson, G. D. (1996) "The analysis and realization of a state switched acoustic transducer," *Ph.D. Dissertation, School of Mechanical Engineering, Georgia Institute of Technology.*

[66] Clark, W. W. (2000) "Vibration control with state-switched piezoelectric materials," *Journal of Intelligent Material Systems and Structures*, **11**(4), pp. 263–271.

[67] Cunefare, K. A., S. De Rosa, N. Sadegh, and G. Larson (2000) "State-switched absorber for semi-active structural control," *Journal of Intelligent Material Systems and Structures*, **11**(4), pp. 300–310.

[68] Philen, M., Y. Shan, P. Prakash, K. Wang, C. Rahn, A. Zydney, and C. Bakis (2007) "Fibrillar network adaptive structure with ion-transport actuation," *Journal of Intelligent Material Systems and Structures*, **18**(4), pp. 323–334.

[69] Caldwell, D., G. Medrano-Cerda, and M. Goodwin (1993) "Braided pneumatic actuator control of a multi-jointed manipulator," in *Proceedings of the IEEE International Conference on Systems, Man and Cybernetics*, vol. 1, pp. 423–428.

[70] Chou, C. and B. Hannaford (1994) "Static and dynamic characteristics of McKibben pneumatic artificial muscles," in *Proceedings - IEEE International Conference on Robotics and Automation*, pp. 281–286.

[71] Pritts, M. and C. Rahn (2004) "Design of an artificial muscle continuum robot," in *Proceedings - IEEE International Conference on Robotics and Automation*, pp. 4743–4746.

[72] Shan, Y., M. Philen, C. Bakis, K. Wang, and C. Rahn (2006) "Nonlinear-elastic finite axisymmetric deformation of flexible matrix composite membranes under internal pressure and axial force," *Composites Science and Technology*, **66**(15), pp. 3053–3063.

[73] Philen, M., Y. Shan, C. Bakis, K. Wang, and C. Rahn (2006) "Variable stiffness adaptive structures utilizing hydraulically pressurized flexible matrix composites with valve control," in *AIAA/ASME/ASCE/AHS/ASC Structures, Structural Dynamics and Materials Conference*, vol. 9, pp. 6387–6397.

[74] Shan, Y., A. Lotfi, M. Philen, S. Li, C. E. Bakis, C. Rahn, and K. Wang (2007) "Fluidic flexible matrix composites for autonomous structural tailoring," in *Proceedings of SPIE - Active and Passive Smart Structures and Integrated Systems*, vol. 6525, p. 652517.

[75] Kozak, K., J. Huey, and W. E. Singhose (2003) "Performance measures for input shaping„" in *Proc. of IEEE Conference on Control Applications*, pp. 1227–1232.

[76] Lekhnitskii, S. (1963) "Theory of elasticity of an anisotropic body," Holden-Day Inc., San Fransisco.

[77] Timoshenko, S. (1983) "History of strength of materials," *Dover Publications*.

[78] White, F. (2002) "Fluid mechanics," *McGraw-Hill, New York*.

[79] Lotfi-Gaskarimahalle, A., Y. Shan, S. Li, C. D. Rahn, C. E. Bakis, and K. W. Wang (2008) "Stiffness shaping for zero vibration fluidic flexible matrix

composites," in *ASME Conference on Smart Materials, Adaptive Structures and Intelligent Systems*.

[80] Richard, C., D. Guyomar, D. Audigier, and H. Bassaler (2000) "Enhanced semi-passive damping using continuous switching of a piezoelectric device on an inductor," in *Proc of SPIE - Smart Structures and Materials: Damping and Isolation*, vol. 3989, pp. 288–299.

# Appendix A: F$^2$MC Compliance Matrix - MATLAB Code

The following function receives the fiber angle and the material properties of the laminate and outputs the compliance matrix.

```
function Amatrix = ComplianceMatrixGenerator2(angle,v12,v23,E11,E22,G12,G23)
% E11 = Fiber elastic modulus
% E22 = Resin elastic modulus
% G12 = Shear modulus in 1-2 plane
% G23 = Shear modulus in 2-3 plane
% v12 = Poisson ratio in 1-2 plane
% v23 = Poisson ratio in 2-3 plane
FiberAngle=[angle,-angle,-angle,+angle];
PlyNum=length(FiberAngle);
Layer_Thickness=[1,1,1,1];
Total_Thickness=sum(Layer_Thickness);
V=((1+v23)*(1-v23-2*v12^2*E22/E11));
c11=(1-v23^2)*E11/V;
c12=v12*(1+v23)*E22/V;
c13=c12;
c23=(v23+v12^2*E22/E11)*E22/V;
c22=(1-v12^2*E22/E11)*E22/V;
c33=c22;
c44=G23;
c55=G12;
c66=c55;
C0=[c11,c12,c13,0,0,0;
c12,c22,c23,0,0,0;
c13,c23,c33,0,0,0;
0,0,0,c44,0,0;
0,0,0,0,c55,0;
0,0,0,0,0,c66];
a=0;b=0;c=0;
for k=1:PlyNum
theta=FiberAngle(k)*pi/180;
vk=Layer_Thickness(k)/Total_Thickness;
```

```
m=cos(theta);
n=sin(theta);
T_s=[m^2, n^2, 0,0,0,2*m*n;
n^2,m^2,0,0,0,-2*m*n;
0,0,1,0,0,0;
0,0,0,m,-n,0;
0,0,0,n,m,0;
-m*n,m*n,0,0,0,(m^2-n^2)];
T_e=[m^2,n^2,0,0,0,m*n; % w.r.t. engineering strain
n^2,m^2,0,0,0,-m*n;
0,0,1,0,0,0;
0,0,0,m,-n,0;
0,0,0,n,m,0;
-2*m*n,2*m*n,0,0,0,(m^2-n^2)];
C=inv(T_s)*C0*T_e;
delta_k=C(4,4)*C(5,5)-(C(4,5))^2;
a=a+vk*C(4,4)/delta_k;
b=b+vk*C(5,5)/delta_k;
c=c+vk*C(4,5)/delta_k;
end %Just for calculation of delta
delta=a*b-c^2;
%The following is for the calculation of Cij
C_bar=[0,0,0,0,0,0;
0,0,0,0,0,0;
0,0,0,0,0,0;
0,0,0,0,0,0;
0,0,0,0,0,0;
0,0,0,0,0,0];
for k=1:PlyNum
theta=FiberAngle(k)*pi/180;
vk=Layer_Thickness(k)/Total_Thickness;
m=cos(theta);
n=sin(theta);
T_s=[m^2, n^2, 0,0,0,2*m*n;
n^2,m^2,0,0,0,-2*m*n;
0,0,1,0,0,0;
0,0,0,m,-n,0;
0,0,0,n,m,0;
-m*n,m*n,0,0,0,(m^2-n^2)];
T_e=[m^2,n^2,0,0,0,m*n;
n^2,m^2,0,0,0,-m*n;
0,0,1,0,0,0;
0,0,0,m,-n,0;
0,0,0,n,m,0;
-2*m*n,2*m*n,0,0,0,(m^2-n^2)];
```

```
C=inv(T_s)*C0*T_e;
delta_k=C(4,4)*C(5,5)-(C(4,5))^2;
C_bar(1,1)=C_bar(1,1)+vk*C(1,1);
C_bar(1,2)=C_bar(1,2)+vk*C(1,2);
C_bar(1,3)=C_bar(1,3)+vk*C(1,3);
C_bar(1,6)=C_bar(1,6)+vk*C(1,6);
C_bar(2,1)=C_bar(1,2);
C_bar(2,2)=C_bar(2,2)+vk*C(2,2);
C_bar(2,3)=C_bar(2,3)+vk*C(2,3);
C_bar(2,6)=C_bar(2,6)+vk*C(2,6);
C_bar(3,1)=C_bar(1,3);
C_bar(3,2)=C_bar(2,3);
C_bar(3,3)=C_bar(3,3)+vk*C(3,3);
C_bar(3,6)=C_bar(3,6)+vk*C(3,6);
C_bar(6,1)=C_bar(1,6);
C_bar(6,2)=C_bar(2,6);
C_bar(6,3)=C_bar(3,6);
C_bar(6,6)=C_bar(6,6)+vk*C(6,6);
C_bar(4,4)=C_bar(4,4)+vk*C(4,4)/delta_k/delta;
C_bar(4,5)=C_bar(4,5)+vk*C(4,5)/delta_k/delta;
C_bar(5,4)=C_bar(4,5);
C_bar(5,5)=C_bar(5,5)+vk*C(5,5)/delta_k/delta;
end
S_bar=inv(C_bar);
%The following follows Lekniskii's Elastic Solution for Cylindrically Orthotropic Tubes
%In the following, 1 refers to the radial direction
%2 refers to the hoop direction, 3 refers to the axial direction
a11=S_bar(3,3);
a12=S_bar(2,3);
a13=S_bar(1,3);
a22=S_bar(2,2);
a23=S_bar(1,2);
a33=S_bar(1,1);
a66=S_bar(4,4);
a55=S_bar(5,5);
a44=S_bar(6,6);
Amatrix = [a11 a12 a13 0 0 0;
a12 a22 a23 0 0 0;
a13 a23 a33 0 0 0;
0 0 0 a44 0 0;
0 0 0 0 a55 0;
0 0 0 0 0 a66];
```

# Appendix B: F$^2$MC Elastic Energy-MATLAB Code

The following function generates the parameters $a_1, a_2$ and $a_3$ from the given compliance matrix, A.

```
function U = Ugenerator_closedForm2(A)
a11 = A(1,1);
a12 = A(1,2);
a13 = A(1,3);
a22 = A(2,2);
a23 = A(2,3);
a33 = A(3,3);
a44 = A(4,4);
beta11=a11-a13*a13/a33;
beta22=a22-a23*a23/a33;
beta44=a44;
beta14=0; beta24=0;
k =sqrt((beta11*beta44-beta14^2)/(beta22*beta44-beta24^2));
x1 = ((a13-a23)*beta44)/(beta22*beta44-beta24^2-(beta11*beta44-beta14^2));
nu=v;
C1 = -(a2^(k+1)-a1^(k+1))/(a2^(2*k)-a1^(2*k));
C2 = -(a2^(k-1)-a1^(k-1))/(a2^(k*2)-a1^(k*2))*a1^(k+1)*a2^(k+1);
H1 = (a1^(k+1))/(a2^(2*k)-a1^(2*k));
H2 = (a2^(k-1))/(a2^(k*2)-a1^(k*2))*a1^(k+1)*a2^(k+1);
```

```
coef_CC_FF1 = (-(-a33*a2^k*a1^k*k^2+a33*a2^k*a1^k)/pi/(a1^(k+2)*a2^k*a23*x1*k^2-
2*a1^k*a2^(2*k+1)*x1*k^2*C1*a23+a2^(k+2)*a1^k*a33*k^2-
2*a2^k*a1^(2*k+1)*x1*k*C1*a23+2*a1^k*a2^(2*k+1)*a13*x1*C1-
a1^(k+2)*a2^k*a23*x1+2*a1^k*a2^(2*k+1)*x1*k*C1*a23-
a1^(k+2)*a2^k*a33*k^2+2*a2^k*a1^(2*k+1)*x1*k^2*C1*a23+a1^(k+2)*a2^k*a13*x1*k^2+2*a2^k*a1^
(2*k+1)*a13*x1*C1*k+2*a2^k*x1*k*C2*a23*a1+2*a2^k*x1*k^2*C2*a23*a1-
2*a2^k*a13*x1*C2*k*a1+2*a1^k*a13*x1*C2*k*a2-2*a1^k*x1*k^2*C2*a23*a2-
2*a2^k*a13*x1*C2*a1+2*a1^k*a13*x1*C2*a2-2*a1^k*x1*k*C2*a23*a2+a1^(k+2)*a2^k*a33-
a2^(k+2)*a1^k*a33+a2^(k+2)*a1^k*a13*x1+a2^(k+2)*a1^k*a23*x1-
2*a1^k*a2^(2*k+1)*a13*x1*C1*k-a1^(k+2)*a2^k*a13*x1-2*a2^k*a1^(2*k+1)*a13*x1*C1-
a2^(k+2)*a1^k*a23*x1*k^2-a2^(k+2)*a1^k*a13*x1*k^2));

coef_CC_PP1 = (-(-2*a2*pi*a1^k*a13*H2+2*a2^(2*k+1)*pi*a1^k*H1*k*a23-
2*a2^(2*k+1)*pi*a1^k*H1*k^2*a23-
2*a2^(2*k+1)*pi*a1^k*a13*H1*k+2*a2^(2*k+1)*pi*a1^k*a13*H1-
2*a2*pi*a1^k*a13*H2*k+2*a1*pi*a2^k*a13*H2+2*a2*pi*a1^k*H2*k*a23+2*a2*pi*a1^k*H2*k^2*a23-
2*a1*pi*a2^k*H2*k*a23+2*a1^(2*k+1)*pi*a2^k*a13*H1*k+2*a1^(2*k+1)*pi*a2^k*H1*k^2*a23-
2*a1^(2*k+1)*pi*a2^k*H1*k*a23-2*a1*pi*a2^k*H2*k^2*a23-
2*a1^(2*k+1)*pi*a2^k*a13*H1+2*a1*pi*a2^k*a13*H2*k)/pi/(a1^(k+2)*a2^k*a23*x1*k^2-
2*a1^k*a2^(2*k+1)*x1*k^2*C1*a23+a2^(k+2)*a1^k*a33*k^2-
2*a2^k*a1^(2*k+1)*x1*k*C1*a23+2*a1^k*a2^(2*k+1)*a13*x1*C1-
a1^(k+2)*a2^k*a23*x1+2*a1^k*a2^(2*k+1)*x1*k*C1*a23-
a1^(k+2)*a2^k*a33*k^2+2*a2^k*a1^(2*k+1)*x1*k^2*C1*a23+a1^(k+2)*a2^k*a13*x1*k^2+2*a2^k*a1^
(2*k+1)*a13*x1*C1*k+2*a2^k*x1*k*C2*a23*a1+2*a2^k*x1*k^2*C2*a23*a1-
2*a2^k*a13*x1*C2*k*a1+2*a1^k*a13*x1*C2*k*a2-2*a1^k*x1*k^2*C2*a23*a2-
2*a2^k*a13*x1*C2*a1+2*a1^k*a13*x1*C2*a2-2*a1^k*x1*k*C2*a23*a2+a1^(k+2)*a2^k*a33-
a2^(k+2)*a1^k*a33+a2^(k+2)*a1^k*a13*x1+a2^(k+2)*a1^k*a23*x1-
2*a1^k*a2^(2*k+1)*a13*x1*C1*k-a1^(k+2)*a2^k*a13*x1-2*a2^k*a1^(2*k+1)*a13*x1*C1-
a2^(k+2)*a1^k*a23*x1*k^2-a2^(k+2)*a1^k*a13*x1*k^2));

coef_PP1_CC = (-E*(a1^2*a12*a33*x1*k*C2+a1^(2+2*k)*a13^2*x1*C1-a1^2*a13*a23*x1*k*C2-
a1^(3+k)*a33^2*nu+a1^(3+k)*a13^2*x1-a1^(3+k)*a13*a33-
a1^(2+2*k)*a12*a33*x1*k*C1+a1^(2*k)*a12*a33*x1*k*C1*a0^2-
a1^(2*k)*a13*a23*x1*k*C1*a0^2+a1^(1+k)*a12*a33*x1*a0^2+a1^(3+k)*a13*a23*x1+a11*a33*x1*C2*
a0^2-a1^(3+k)*a12*a33*x1-a12*a33*x1*k*C2*a0^2-
a1^(2*k)*a13^2*x1*C1*a0^2+a1^(1+k)*a11*a33*x1*a0^2+a1^(2*k)*a11*a33*x1*C1*a0^2+a1^(2+2*k)
*a13*a23*x1*k*C1-a1^(2+2*k)*a11*a33*x1*C1-a1^(3+k)*a11*a33*x1-a1^(1+k)*a13^2*x1*a0^2-
a1^(1+k)*a13*a23*x1*a0^2+a13*a23*x1*k*C2*a0^2+a1^(1+k)*a13*a33*a0^2+a1^(1+k)*a33^2*nu*a0^
2-a1^2*a11*a33*x1*C2-
a13^2*x1*C2*a0^2+a1^2*a13^2*x1*C2)/(E*a13^2*H1*a1^(2+2*k)+E*a13^2*H2*a0^2-
E*a13^2*H2*a1^2-E*a13^2*H1*a1^(2*k)*a0^2-E*a12*a33*H1*k*a1^(2+2*k)+E*a12*a33*H2*k*a0^2-
E*a12*a33*H2*k*a1^2+E*a12*a33*H1*k*a1^(2*k)*a0^2+E*a13*a23*H1*k*a1^(2+2*k)-
E*a13*a23*H1*k*a1^(2*k)*a0^2+E*a13*a23*H2*k*a1^2-
E*a13*a23*H2*k*a0^2+E*a11*a33*H2*a1^2+E*a11*a33*H1*a1^(2*k)*a0^2-E*a11*a33*H1*a1^(2+2*k)-
E*a11*a33*H2*a0^2-
a33*a1^(3+k)+a33*a0^2*a1^(1+k)+a33*nu*a0^2*a1^(1+k)+a33*nu*a1^(3+k)+2*a33*nu^2*a1^(3+k)))
;

coef_PP1_P = (-2*a33*nu*a0^2*(1+nu)*a1/(-E*a13^2*H1*a1^(k+2)-E*a13^2*H2*a1^(-
k)*a0^2+E*a13^2*H2*a1^(2-k)+E*a13^2*H1*a1^k*a0^2+E*a12*a33*H1*k*a1^(k+2)-
E*a12*a33*H2*k*a1^(-k)*a0^2+E*a12*a33*H2*k*a1^(2-k)-E*a12*a33*H1*k*a1^k*a0^2-
E*a13*a23*H1*k*a1^(k+2)+E*a13*a23*H1*k*a1^k*a0^2-E*a13*a23*H2*k*a1^(2-
k)+E*a13*a23*H2*k*a1^(-k)*a0^2-E*a11*a33*H2*a1^(2-k)-
E*a11*a33*H1*a1^k*a0^2+E*a11*a33*H1*a1^(k+2)+E*a11*a33*H2*a1^(-k)*a0^2+a33*a1^3-
a33*a0^2*a1-a33*nu*a0^2*a1-a33*nu*a1^3-2*a33*nu^2*a1^3));
coef_FF1_CC = (pi*E*(2*a1^2*nu*a12*a33*x1*k*C2*a0^2-2*a1^4*nu*a13^2*x1*C2-
2*a1^2*nu*a13*a23*x1*k*C2*a0^2-2*a1^2*a33*E*a13^2*H2*a0^2+2*a1^2*a33*E*a13*a23*H2*k*a0^2-
a1^4*a33^2*E*a11*H2+a1^(1+k)*a33^2*a0^4-
a1^4*a33*E*a13*a23*H2*k+a1^4*a33*E*a13^2*H2+a1^4*a33^2*E*a12*H2*k-
```

```
a33*E*a0^4*a13*a23*H2*k+2*a1^4*nu*a11*a33*x1*C2+2*a1^2*nu*a13^2*x1*C2*a0^2+2*a1^2*a33^2*E
*a11*H2*a0^2-a1^(5+k)*a33^2*nu-
2*a1^(3+k)*a33^2*a0^2+2*a1^4*nu*a13*a23*x1*k*C2+2*a1^(5+k)*nu*a13*a33+a1^(1+k)*a33^2*a0^4
*nu-2*a1^(5+k)*nu*a13^2*x1-2*a1^(4+2*k)*nu*a13^2*x1*C1+2*a1^(4+2*k)*nu*a11*a33*x1*C1-
a1^(2*k)*a33*E*a0^4*a13^2*H1+2*a1^(3+k)*nu*a13*a23*x1*a0^2+a1^(2*k)*a33^2*E*a0^4*a11*H1-
2*a1^(2+2*k)*a33^2*E*a11*H1*a0^2+2*a1^(2+2*k)*a33*E*a13^2*H1*a0^2-
2*a1^(3+k)*nu*a13*a33*a0^2+a1^(5+k)*a33^2-
2*a1^(2+2*k)*a33^2*E*a12*H1*k*a0^2+2*a1^(3+k)*nu*a13^2*x1*a0^2-
2*a1^(2+2*k)*nu*a11*a33*x1*C1*a0^2+a1^(4+2*k)*a33^2*E*a11*H1-
2*a1^(3+k)*nu*a12*a33*x1*a0^2+a1^(2*k)*a33^2*E*a0^4*a12*H1*k-
2*a1^(3+k)*nu*a11*a33*x1*a0^2-2*a1^(5+k)*nu*a13*a23*x1+a1^(4+2*k)*a33^2*E*a12*H1*k-
a1^(4+2*k)*a33*E*a13^2*H1+2*a1^(5+k)*nu*a11*a33*x1+2*a1^(5+k)*nu*a12*a33*x1-
a1^(4+2*k)*a33*E*a13*a23*H1*k+2*a1^(4+2*k)*nu*a12*a33*x1*k*C1-
2*a1^(4+2*k)*nu*a13*a23*x1*k*C1+2*a1^(2+2*k)*a33*E*a13*a23*H1*k*a0^2-
a1^(2*k)*a33*E*a0^4*a13*a23*H1*k+2*a1^(2+2*k)*nu*a13*a23*x1*k*C1*a0^2-
2*a1^(2+2*k)*nu*a12*a33*x1*k*C1*a0^2+2*a1^(2+2*k)*nu*a13^2*x1*C1*a0^2-
2*a1^2*a33^2*E*a12*H2*k*a0^2-
2*a1^4*nu*a12*a33*x1*k*C2+a33*E*a0^4*a13^2*H2+a33^2*E*a0^4*a12*H2*k-a33^2*E*a0^4*a11*H2-
2*a1^2*nu*a11*a33*x1*C2*a0^2)/(E*a13^2*H1*a1^(2+2*k)+E*a13^2*H2*a0^2-E*a13^2*H2*a1^2-
E*a13^2*H1*a1^(2*k)*a0^2-E*a12*a33*H1*k*a1^(2+2*k)+E*a12*a33*H2*k*a0^2-
E*a12*a33*H2*k*a1^2+E*a12*a33*H1*k*a1^(2*k)*a0^2+E*a13*a23*H1*k*a1^(2+2*k)-
E*a13*a23*H1*k*a1^(2*k)*a0^2+E*a13*a23*H2*k*a1^2-
E*a13*a23*H2*k*a0^2+E*a11*a33*H2*a1^2+E*a11*a33*H1*a1^(2*k)*a0^2-E*a11*a33*H1*a1^(2+2*k)-
E*a11*a33*H2*a0^2-
a33*a1^(3+k)+a33*a0^2*a1^(1+k)+a33*nu*a0^2*a1^(1+k)+a33*nu*a1^(3+k)+2*a33*nu^2*a1^(3+k)))
;

coef_FF1_P = (-pi*a0^2*(-
4*a33*nu^2*a1^(3+k)+E*a13*a23*H2*k*a0^2+E*a11*a33*H2*a0^2+E*a13^2*H2*a1^2+E*a12*a33*H2*k*
a1^2-E*a13*a23*H2*k*a1^2-E*a11*a33*H2*a1^2+2*a1^2*nu*E*a11*a33*H2+2*nu*a0^2*E*a13^2*H2-
2*a1^2*nu*E*a13^2*H2-2*nu*a0^2*E*a13*a23*H2*k+E*a13^2*H1*a1^(2*k)*a0^2-
E*a12*a33*H1*k*a1^(2*k)*a0^2+E*a12*a33*H1*k*a1^(2+2*k)+a33*nu*a0^2*a1^(1+k)+a33*a1^(3+k)-
E*a13*a23*H1*k*a1^(2+2*k)-
E*a13^2*H1*a1^(2+2*k)+2*a1^(2+2*k)*nu*E*a13^2*H1+E*a11*a33*H1*a1^(2+2*k)-E*a13^2*H2*a0^2-
E*a12*a33*H2*k*a0^2+2*a1^(1+k)*nu^2*a0^2*a33-2*a1^2*nu*E*a12*a33*H2*k-
2*nu*a0^2*E*a11*a33*H2+2*nu*a0^2*E*a12*a33*H2*k+2*a1^2*nu*E*a13*a23*H2*k+E*a13*a23*H1*k*a
1^(2*k)*a0^2-E*a11*a33*H1*a1^(2*k)*a0^2-2*a1^(2*k)*nu*a0^2*E*a13^2*H1-
2*a1^(2*k)*nu*a0^2*E*a13*a23*H1*k+2*a1^(2*k)*nu*a0^2*E*a12*a33*H1*k-
2*a1^(2+2*k)*nu*E*a12*a33*H1*k-
2*a1^(2+2*k)*nu*E*a11*a33*H1+2*a1^(2*k)*nu*a0^2*E*a11*a33*H1+2*a1^(2+2*k)*nu*E*a13*a23*H1
*k-a33*a0^2*a1^(1+k)-3*a33*nu*a1^(3+k))/(E*a13^2*H1*a1^(2+2*k)+E*a13^2*H2*a0^2-
E*a13^2*H2*a1^2-E*a13^2*H1*a1^(2*k)*a0^2-E*a12*a33*H1*k*a1^(2+2*k)+E*a12*a33*H2*k*a0^2-
E*a12*a33*H2*k*a1^2+E*a12*a33*H1*k*a1^(2*k)*a0^2+E*a13*a23*H1*k*a1^(2+2*k)-
E*a13*a23*H1*k*a1^(2*k)*a0^2+E*a13*a23*H2*k*a1^2-
E*a13*a23*H2*k*a0^2+E*a11*a33*H2*a1^2+E*a11*a33*H1*a1^(2*k)*a0^2-E*a11*a33*H1*a1^(2+2*k)-
E*a11*a33*H2*a0^2-
a33*a1^(3+k)+a33*a0^2*a1^(1+k)+a33*nu*a0^2*a1^(1+k)+a33*nu*a1^(3+k)+2*a33*nu^2*a1^(3+k)))
;

coef_C_P = (coef_CC_FF1*coef_FF1_P+coef_CC_PP1*coef_PP1_P)/(1-
(coef_CC_FF1*coef_FF1_CC+coef_CC_PP1*coef_PP1_CC));
coef_C_F = (coef_CC_FF1)/(1-(coef_CC_FF1*coef_FF1_CC+coef_CC_PP1*coef_PP1_CC));
coef_P1_P = (coef_PP1_CC*coef_C_P+coef_PP1_P);
coef_P1_F = coef_PP1_CC*coef_C_F;
coef_F1_P = (coef_FF1_CC*coef_C_P+coef_FF1_P);
coef_F1_F = coef_FF1_CC*coef_C_F+1;

Ur1_PP = 0.5*(-pi*L*(2*coef_C_P^2*a2^(1-k)*k*x1*C2*a13*a33+a1^2*coef_C_P^2*x1^2*a13^2*k-
a1^2*coef_C_P^2*x1^2*a13^2*k^3-4*log(a2)*coef_C_P*x1*C1*a11*coef_P1_P*H2*a33*k-a1^(-
```

```
2*k)*coef_P1_P^2*H2^2*a13^2+2*a1^(-
2*k)*coef_C_P*x1*C2*a13^2*coef_P1_P*H2+4*coef_C_P*a1^(1-k)*k^2*x1*a11*a33*coef_P1_P*H2-
2*coef_C_P^2*a1^(1-k)*k^2*x1*C2*a13*a33+2*coef_C_P^2*a1^(1-k)*k*x1^2*C2*a13*a23-
4*coef_C_P^2*a1^(1-k)*k*x1^2*a11*a33*C2+2*coef_C_P*a1^(1-
k)*k*coef_P1_P*H2*a13*a33+2*coef_C_P^2*a1^(1-k)*k^3*x1^2*a12*a33*C2-2*coef_C_P^2*a1^(1-
k)*k^3*x1^2*a13*a23*C2-2*coef_C_P*a1^(1-
k)*k^3*x1*a12*a33*coef_P1_P*H2+4*coef_C_P^2*a1^(1-k)*k^2*x1^2*a13^2*C2-
a1^(2*k)*coef_C_P^2*x1^2*C1^2*a11*a33-
a1^(2*k)*coef_P1_P^2*H1^2*a13^2*k^2+4*coef_C_P*a2^(1-k)*k*x1*a13^2*coef_P1_P*H2-
2*coef_C_P*a2^(1-k)*k*coef_P1_P*H2*a12*a33*x1+2*coef_C_P*a2^(1-
k)*k*coef_P1_P*H2*a13*a23*x1-4*coef_C_P^2*a2^(1-k)*k*x1^2*a13^2*C2-2*coef_C_P*a2^(1-
k)*k^3*x1*a13*a23*coef_P1_P*H2-2*coef_C_P*a2^(1-
k)*k^2*coef_P1_P*H2*a13*a33+4*coef_C_P^2*a2^(1-k)*k^2*x1^2*a11*a33*C2-4*coef_C_P*a2^(1-
k)*k^2*x1*a11*a33*coef_P1_P*H2+4*coef_C_P*a2^(1-
k)*k^2*x1*a13^2*coef_P1_P*H2+2*coef_C_P^2*a2^(1-k)*k^2*x1*C2*a13*a33-2*coef_C_P^2*a2^(1-
k)*k*x1^2*C2*a13*a23+4*coef_C_P^2*a2^(1-k)*k*x1^2*a11*a33*C2-2*coef_C_P*a2^(1-
k)*k*coef_P1_P*H2*a13*a33-2*coef_C_P^2*a2^(1-k)*k^3*x1^2*a12*a33*C2+2*coef_C_P^2*a2^(1-
k)*k^3*x1^2*a13*a23*C2+a1^(2*k)*coef_P1_P^2*H1^2*a11*a33*k^2-
a2^2*coef_C_P^2*x1^2*a13*a23*k+a2^2*coef_C_P^2*x1^2*a13*a23*k^3-
a2^(2*k)*coef_P1_P^2*H1^2*a13^2-
a2^2*coef_C_P^2*x1^2*a13^2*k+a2^2*coef_C_P^2*x1^2*a13^2*k^3+a2^2*coef_C_P^2*x1*a13*a33*k-
a2^2*coef_C_P^2*x1*a13*a33*k^3+a2^2*coef_C_P^2*x1^2*a12*a33*k-
a2^2*coef_C_P^2*x1^2*a12*a33*k^3+a2^2*coef_C_P^2*x1^2*a11*a33*k-
a2^2*coef_C_P^2*x1^2*a11*a33*k^3-
a1^2*coef_C_P^2*x1^2*a12*a33*k+a1^2*coef_C_P^2*x1^2*a12*a33*k^3+4*coef_C_P^2*a1^(1+k)*x1^
2*a13^2*C1*k-4*coef_C_P*a1^(1-k)*k^2*x1*a13^2*coef_P1_P*H2-
a2^(2*k)*coef_C_P^2*x1^2*C1^2*a13^2-
2*a2^(2*k)*coef_C_P*x1*C1*a13*a23*coef_P1_P*H1*k+2*a2^(2*k)*coef_C_P*x1*C1*a11*a33*coef_P
1_P*H1+2*a2^(2*k)*coef_C_P*x1*C1*a13^2*coef_P1_P*H1*k^2+a2^(2*k)*coef_C_P^2*x1^2*C1^2*a13
^2*k^2+a2^(2*k)*coef_C_P^2*x1^2*C1^2*a13*a23*k^3+2*a2^(2*k)*coef_C_P*x1*C1*a13*a23*coef_P
1_P*H1*k^3-a2^(2*k)*coef_P1_P^2*H1^2*a12*a33*k^3-
2*a2^(2*k)*coef_C_P*x1*C1*a13^2*coef_P1_P*H1+2*coef_C_P*a2^(1+k)*coef_P1_P*H1*a13*a23*x1*
k^3+4*log(a2)*coef_P1_P^2*H1*a13^2*H2*k-4*log(a2)*coef_P1_P^2*H1*a13^2*H2*k^3-
4*coef_C_P^2*a1^(1+k)*x1^2*a13^2*C1*k^2+4*log(a2)*coef_C_P*x1*C2*a11*coef_P1_P*H1*a33*k-
4*log(a2)*coef_C_P*x1*C2*a11*coef_P1_P*H1*a33*k^3-
4*log(a2)*coef_C_P*x1*C1*a13^2*coef_P1_P*H2*k^3-a2^(-
2*k)*coef_C_P^2*x1^2*C2^2*a11*a33+a2^(-2*k)*coef_P1_P^2*H2^2*a12*a33*k-a2^(-
2*k)*coef_C_P^2*x1^2*C2^2*a13*a23*k-a2^(-2*k)*coef_P1_P^2*H2^2*a13*a23*k+2*a2^(-
2*k)*coef_C_P*x1*C2*a13*a23*coef_P1_P*H2*k+a2^(-2*k)*coef_C_P^2*x1^2*C2^2*a13^2-a2^(-
2*k)*coef_P1_P^2*H2^2*a13^2*k^2+2*a2^(-2*k)*coef_C_P*x1*C2*a13^2*coef_P1_P*H2*k^2+a2^(-
2*k)*coef_P1_P^2*H2^2*a13*a23*k^3-2*a2^(-
2*k)*coef_C_P*x1*C2*a11*a33*coef_P1_P*H2*k^2+a2^(-2*k)*coef_C_P^2*x1^2*C2^2*a13*a23*k^3-
2*coef_C_P*a2^(1+k)*coef_P1_P*H1*a12*x1*a33*k^3-
2*coef_C_P^2*a1^(1+k)*x1*C1*a13*a33*k+2*coef_C_P^2*a1^(1+k)*x1*C1*a13*a33*k^2-
2*coef_C_P^2*a1^(1-k)*k*x1^2*C2*a12*a33+4*coef_C_P*a1^(1-k)*k*x1*a11*a33*coef_P1_P*H2-
2*coef_C_P^2*a1^(1-k)*k*x1*C2*a13*a33-
4*coef_C_P*a2^(1+k)*x1*a13^2*coef_P1_P*H1*k+4*coef_C_P*a2^(1+k)*x1*a13^2*coef_P1_P*H1*k^2
-2*coef_C_P*a2^(1+k)*coef_P1_P*H1*a13*a23*x1*k-
4*log(a2)*coef_C_P*x1*C2*a13^2*coef_P1_P*H1*k+4*log(a2)*coef_C_P*x1*C2*a13^2*coef_P1_P*H1
*k^3+2*coef_C_P^2*a2^(1+k)*x1^2*a13*a23*k^3*C1+2*coef_C_P*a2^(1+k)*coef_P1_P*H1*a13*a33*k
-
2*coef_C_P*a2^(1+k)*coef_P1_P*H1*a13*a33*k^2+4*log(a2)*coef_C_P*x1*C1*a13^2*coef_P1_P*H2*
k-a2^(2*k)*coef_P1_P^2*H1^2*a11*a33*k^2-a2^(2*k)*coef_C_P^2*x1^2*C1^2*a11*a33*k^2-
2*a2^(2*k)*coef_C_P*x1*C1*a11*a33*coef_P1_P*H1*k^2-
a2^(2*k)*coef_C_P^2*x1^2*C1^2*a12*a33*k^3-
2*a2^(2*k)*coef_C_P*x1*C1*a12*a33*coef_P1_P*H1*k^3+a2^(2*k)*coef_P1_P^2*H1^2*a13*a23*k^3+
a2^(2*k)*coef_P1_P^2*H1^2*a11*a33+a2^(2*k)*coef_P1_P^2*H1^2*a12*a33*k-
a2^(2*k)*coef_C_P^2*x1^2*C1^2*a13*a23*k+a2^(2*k)*coef_C_P^2*x1^2*C1^2*a12*a33*k+a2^(2*k)*
coef_C_P^2*x1^2*C1^2*a11*a33-
```

```
a2^(2*k)*coef_P1_P^2*H1^2*a13*a23*k+2*a2^(2*k)*coef_C_P*x1*C1*a12*a33*coef_P1_P*H1*k+a2^(
2*k)*coef_P1_P^2*H1^2*a13^2*k^2+2*a2^(-2*k)*coef_C_P*x1*C2*a12*a33*coef_P1_P*H2*k^3-a2^(-
2*k)*coef_C_P^2*x1^2*C2^2*a13^2*k^2-a2^(-2*k)*coef_P1_P^2*H2^2*a12*a33*k^3+a2^(-
2*k)*coef_C_P^2*x1^2*C2^2*a11*a33*k^2+a2^(-2*k)*coef_C_P^2*x1^2*C2^2*a12*a33*k-2*a2^(-
2*k)*coef_C_P*x1*C2*a13^2*coef_P1_P*H2+2*a2^(-2*k)*coef_C_P*x1*C2*a11*a33*coef_P1_P*H2-
2*a2^(-2*k)*coef_C_P*x1*C2*a12*a33*coef_P1_P*H2*k-a2^(-2*k)*coef_P1_P^2*H2^2*a11*a33-
2*a2^(-2*k)*coef_C_P*x1*C2*a13*a23*coef_P1_P*H2*k^3+a2^(-
2*k)*coef_P1_P^2*H2^2*a11*a33*k^2-a2^(-2*k)*coef_C_P^2*x1^2*C2^2*a12*a33*k^3-
4*coef_C_P^2*a1^(1+k)*x1^2*a11*C1*a33*k+4*coef_C_P^2*a1^(1+k)*x1^2*a11*C1*a33*k^2+4*coef_
C_P*a1^(1+k)*x1*a13^2*coef_P1_P*H1*k-4*coef_C_P^2*a2^(1-
k)*k^2*x1^2*a13^2*C2+2*coef_C_P^2*a2^(1-k)*k*x1^2*C2*a12*a33-4*coef_C_P*a2^(1-
k)*k*x1*a11*a33*coef_P1_P*H2+4*coef_C_P*a2^(1+k)*x1*a11*coef_P1_P*H1*a33*k-
4*coef_C_P*a2^(1+k)*x1*a11*coef_P1_P*H1*a33*k^2+a1^(2*k)*coef_P1_P^2*H1^2*a13^2+2*coef_C_
P^2*a2^(1+k)*x1^2*C1*a12*a33*k+2*coef_C_P^2*a2^(1+k)*x1*C1*a13*a33*k-
2*coef_C_P^2*a2^(1+k)*x1*C1*a13*a33*k^2+4*log(a1)*coef_C_P*x1*C2*a13^2*coef_P1_P*H1*k-
4*log(a1)*coef_C_P*x1*C2*a13^2*coef_P1_P*H1*k^3-
2*coef_C_P*a1^(1+k)*coef_P1_P*H1*a12*x1*a33*k-
4*coef_C_P*a1^(1+k)*x1*a11*coef_P1_P*H1*a33*k+4*coef_C_P*a1^(1+k)*x1*a11*coef_P1_P*H1*a33
*k^2-2*coef_C_P^2*a2^(1+k)*x1^2*C1*a13*a23*k-
4*log(a1)*coef_C_P*x1*C1*a13^2*coef_P1_P*H2*k+4*log(a1)*coef_C_P*x1*C1*a13^2*coef_P1_P*H2
*k^3+2*coef_C_P*a2^(1+k)*coef_P1_P*H1*a12*x1*a33*k-
2*coef_C_P*a1^(1+k)*coef_P1_P*H1*a13*a33*k+2*a1^(-
2*k)*coef_C_P*x1*C2*a12*a33*coef_P1_P*H2*k+2*a1^(-
2*k)*coef_C_P*x1*C2*a13*a23*coef_P1_P*H2*k^3-a1^(-2*k)*coef_P1_P^2*H2^2*a11*a33*k^2+a1^(-
2*k)*coef_C_P^2*x1^2*C2^2*a12*a33*k^3-
4*log(a2)*coef_C_P^2*x1^2*C1*a13^2*C2*k+4*log(a2)*coef_C_P*x1*C1*a11*coef_P1_P*H2*a33*k^3
-4*log(a1)*coef_C_P^2*x1^2*C1*a11*C2*a33*k+4*log(a1)*coef_C_P^2*x1^2*C1*a11*C2*a33*k^3-
4*log(a2)*coef_P1_P^2*H1*a11*H2*a33*k+4*log(a2)*coef_P1_P^2*H1*a11*H2*a33*k^3+4*log(a1)*c
oef_C_P*x1*C1*a11*coef_P1_P*H2*a33*k-
4*log(a1)*coef_C_P*x1*C1*a11*coef_P1_P*H2*a33*k^3+4*log(a1)*coef_P1_P^2*H1*a11*H2*a33*k-
4*log(a1)*coef_P1_P^2*H1*a11*H2*a33*k^3+4*log(a2)*coef_C_P^2*x1^2*C1*a11*C2*a33*k-
4*log(a2)*coef_C_P^2*x1^2*C1*a11*C2*a33*k^3-
4*log(a1)*coef_C_P*x1*C2*a11*coef_P1_P*H1*a33*k+4*log(a1)*coef_C_P*x1*C2*a11*coef_P1_P*H1
*a33*k^3-4*coef_C_P^2*a2^(1+k)*x1^2*a13^2*C1*k+4*coef_C_P^2*a2^(1+k)*x1^2*a13^2*C1*k^2-
4*coef_C_P*a1^(1-k)*k*x1*a13^2*coef_P1_P*H2+2*coef_C_P*a1^(1-
k)*k*coef_P1_P*H2*a12*a33*x1-2*coef_C_P*a1^(1-
k)*k*coef_P1_P*H2*a13*a23*x1+4*coef_C_P^2*a1^(1-k)*k*x1^2*a13^2*C2+2*coef_C_P*a1^(1-
k)*k^3*x1*a13*a23*coef_P1_P*H2+2*coef_C_P*a1^(1-k)*k^2*coef_P1_P*H2*a13*a33-
4*coef_C_P^2*a1^(1-k)*k^2*x1^2*a11*a33*C2+a1^2*coef_C_P^2*x1^2*a13*a23*k-
a1^2*coef_C_P^2*x1^2*a13*a23*k^3+2*coef_C_P*a1^(1+k)*coef_P1_P*H1*a13*a33*k^2-
2*coef_C_P^2*a2^(1+k)*x1^2*a12*k^3*C1*a33+2*coef_C_P*a1^(1+k)*coef_P1_P*H1*a13*a23*x1*k+2
*coef_C_P^2*a1^(1+k)*x1^2*C1*a13*a23*k+4*coef_C_P^2*a2^(1+k)*x1^2*a11*C1*a33*k-
4*coef_C_P^2*a2^(1+k)*x1^2*a11*C1*a33*k^2-2*coef_C_P^2*a1^(1+k)*x1^2*C1*a13*a23*k^3-
4*log(a1)*coef_P1_P^2*H1*a13^2*H2*k+4*log(a1)*coef_P1_P^2*H1*a13^2*H2*k^3+a1^(-
2*k)*coef_C_P^2*x1^2*C2^2*a11*a33-a1^(-2*k)*coef_P1_P^2*H2^2*a12*a33*k+a1^(-
2*k)*coef_C_P^2*x1^2*C2^2*a13*a23*k+a1^(-2*k)*coef_P1_P^2*H2^2*a13*a23*k-2*a1^(-
2*k)*coef_C_P*x1*C2*a13*a23*coef_P1_P*H2*k-a1^(-2*k)*coef_C_P^2*x1^2*C2^2*a13^2+a1^(-
2*k)*coef_P1_P^2*H2^2*a13^2*k^2-2*a1^(-2*k)*coef_C_P*x1*C2*a13^2*coef_P1_P*H2*k^2-a1^(-
2*k)*coef_P1_P^2*H2^2*a13*a23*k^3+2*a1^(-2*k)*coef_C_P*x1*C2*a11*a33*coef_P1_P*H2*k^2-
a1^(-2*k)*coef_C_P^2*x1^2*C2^2*a13*a23*k^3-2*a1^(-
2*k)*coef_C_P*x1*C2*a12*a33*coef_P1_P*H2*k^3+a1^(-
2*k)*coef_C_P^2*x1^2*C2^2*a13^2*k^2+a1^(-2*k)*coef_P1_P^2*H2^2*a12*a33*k^3-a1^(-
2*k)*coef_C_P^2*x1^2*C2^2*a11*a33*k^2-a1^(-2*k)*coef_C_P^2*x1^2*C2^2*a12*a33*k-2*a1^(-
2*k)*coef_C_P*x1*C2*a11*a33*coef_P1_P*H2+a1^(-2*k)*coef_P1_P^2*H2^2*a11*a33+a2^(-
2*k)*coef_P1_P^2*H2^2*a13^2+2*coef_C_P*a2^(1-k)*k^3*x1*a12*a33*coef_P1_P*H2-
4*coef_C_P*a1^(1+k)*x1*a13^2*coef_P1_P*H1*k^2+2*coef_C_P^2*a1^(1+k)*x1^2*C1*a12*a33*k^3-
2*coef_C_P*a1^(1+k)*coef_P1_P*H1*a13*a23*x1*k^3+4*log(a2)*coef_C_P^2*x1^2*C1*a13^2*C2*k^3
+2*coef_C_P*a1^(1+k)*x1*a12*coef_P1_P*H1*k^3*a33+4*log(a1)*coef_C_P^2*x1^2*C1*a13^2*C2*k-
4*log(a1)*coef_C_P^2*x1^2*C1*a13^2*C2*k^3-
```

```
2*coef_C_P^2*a1^(1+k)*x1^2*C1*a12*a33*k+a1^(2*k)*coef_C_P^2*x1^2*C1^2*a11*a33*k^2+2*a1^(2
*k)*coef_C_P*x1*C1*a11*a33*coef_P1_P*H1*k^2+a1^(2*k)*coef_C_P^2*x1^2*C1^2*a12*a33*k^3+2*a
1^(2*k)*coef_C_P*x1*C1*a12*a33*coef_P1_P*H1*k^3-a1^(2*k)*coef_P1_P^2*H1^2*a13*a23*k^3-
a1^(2*k)*coef_P1_P^2*H1^2*a11*a33-
a1^(2*k)*coef_P1_P^2*H1^2*a12*a33*k+a1^(2*k)*coef_C_P^2*x1^2*C1^2*a13*a23*k-
a1^(2*k)*coef_C_P^2*x1^2*C1^2*a12*a33*k+a1^(2*k)*coef_P1_P^2*H1^2*a13*a23*k-
2*a1^(2*k)*coef_C_P*x1*C1*a12*a33*coef_P1_P*H1*k+a1^(2*k)*coef_C_P^2*x1^2*C1^2*a13^2+2*a1
^(2*k)*coef_C_P*x1*C1*a13*a23*coef_P1_P*H1*k-
2*a1^(2*k)*coef_C_P*x1*C1*a11*a33*coef_P1_P*H1-
2*a1^(2*k)*coef_C_P*x1*C1*a13^2*coef_P1_P*H1*k^2-a1^(2*k)*coef_C_P^2*x1^2*C1^2*a13^2*k^2-
a1^(2*k)*coef_C_P^2*x1^2*C1^2*a13*a23*k^3-
2*a1^(2*k)*coef_C_P*x1*C1*a13*a23*coef_P1_P*H1*k^3+a1^(2*k)*coef_P1_P^2*H1^2*a12*a33*k^3+
2*a1^(2*k)*coef_C_P*x1*C1*a13^2*coef_P1_P*H1-
a1^2*coef_C_P^2*x1^2*a11*a33*k+a1^2*coef_C_P^2*x1^2*a11*a33*k^3-
a1^2*coef_C_P^2*x1*a13*a33*k+a1^2*coef_C_P^2*x1*a13*a33*k^3)/a33/k/(-1+k^2));
Ut1_PP = 0.5*(-L*pi*(-a2^(2*k)*coef_C_P^2*x1^2*k^3*C1^2*a22*a33-
2*a1^(2*k)*coef_C_P*x1*k^3*C1*a23^2*coef_P1_P*H1+2*coef_C_P*a1^(1+k)*a33*coef_P1_P*H1*k^2
*a23+2*coef_C_P^2*a1^(1+k)*a33*x1*k^2*C1*a23-
2*coef_C_P*a1^(1+k)*x1*a13*a23*coef_P1_P*H1*k^2-
2*coef_C_P^2*a1^(1+k)*x1^2*a13*a23*k^2*C1+4*log(a1)*coef_C_P^2*x1^2*k^2*C1*a22*C2*a33-
4*log(a1)*coef_C_P^2*x1^2*k^4*C1*a22*C2*a33+4*coef_C_P^2*a2^(1+k)*a33*x1^2*k*C1*a22+4*coe
f_C_P*a2^(1+k)*a33*coef_P1_P*H1*k*a22*x1+2*coef_C_P^2*a2^(1+k)*a33*x1*k*C1*a23-
4*coef_C_P^2*a2^(1+k)*x1^2*k*C1*a23^2+2*coef_C_P*a2^(1+k)*coef_P1_P*H1*a12*a33*x1-
2*coef_C_P*a2^(1+k)*coef_P1_P*H1*a13*a23*x1-a2^(-
2*k)*coef_C_P^2*x1^2*k*C2^2*a22*a33+a2^(-2*k)*coef_C_P^2*x1^2*k^3*C2^2*a22*a33-
a1^(2*k)*coef_P1_P^2*H1^2*a12*a33+a1^(2*k)*coef_P1_P^2*H1^2*a12*a33*k^2+a2^2*coef_C_P^2*x
1^2*a12*a33-a2^2*coef_C_P^2*x1^2*a12*a33*k^2+a1^2*coef_C_P^2*x1^2*a13*a23-
a1^2*coef_C_P^2*x1^2*a13*a23*k^2-
a1^2*coef_C_P^2*x1^2*a12*a33+a1^2*coef_C_P^2*x1^2*a12*a33*k^2+4*log(a1)*coef_C_P*x1*k^2*C
2*a22*coef_P1_P*H1*a33-
4*log(a1)*coef_C_P*x1*k^4*C2*a22*coef_P1_P*H1*a33+4*log(a2)*coef_P1_P^2*H1*k^2*a22*H2*a33
-4*log(a2)*coef_P1_P^2*H1*k^4*a22*H2*a33-
4*log(a1)*coef_C_P*x1*k^2*C1*a22*coef_P1_P*H2*a33+a1^(2*k)*coef_C_P^2*x1^2*k^3*C1^2*a22*a
33+4*log(a1)*coef_C_P*x1*k^4*C1*a22*coef_P1_P*H2*a33-
a1^(2*k)*coef_C_P^2*x1^2*k*C1^2*a22*a33-
4*log(a2)*coef_C_P*x1*k^2*C2*a22*coef_P1_P*H1*a33+4*log(a2)*coef_C_P*x1*k^4*C2*a22*coef_P
1_P*H1*a33-a1^(2*k)*coef_P1_P^2*H1^2*k*a22*a33-2*a2^(-
2*k)*coef_C_P*x1*C2*a12*coef_P1_P*H2*a33+2*a2^(-
2*k)*coef_C_P*x1*C2*a12*coef_P1_P*H2*a33*k^2-a1^(-2*k)*coef_C_P^2*x1^2*C2^2*a12*a33+a1^(-
2*k)*coef_C_P^2*x1^2*C2^2*a12*a33*k^2+4*log(a2)*coef_C_P^2*x1^2*k^2*C1*a23^2*C2-
a1^(2*k)*coef_P1_P^2*H1^2*a13*a23*k^2-
4*log(a1)*coef_C_P^2*x1^2*k^2*C1*a23^2*C2+4*log(a1)*coef_C_P^2*x1^2*k^4*C1*a23^2*C2+2*a1^
(2*k)*coef_C_P*x1*k*C1*a23^2*coef_P1_P*H1+2*a2^(-
2*k)*coef_C_P*x1*C2*a13*a23*coef_P1_P*H2-
a2^(2*k)*coef_P1_P^2*H1^2*k*a23^2+2*a1^(2*k)*coef_C_P*x1*C1*a12*coef_P1_P*H1*a33*k^2-
a2^(-2*k)*coef_P1_P^2*H2^2*k*a22*a33+a2^(-
2*k)*coef_P1_P^2*H2^2*k^3*a22*a33+2*a1^(2*k)*coef_C_P*x1*k^3*C1*a22*coef_P1_P*H1*a33+2*a1
^(-2*k)*coef_C_P*x1*C2*a13*a23*coef_P1_P*H2*k^2+a1^(2*k)*coef_P1_P^2*H1^2*a13*a23-
2*a2^(2*k)*coef_C_P*x1*k^3*C1*a22*coef_P1_P*H1*a33+2*a2^(2*k)*coef_C_P*x1*k*C1*a22*coef_P
1_P*H1*a33-4*log(a2)*coef_C_P^2*x1^2*k^4*C1*a23^2*C2-2*a1^(-
2*k)*coef_C_P*x1*C2*a13*a23*coef_P1_P*H2-
2*a1^(2*k)*coef_C_P*x1*C1*a12*coef_P1_P*H1*a33+2*coef_C_P^2*a1^(1+k)*x1^2*a12*a33*k^2*C1+
4*coef_C_P^2*a1^(1+k)*a33*x1^2*k^2*C1*a22-4*coef_C_P^2*a1^(1+k)*x1^2*k^2*C1*a23^2-
4*coef_C_P*a1^(1+k)*coef_P1_P*H1*k^2*a23^2*x1+2*coef_C_P*a1^(1+k)*x1*a12*a33*coef_P1_P*H1
*k^2+4*coef_C_P*a1^(1+k)*a33*coef_P1_P*H1*k^2*a22*x1+4*coef_C_P*a1^(1+k)*coef_P1_P*H1*k*a
23^2*x1-2*coef_C_P*a1^(1+k)*a33*coef_P1_P*H1*k*a23-2*coef_C_P^2*a1^(1+k)*x1^2*C1*a12*a33-
4*coef_C_P^2*a1^(1+k)*a33*x1^2*k*C1*a22-4*coef_C_P*a1^(1+k)*a33*coef_P1_P*H1*k*a22*x1-
2*coef_C_P^2*a1^(1+k)*a33*x1*k*C1*a23+4*log(a2)*coef_C_P*x1*k^2*C2*a23^2*coef_P1_P*H1-
4*log(a2)*coef_C_P*x1*k^4*C2*a23^2*coef_P1_P*H1+a2^(-
```

```
2*k)*coef_C_P^2*x1^2*C2^2*a13*a23*k^2-2*a2^(-
2*k)*coef_C_P*x1*k*C2*a23^2*coef_P1_P*H2+2*a2^(-
2*k)*coef_C_P*x1*k^3*C2*a23^2*coef_P1_P*H2-a2^(-2*k)*coef_P1_P^2*H2^2*a13*a23+a1^(-
2*k)*coef_C_P^2*x1^2*k^3*C2^2*a23^2+4*log(a1)*coef_C_P*x1*k^2*C1*a23^2*coef_P1_P*H2-
4*log(a1)*coef_C_P*x1*k^4*C1*a23^2*coef_P1_P*H2-
4*log(a1)*coef_C_P*x1*k^2*C2*a23^2*coef_P1_P*H1+4*log(a1)*coef_C_P*x1*k^4*C2*a23^2*coef_P
1_P*H1-a2^(-2*k)*coef_C_P^2*x1^2*C2^2*a13*a23-2*a2^(-
2*k)*coef_C_P*x1*C2*a13*a23*coef_P1_P*H2*k^2+a2^(2*k)*coef_P1_P^2*H1^2*k^3*a23^2-
2*a1^(2*k)*coef_C_P*x1*k*C1*a22*coef_P1_P*H1*a33+a2^(2*k)*coef_P1_P^2*H1^2*a12*a33-
a2^(2*k)*coef_P1_P^2*H1^2*a12*a33*k^2-a1^(-2*k)*coef_C_P^2*x1^2*k*C2^2*a23^2-
2*coef_C_P*a1^(1+k)*coef_P1_P*H1*a12*a33*x1+2*coef_C_P*a1^(1+k)*coef_P1_P*H1*a13*a23*x1+4
*coef_C_P^2*a1^(1+k)*x1^2*k*C1*a23^2+2*coef_C_P^2*a1^(1+k)*x1^2*C1*a13*a23-2*a1^(-
2*k)*coef_C_P*x1*k*C2*a22*coef_P1_P*H2*a33+2*a1^(-
2*k)*coef_C_P*x1*k^3*C2*a22*coef_P1_P*H2*a33-
a2^(2*k)*coef_C_P^2*x1^2*k*C1^2*a23^2+a2^(2*k)*coef_C_P^2*x1^2*k^3*C1^2*a23^2+2*a1^(-
2*k)*coef_C_P*x1*k*C2*a23^2*coef_P1_P*H2-2*a1^(-
2*k)*coef_C_P*x1*k^3*C2*a23^2*coef_P1_P*H2+a1^(2*k)*coef_C_P^2*x1^2*C1^2*a13*a23-
a1^(2*k)*coef_C_P^2*x1^2*C1^2*a13*a23*k^2+2*a1^(2*k)*coef_C_P*x1*C1*a13*a23*coef_P1_P*H1-
2*a1^(2*k)*coef_C_P*x1*C1*a13*a23*coef_P1_P*H1*k^2-
2*a2^(2*k)*coef_C_P*x1*k*C1*a23^2*coef_P1_P*H1+2*a2^(2*k)*coef_C_P*x1*k^3*C1*a23^2*coef_P
1_P*H1+a2^(-2*k)*coef_P1_P^2*H2^2*a13*a23*k^2-a1^(-2*k)*coef_P1_P^2*H2^2*k*a23^2+a1^(-
2*k)*coef_P1_P^2*H2^2*k^3*a23^2-
a2^(2*k)*coef_P1_P^2*H1^2*a13*a23+a2^(2*k)*coef_P1_P^2*H1^2*a13*a23*k^2-
4*log(a2)*coef_C_P*x1*k^2*C1*a23^2*coef_P1_P*H2+4*log(a2)*coef_C_P*x1*k^4*C1*a23^2*coef_P
1_P*H2+4*log(a1)*coef_P1_P^2*H1*k^2*a23^2*H2+a1^(2*k)*coef_P1_P^2*H1^2*k*a23^2-
a2^2*coef_C_P^2*x1*a23*a33*k^2-4*log(a1)*coef_P1_P^2*H1*k^4*a23^2*H2-
2*a2^(2*k)*coef_C_P*x1*C1*a13*a23*coef_P1_P*H1+2*a2^(2*k)*coef_C_P*x1*C1*a13*a23*coef_P1_
P*H1*k^2-a1^(2*k)*coef_P1_P^2*H1^2*k^3*a23^2+a1^(2*k)*coef_C_P^2*x1^2*k*C1^2*a23^2-
a1^(2*k)*coef_C_P^2*x1^2*k^3*C1^2*a23^2+a2^2*coef_C_P^2*x1^2*a23^2*k^2+a1^(-
2*k)*coef_C_P^2*x1^2*C2^2*a13*a23+4*log(a2)*coef_P1_P^2*H1*k^4*a23^2*H2+a2^(-
2*k)*coef_P1_P^2*H2^2*a12*a33-a2^(-2*k)*coef_P1_P^2*H2^2*a12*a33*k^2-a1^(-
2*k)*coef_C_P^2*x1^2*C2^2*a13*a23*k^2+a1^(-2*k)*coef_P1_P^2*H2^2*a13*a23-a1^(-
2*k)*coef_P1_P^2*H2^2*a13*a23*k^2-a2^2*coef_C_P^2*x1^2*a23^2-
a1^2*coef_C_P^2*x1^2*a22*a33+a1^2*coef_C_P^2*x1^2*a22*a33*k^2-
4*log(a2)*coef_P1_P^2*H1*k^2*a23^2*H2-4*log(a1)*coef_P1_P^2*H1*k^2*a22*H2*a33-2*a2^(-
2*k)*coef_C_P*x1*k^3*C2*a22*coef_P1_P*H2*a33+a2^(-2*k)*coef_C_P^2*x1^2*C2^2*a12*a33-a2^(-
2*k)*coef_C_P^2*x1^2*C2^2*a12*a33*k^2-
a1^2*coef_C_P^2*x1*a23*a33+a1^2*coef_C_P^2*x1*a23*a33*k^2+2*a2^(2*k)*coef_C_P*x1*C1*a12*c
oef_P1_P*H1*a33-2*a2^(2*k)*coef_C_P*x1*C1*a12*coef_P1_P*H1*a33*k^2-
a1^(2*k)*coef_C_P^2*x1^2*C1^2*a12*a33+2*coef_C_P*a2^(1-k)*a33*coef_P1_P*H2*k*a23+2*a2^(-
2*k)*coef_C_P*x1*k*C2*a22*coef_P1_P*H2*a33-
a1^2*coef_C_P^2*x1^2*a23^2*k^2+a1^2*coef_C_P^2*x1^2*a23^2-a1^(-
2*k)*coef_P1_P^2*H2^2*a12*a33+a1^(-2*k)*coef_P1_P^2*H2^2*a12*a33*k^2+a1^(-
2*k)*coef_P1_P^2*H2^2*k*a22*a33-a1^(-2*k)*coef_P1_P^2*H2^2*k^3*a22*a33-
2*coef_C_P*a2^(1+k)*a33*coef_P1_P*H1*k^2*a23+4*coef_C_P*a2^(1+k)*coef_P1_P*H1*k^2*a23^2*x
1+2*coef_C_P^2*a2^(1+k)*x1^2*C1*a12*a33-2*coef_C_P*a2^(1+k)*x1*a12*a33*coef_P1_P*H1*k^2-
4*coef_C_P*a2^(1+k)*a33*coef_P1_P*H1*k^2*a22*x1-
2*coef_C_P^2*a2^(1+k)*a33*x1*k^2*C1*a23+2*coef_C_P*a2^(1+k)*x1*a13*a23*coef_P1_P*H1*k^2+2
*coef_C_P^2*a2^(1+k)*x1^2*a13*a23*k^2*C1+4*coef_C_P^2*a2^(1+k)*x1^2*k^2*C1*a23^2+4*log(a2
)*coef_C_P*x1*k^2*C1*a22*coef_P1_P*H2*a33-
4*log(a2)*coef_C_P*x1*k^4*C1*a22*coef_P1_P*H2*a33-a2^(-
2*k)*coef_C_P^2*x1^2*k^3*C2^2*a23^2+2*a1^(-
2*k)*coef_C_P*x1*C2*a12*coef_P1_P*H2*a33+a2^(2*k)*coef_P1_P^2*H1^2*k*a22*a33-a2^(-
2*k)*coef_P1_P^2*H2^2*k^3*a23^2+a1^(-2*k)*coef_C_P^2*x1^2*k*C2^2*a22*a33-a1^(-
2*k)*coef_C_P^2*x1^2*k^3*C2^2*a22*a33+a2^(2*k)*coef_C_P^2*x1^2*C1^2*a12*a33-
a2^(2*k)*coef_C_P^2*x1^2*C1^2*a12*a33*k^2-2*a1^(-
2*k)*coef_C_P*x1*C2*a12*coef_P1_P*H2*a33*k^2+a2^(-2*k)*coef_C_P^2*x1^2*k*C2^2*a23^2-
a2^2*coef_C_P^2*x1^2*a13*a23+a2^2*coef_C_P^2*x1^2*a13*a23*k^2-
a2^(2*k)*coef_P1_P^2*H1^2*k^3*a22*a33-
```

```
a2^(2*k)*coef_C_P^2*x1^2*C1^2*a13*a23+a2^(2*k)*coef_C_P^2*x1^2*C1^2*a13*a23*k^2+a1^(2*k)*
coef_C_P^2*x1^2*C1^2*a12*a33*k^2-
4*log(a2)*coef_C_P^2*x1^2*k^2*C1*a22*C2*a33+4*log(a2)*coef_C_P^2*x1^2*k^4*C1*a22*C2*a33+4
*coef_C_P*a2^(1-k)*a33*coef_P1_P*H2*k*a22*x1+2*coef_C_P^2*a2^(1-
k)*x1^2*a13*a23*k^2*C2+4*coef_C_P*a2^(1-k)*a33*coef_P1_P*H2*k^2*a22*x1-4*coef_C_P*a1^(1-
k)*a33*coef_P1_P*H2*k*a22*x1-2*coef_C_P*a1^(1-k)*a33*coef_P1_P*H2*k*a23+a2^(-
2*k)*coef_P1_P^2*H2^2*k*a23^2-2*coef_C_P^2*a1^(1-k)*x1^2*a13*a23*k^2*C2-4*coef_C_P*a1^(1-
k)*a33*coef_P1_P*H2*k^2*a22*x1-2*coef_C_P*a1^(1-k)*a33*coef_P1_P*H2*k^2*a23-
4*coef_C_P*a2^(1-k)*coef_P1_P*H2*k^2*a23^2*x1-2*coef_C_P^2*a2^(1-k)*a33*x1*k^2*C2*a23-
4*coef_C_P^2*a2^(1-k)*a33*x1^2*k*C2*a22-2*coef_C_P^2*a2^(1+k)*x1^2*a12*a33*k^2*C1-
4*coef_C_P^2*a2^(1+k)*a33*x1^2*k^2*C1*a22-
4*coef_C_P*a2^(1+k)*coef_P1_P*H1*k*a23^2*x1+2*coef_C_P*a2^(1+k)*a33*coef_P1_P*H1*k*a23+4*
log(a1)*coef_P1_P^2*H1*k^4*a22*H2*a33-
2*coef_C_P^2*a2^(1+k)*x1^2*C1*a13*a23+4*coef_C_P^2*a2^(1-k)*x1^2*k*C2*a23^2-
2*coef_C_P*a2^(1-k)*coef_P1_P*H2*a12*a33*x1+2*coef_C_P*a2^(1-
k)*coef_P1_P*H2*a13*a23*x1+a1^(2*k)*coef_P1_P^2*H1^2*k^3*a22*a33+2*coef_C_P*a2^(1-
k)*a33*coef_P1_P*H2*k^2*a23-2*coef_C_P*a2^(1-k)*x1*a13*a23*coef_P1_P*H2*k^2-
2*coef_C_P^2*a2^(1-k)*x1^2*a12*a33*k^2*C2-4*coef_C_P^2*a2^(1-
k)*a33*x1^2*k^2*C2*a22+4*coef_C_P^2*a2^(1-k)*x1^2*k^2*C2*a23^2+2*coef_C_P*a2^(1-
k)*x1*a12*a33*coef_P1_P*H2*k^2-4*coef_C_P*a2^(1-k)*coef_P1_P*H2*k*a23^2*x1-
2*coef_C_P^2*a2^(1-k)*a33*x1*k*C2*a23-2*coef_C_P*a1^(1-k)*x1*a12*a33*coef_P1_P*H2*k^2-
4*coef_C_P^2*a1^(1-k)*x1^2*k*C2*a23^2+4*coef_C_P*a1^(1-
k)*coef_P1_P*H2*k^2*a23^2*x1+2*coef_C_P^2*a1^(1-k)*a33*x1*k^2*C2*a23+4*coef_C_P^2*a1^(1-
k)*a33*x1^2*k*C2*a22+2*coef_C_P*a1^(1-k)*coef_P1_P*H2*a12*a33*x1-2*coef_C_P^2*a2^(1-
k)*x1^2*C2*a13*a23+2*coef_C_P^2*a2^(1-k)*x1^2*C2*a12*a33+2*coef_C_P*a1^(1-
k)*x1*a13*a23*coef_P1_P*H2*k^2+2*coef_C_P^2*a1^(1-
k)*x1^2*a12*a33*k^2*C2+4*coef_C_P^2*a1^(1-k)*a33*x1^2*k^2*C2*a22-4*coef_C_P^2*a1^(1-
k)*x1^2*k^2*C2*a23^2+a2^2*coef_C_P^2*x1^2*a22*a33-
a2^2*coef_C_P^2*x1^2*a22*a33*k^2+a2^2*coef_C_P^2*x1*a23*a33-2*coef_C_P*a1^(1-
k)*coef_P1_P*H2*a13*a23*x1+4*coef_C_P*a1^(1-
k)*coef_P1_P*H2*k*a23^2*x1+2*coef_C_P^2*a1^(1-k)*a33*x1*k*C2*a23+2*coef_C_P^2*a1^(1-
k)*x1^2*C2*a13*a23-2*coef_C_P^2*a1^(1-
k)*x1^2*C2*a12*a33+a2^(2*k)*coef_C_P^2*x1^2*k*C1^2*a22*a33)/a33/(-1+k^2));

Uz1_PP = 0.5*(coef_C_P*L*pi*(-a2^2*coef_C_P*a33+a2^2*coef_C_P*a13*x1-
a2^2*coef_C_P*a13*x1*k^2+a2^2*coef_C_P*x1*a23-a2^2*coef_C_P*x1*a23*k^2+a1^2*coef_C_P*a33-
a1^2*coef_C_P*a13*x1+a1^2*coef_C_P*a13*x1*k^2-2*a2^(1-k)*a13*coef_P1_P*H2*k-2*a2^(1-
k)*a13*coef_P1_P*H2+2*a2^(1-k)*coef_C_P*a13*x1*C2+a2^2*coef_C_P*a33*k^2-
a1^2*coef_C_P*x1*a23+a1^2*coef_C_P*x1*a23*k^2+2*a2^(1-k)*coef_C_P*a13*x1*C2*k-2*a2^(1-
k)*coef_C_P*x1*k*C2*a23-2*a2^(1-k)*coef_C_P*x1*k^2*C2*a23+2*a2^(1-
k)*coef_P1_P*H2*k*a23+2*a2^(1-k)*coef_P1_P*H2*k^2*a23-
2*a1^(1+k)*coef_C_P*x1*k*C1*a23+2*a1^(1+k)*coef_C_P*x1*k^2*C1*a23-
2*a1^(1+k)*coef_P1_P*H1*k*a23+2*a1^(1+k)*coef_P1_P*H1*k^2*a23-
2*a1^(1+k)*coef_C_P*a13*x1*C1+2*a1^(1+k)*coef_C_P*a13*x1*C1*k+2*a1^(1+k)*a13*coef_P1_P*H1
*k-2*a1^(1-k)*coef_C_P*a13*x1*C2-2*a1^(1-k)*coef_C_P*a13*x1*C2*k+2*a1^(1-
k)*a13*coef_P1_P*H2+2*a2^(1+k)*a13*coef_P1_P*H1-2*a1^(1+k)*a13*coef_P1_P*H1-
a1^2*coef_C_P*a33*k^2+2*a1^(1-k)*a13*coef_P1_P*H2*k+2*a1^(1-
k)*coef_C_P*x1*k*C2*a23+2*a1^(1-k)*coef_C_P*x1*k^2*C2*a23-2*a1^(1-k)*coef_P1_P*H2*k*a23-
2*a1^(1-k)*coef_P1_P*H2*k^2*a23-
2*a2^(1+k)*coef_P1_P*H1*k^2*a23+2*a2^(1+k)*coef_C_P*x1*k*C1*a23-
2*a2^(1+k)*coef_C_P*x1*k^2*C1*a23+2*a2^(1+k)*coef_P1_P*H1*k*a23+2*a2^(1+k)*coef_C_P*a13*x
1*C1-2*a2^(1+k)*coef_C_P*a13*x1*C1*k-2*a2^(1+k)*a13*coef_P1_P*H1*k)/(-1+k^2));

Ur2_PP = 0.5*(-L*(4*a0^2*a1^4*log(a1)*coef_P1_P^2*pi+2*a0^4*a1^2*log(a1)*coef_P1_P*nu*pi-
a0^2*a1^2*nu*coef_F1_P+4*a0^2*a1^4*log(a0)*pi*coef_P1_P+a0^6*pi-a1^4*a0^2*pi*nu-
2*a0^4*a1^2*log(a1)*nu*pi-
4*a0^4*a1^2*log(a0)*pi+4*a0^4*a1^2*log(a1)*pi+3*a0^4*a1^2*nu*pi+2*a0^4*a1^2*log(a0)*nu*pi
+a1^2*a0^4*pi*coef_P1_P^2-4*a0^2*a1^4*log(a0)*coef_P1_P^2*pi+a1^6*coef_P1_P^2*nu*pi-
coef_P1_P*a0^2*a1^2*nu*coef_F1_P-
```

```
2*a0^6*nu*pi+4*a0^4*a1^2*log(a0)*coef_P1_P*pi+2*a0^2*a1^2*log(a1)*nu*coef_F1_P+a0^4*nu*co
ef_F1_P-a1^6*coef_P1_P^2*pi-
2*a0^4*a1^2*log(a0)*coef_P1_P*nu*pi+a1^2*a0^4*pi*nu*coef_P1_P^2-
4*a0^2*a1^4*log(a1)*pi*coef_P1_P+a1^4*coef_P1_P*nu*coef_F1_P-
4*a0^4*a1^2*log(a1)*coef_P1_P*pi-
4*coef_P1_P*a0^4*a1^2*pi+2*a0^2*a1^2*log(a0)*coef_P1_P*nu*coef_F1_P+4*a0^2*a1^4*pi*coef_P
1_P-2*a0^2*a1^2*log(a0)*nu*coef_F1_P-a0^2*a1^4*nu*pi*coef_P1_P-
2*a0^2*a1^2*log(a1)*coef_P1_P*nu*coef_F1_P-a1^4*a0^2*pi-
2*coef_P1_P^2*a0^2*a1^4*nu*pi+coef_P1_P*a0^4*a1^2*nu*pi)/E/(-a1^2+a0^2)^2);

Ut2_PP =
0.5*(L*(4*a0^2*a1^4*log(a1)*coef_P1_P^2*pi+2*a0^4*a1^2*log(a1)*coef_P1_P*nu*pi+a0^2*a1^2*
nu*coef_F1_P+4*a0^2*a1^4*log(a0)*pi*coef_P1_P-a0^6*pi+a1^4*a0^2*pi*nu-
2*a0^4*a1^2*log(a1)*nu*pi-4*a0^4*a1^2*log(a0)*pi+4*a0^4*a1^2*log(a1)*pi-
3*a0^4*a1^2*nu*pi+2*a0^4*a1^2*log(a0)*nu*pi-a1^2*a0^4*pi*coef_P1_P^2-
4*a0^2*a1^4*log(a0)*coef_P1_P^2*pi-
a1^6*coef_P1_P^2*nu*pi+coef_P1_P*a0^2*a1^2*nu*coef_F1_P+2*a0^6*nu*pi+4*a0^4*a1^2*log(a0)*
coef_P1_P*pi+2*a0^2*a1^2*log(a1)*nu*coef_F1_P-a0^4*nu*coef_F1_P+a1^6*coef_P1_P^2*pi-
2*a0^4*a1^2*log(a0)*coef_P1_P*nu*pi-a1^2*a0^4*pi*nu*coef_P1_P^2-
4*a0^2*a1^4*log(a1)*pi*coef_P1_P-a1^4*coef_P1_P*nu*coef_F1_P-
4*a0^4*a1^2*log(a1)*coef_P1_P*pi+4*coef_P1_P*a0^4*a1^2*pi+2*a0^2*a1^2*log(a0)*coef_P1_P*n
u*coef_F1_P-4*a0^2*a1^4*pi*coef_P1_P-
2*a0^2*a1^2*log(a0)*nu*coef_F1_P+a0^2*a1^4*nu*pi*coef_P1_P-
2*a0^2*a1^2*log(a1)*coef_P1_P*nu*coef_F1_P+a1^4*a0^2*pi+2*coef_P1_P^2*a0^2*a1^4*nu*pi-
coef_P1_P*a0^4*a1^2*nu*pi)/E/(-a1^2+a0^2)^2);

Uz2_PP = 0.5*(-(coef_F1_P^2-2*coef_F1_P*pi*a0^2+2*coef_F1_P*nu*pi*a0^2-
2*coef_F1_P*nu*pi*coef_P1_P*a1^2+pi^2*a0^4-
2*pi^2*a0^4*nu+2*pi^2*a0^2*nu*coef_P1_P*a1^2)*L/pi/E/(-a1^2+a0^2));

Ur1_FF = 0.5*(L*pi*(-a2^(-2*k)*coef_P1_F^2*H2^2*a13*a23*k^3-
2*coef_C_F^2*a2^(k+1)*x1^2*C1*a13*a23*k^3+4*log(a2)*coef_P1_F^2*H1*a13^2*H2*k^3+2*coef_C_
F*a2^(k+1)*coef_P1_F*H1*a13*a23*x1*k-2*coef_C_F^2*a2^(k+1)*x1^2*C1*a12*a33*k-
2*coef_C_F*a2^(k+1)*coef_P1_F*H1*a13*a23*x1*k^3+2*coef_C_F^2*a1^(1-
k)*k^3*x1^2*a13*a23*C2-2*coef_C_F^2*a1^(1-k)*k^3*x1^2*a12*a33*C2+2*coef_C_F*a1^(1-
k)*k^3*x1*a12*a33*coef_P1_F*H2-2*coef_C_F*a1^(1-
k)*k^3*x1*a13*a23*coef_P1_F*H2+4*coef_C_F^2*a1^(1-k)*k^2*x1^2*a11*a33*C2-
4*coef_C_F^2*a1^(1-k)*k^2*x1^2*a13^2*C2+2*coef_C_F^2*a1^(1-k)*k^2*x1*C2*a13*a33-
2*coef_C_F*a1^(1-k)*k^2*coef_P1_F*H2*a13*a33-4*coef_C_F*a1^(1-
k)*k^2*x1*a11*a33*coef_P1_F*H2+4*coef_C_F*a1^(1-
k)*k^2*x1*a13^2*coef_P1_F*H2+4*coef_C_F*a1^(1-k)*k*x1*a13^2*coef_P1_F*H2-
4*coef_C_F^2*a1^(1-k)*k*x1^2*a13^2*C2+4*coef_C_F^2*a1^(1-
k)*k*x1^2*a11*a33*C2+2*coef_C_F^2*a1^(1-k)*k*x1*C2*a13*a33-2*coef_C_F^2*a1^(1-
k)*k*x1^2*C2*a13*a23+2*coef_C_F^2*a1^(1-k)*k*x1^2*C2*a12*a33-2*coef_C_F*a1^(1-
k)*k*coef_P1_F*H2*a13*a33-2*a1^(-2*k)*coef_C_F*x1*C2*a13^2*coef_P1_F*H2+2*a1^(-
2*k)*coef_C_F*x1*C2*a11*a33*coef_P1_F*H2-2*a1^(-
2*k)*coef_C_F*x1*C2*a12*a33*coef_P1_F*H2*k+a1^(-2*k)*coef_C_F^2*x1^2*C2^2*a13^2-a1^(-
2*k)*coef_P1_F^2*H2^2*a13*a23*k-a1^(-2*k)*coef_P1_F^2*H2^2*a11*a33+a1^(-
2*k)*coef_P1_F^2*H2^2*a12*a33*k+2*a1^(-2*k)*coef_C_F*x1*C2*a13*a23*coef_P1_F*H2*k+a1^(-
2*k)*coef_C_F^2*x1^2*C2^2*a12*a33*k+2*a1^(-
2*k)*coef_C_F*x1*C2*a12*a33*coef_P1_F*H2*k^3+a1^(-2*k)*coef_P1_F^2*H2^2*a11*a33*k^2+a1^(-
2*k)*coef_C_F^2*x1^2*C2^2*a13*a23*k^3-2*a1^(-
2*k)*coef_C_F*x1*C2*a13*a23*coef_P1_F*H2*k^3+2*a1^(-
2*k)*coef_C_F*x1*C2*a13^2*coef_P1_F*H2*k^2+a1^(-
2*k)*coef_C_F^2*x1^2*C2^2*a11*a33*k^2+a1^(-2*k)*coef_P1_F^2*H2^2*a13*a23*k^3-2*a1^(-
2*k)*coef_C_F*x1*C2*a11*a33*coef_P1_F*H2*k^2-a1^(-2*k)*coef_C_F^2*x1^2*C2^2*a13^2*k^2-
a1^(-2*k)*coef_C_F^2*x1^2*C2^2*a12*a33*k^3-a1^(-2*k)*coef_P1_F^2*H2^2*a13^2*k^2-a1^(-
2*k)*coef_C_F^2*x1^2*C2^2*a13*a23*k+2*coef_C_F*a1^(k+1)*coef_P1_F*H1*a12*x1*a33*k+2*coef_
C_F^2*a2^(k+1)*x1*C1*a13*a33*k^2-
```

```
2*coef_C_F^2*a2^(k+1)*x1*C1*a13*a33*k+a2^2*coef_C_F^2*x1^2*a13^2*k+a2^2*coef_C_F^2*x1^2*a
13*a23*k-a2^2*coef_C_F^2*x1^2*a13*a23*k^3+2*coef_C_F*a2^(1-
k)*k^3*x1*a13*a23*coef_P1_F*H2+a1^(2*k)*coef_C_F^2*x1^2*C1^2*a11*a33+a1^(2*k)*coef_C_F^2*
x1^2*C1^2*a13^2*k^2+4*log(a1)*coef_C_F*x1*C1*a13^2*coef_P1_F*H2*k-
4*log(a1)*coef_C_F*x1*C1*a13^2*coef_P1_F*H2*k^3-
2*coef_C_F*a2^(k+1)*coef_P1_F*H1*a12*x1*a33*k+a1^(2*k)*coef_P1_F^2*H1^2*a12*a33*k-
a1^(2*k)*coef_P1_F^2*H1^2*a13*a23*k-a1^(2*k)*coef_P1_F^2*H1^2*a11*a33*k^2+a2^(-
2*k)*coef_P1_F^2*H2^2*a12*a33*k^3-
a1^2*coef_C_F^2*x1^2*a12*a33*k^3+a2^2*coef_C_F^2*x1*a13*a33*k^3+4*log(a1)*coef_P1_F^2*H1*
a13^2*H2*k+a1^2*coef_C_F^2*x1^2*a13^2*k^3-a1^2*coef_C_F^2*x1^2*a13^2*k-
a1^2*coef_C_F^2*x1^2*a13*a23*k+a1^2*coef_C_F^2*x1^2*a13*a23*k^3+a1^2*coef_C_F^2*x1^2*a11*
a33*k-a1^2*coef_C_F^2*x1^2*a11*a33*k^3-a2^2*coef_C_F^2*x1^2*a13^2*k^3-4*coef_C_F*a1^(1-
k)*k*x1*a11*a33*coef_P1_F*H2+2*coef_C_F*a1^(1-k)*k*coef_P1_F*H2*a13*a23*x1-
2*coef_C_F*a1^(1-k)*k*coef_P1_F*H2*a12*a33*x1-
a2^(2*k)*coef_P1_F^2*H1^2*a12*a33*k+a2^(2*k)*coef_P1_F^2*H1^2*a13*a23*k-
2*a2^(2*k)*coef_C_F*x1*C1*a13*a23*coef_P1_F*H1*k^3+a2^(2*k)*coef_P1_F^2*H1^2*a11*a33*k^2+
2*a2^(2*k)*coef_C_F*x1*C1*a12*a33*coef_P1_F*H1*k^3+a2^(2*k)*coef_C_F^2*x1^2*C1^2*a12*a33*
k^3+a2^(2*k)*coef_P1_F^2*H1^2*a12*a33*k^3-a2^(2*k)*coef_P1_F^2*H1^2*a13*a23*k^3-
2*a2^(2*k)*coef_C_F*x1*C1*a13^2*coef_P1_F*H1*k^2-
a2^(2*k)*coef_C_F^2*x1^2*C1^2*a13^2*k^2+a2^(2*k)*coef_C_F^2*x1^2*C1^2*a11*a33*k^2+a2^(2*k
)*coef_C_F^2*x1^2*C1^2*a13*a23*k-
a2^(2*k)*coef_C_F^2*x1^2*C1^2*a11*a33+2*a2^(2*k)*coef_C_F*x1*C1*a13*a23*coef_P1_F*H1*k+2*
a2^(2*k)*coef_C_F*x1*C1*a13^2*coef_P1_F*H1+2*a2^(2*k)*coef_C_F*x1*C1*a11*a33*coef_P1_F*H1
*k^2-a2^(2*k)*coef_C_F^2*x1^2*C1^2*a13*a23*k^3-
2*a2^(2*k)*coef_C_F*x1*C1*a12*a33*coef_P1_F*H1*k-
2*a2^(2*k)*coef_C_F*x1*C1*a11*a33*coef_P1_F*H1-a2^(2*k)*coef_C_F^2*x1^2*C1^2*a12*a33*k-
a2^(2*k)*coef_P1_F^2*H1^2*a13^2*k^2-
a2^(2*k)*coef_P1_F^2*H1^2*a11*a33+a2^(2*k)*coef_C_F^2*x1^2*C1^2*a13^2+4*coef_C_F*a2^(k+1)
*x1*a13^2*coef_P1_F*H1*k-4*coef_C_F*a2^(k+1)*x1*a13^2*coef_P1_F*H1*k^2-
2*coef_C_F^2*a1^(k+1)*x1^2*C1*a12*a33*k^3-
2*coef_C_F^2*a1^(k+1)*x1^2*C1*a13*a23*k+2*coef_C_F*a1^(k+1)*coef_P1_F*H1*a13*a33*k-
2*coef_C_F*a1^(k+1)*coef_P1_F*H1*a13*a33*k^2+4*coef_C_F^2*a1^(k+1)*x1^2*a11*C1*a33*k-
4*coef_C_F^2*a1^(k+1)*x1^2*a11*C1*a33*k^2-
2*coef_C_F*a1^(k+1)*coef_P1_F*H1*a12*x1*a33*k^3+2*coef_C_F^2*a1^(k+1)*x1^2*C1*a13*a23*k^3
+2*coef_C_F*a1^(k+1)*coef_P1_F*H1*a13*a23*x1*k^3+4*coef_C_F*a1^(k+1)*x1*a11*coef_P1_F*H1*
a33*k-4*coef_C_F*a1^(k+1)*x1*a11*coef_P1_F*H1*a33*k^2-
4*log(a1)*coef_P1_F^2*H1*a13^2*H2*k^3+2*coef_C_F^2*a2^(1-k)*k^3*x1^2*a12*a33*C2-
2*coef_C_F*a2^(1-k)*k^3*x1*a12*a33*coef_P1_F*H2-4*coef_C_F^2*a2^(1-
k)*k^2*x1^2*a11*a33*C2-2*coef_C_F^2*a2^(1-k)*k^2*x1*C2*a13*a33+2*coef_C_F*a2^(1-
k)*k^2*coef_P1_F*H2*a13*a33-a1^(-
2*k)*coef_C_F^2*x1^2*C2^2*a11*a33+a2^2*coef_C_F^2*x1^2*a12*a33*k^3+4*coef_C_F*a2^(1-
k)*k^2*x1*a11*a33*coef_P1_F*H2-4*coef_C_F*a2^(1-k)*k^2*x1*a13^2*coef_P1_F*H2-
4*coef_C_F*a2^(1-k)*k*x1*a13^2*coef_P1_F*H2+4*coef_C_F^2*a2^(1-k)*k*x1^2*a13^2*C2-
4*coef_C_F^2*a2^(1-k)*k*x1^2*a11*a33*C2-2*coef_C_F^2*a2^(1-
k)*k*x1*C2*a13*a33+2*coef_C_F^2*a2^(1-k)*k*x1^2*C2*a13*a23-2*coef_C_F^2*a2^(1-
k)*k*x1^2*C2*a12*a33+2*coef_C_F*a2^(1-k)*k*coef_P1_F*H2*a13*a33+4*coef_C_F*a2^(1-
k)*k*x1*a11*a33*coef_P1_F*H2-2*coef_C_F*a2^(1-
k)*k*coef_P1_F*H2*a13*a23*x1+2*coef_C_F*a2^(1-k)*k*coef_P1_F*H2*a12*a33*x1-
2*coef_C_F*a1^(k+1)*coef_P1_F*H1*a13*a23*x1*k+2*coef_C_F^2*a1^(k+1)*x1*C1*a13*a33*k-
2*coef_C_F^2*a1^(k+1)*x1*C1*a13*a33*k^2-
4*log(a1)*coef_C_F*x1*C2*a13^2*coef_P1_F*H1*k+4*log(a1)*coef_C_F*x1*C2*a13^2*coef_P1_F*H1
*k^3+4*log(a1)*coef_C_F*x1*C2*a11*coef_P1_F*H1*a33*k-
4*log(a2)*coef_P1_F^2*H1*a11*H2*a33*k^3-
4*log(a1)*coef_C_F*x1*C2*a11*coef_P1_F*H1*a33*k^3-
4*log(a1)*coef_P1_F^2*H1*a11*H2*a33*k+4*log(a1)*coef_P1_F^2*H1*a11*H2*a33*k^3-
4*log(a2)*coef_C_F*x1*C2*a11*coef_P1_F*H1*a33*k+4*log(a2)*coef_C_F*x1*C2*a11*coef_P1_F*H1
*a33*k^3-
4*log(a1)*coef_C_F*x1*C1*a11*coef_P1_F*H2*a33*k+4*log(a1)*coef_C_F*x1*C1*a11*coef_P1_F*H2
*a33*k^3-
```

```
4*log(a2)*coef_C_F^2*x1^2*C1*a11*C2*a33*k+4*log(a2)*coef_C_F^2*x1^2*C1*a11*C2*a33*k^3+4*l
og(a2)*coef_P1_F^2*H1*a11*H2*a33*k+4*log(a1)*coef_C_F^2*x1^2*C1*a11*C2*a33*k-
4*log(a1)*coef_C_F^2*x1^2*C1*a11*C2*a33*k^3+2*coef_C_F^2*a1^(k+1)*x1^2*C1*a12*a33*k+4*log
(a2)*coef_C_F*x1*C1*a11*coef_P1_F*H2*a33*k-
4*log(a2)*coef_C_F*x1*C1*a11*coef_P1_F*H2*a33*k^3+2*a2^(-
2*k)*coef_C_F*x1*C2*a13^2*coef_P1_F*H2-2*a2^(-
2*k)*coef_C_F*x1*C2*a11*a33*coef_P1_F*H2+2*a2^(-
2*k)*coef_C_F*x1*C2*a12*a33*coef_P1_F*H2*k+a2^(-2*k)*coef_P1_F^2*H2^2*a13*a23*k+a2^(-
2*k)*coef_P1_F^2*H2^2*a11*a33-2*a2^(-2*k)*coef_C_F*x1*C2*a13*a23*coef_P1_F*H2*k-a2^(-
2*k)*coef_C_F^2*x1^2*C2^2*a12*a33*k+a2^(-2*k)*coef_C_F^2*x1^2*C2^2*a11*a33-2*a2^(-
2*k)*coef_C_F*x1*C2*a12*a33*coef_P1_F*H2*k^3-a2^(-2*k)*coef_P1_F^2*H2^2*a11*a33*k^2-a2^(-
2*k)*coef_C_F^2*x1^2*C2^2*a13*a23*k^3+2*a2^(-
2*k)*coef_C_F*x1*C2*a13*a23*coef_P1_F*H2*k^3-2*a2^(-
2*k)*coef_C_F*x1*C2*a13^2*coef_P1_F*H2*k^2-a2^(-
2*k)*coef_C_F^2*x1^2*C2^2*a11*a33*k^2+2*a2^(-
2*k)*coef_C_F*x1*C2*a11*a33*coef_P1_F*H2*k^2+a2^(-
2*k)*coef_C_F^2*x1^2*C2^2*a13^2*k^2+a2^(-2*k)*coef_C_F^2*x1^2*C2^2*a12*a33*k^3+a2^(-
2*k)*coef_P1_F^2*H2^2*a13^2*k^2+a2^(-
2*k)*coef_C_F^2*x1^2*C2^2*a13*a23*k+2*coef_C_F^2*a2^(k+1)*x1^2*C1*a13*a23*k+4*coef_C_F^2*
a1^(k+1)*x1^2*a13^2*C1*k^2+2*a1^(2*k)*coef_C_F*x1*C1*a13*a23*coef_P1_F*H1*k^3-
2*a1^(2*k)*coef_C_F*x1*C1*a12*a33*coef_P1_F*H1*k^3-
a1^(2*k)*coef_C_F^2*x1^2*C1^2*a12*a33*k^3-
a1^(2*k)*coef_P1_F^2*H1^2*a12*a33*k^3+a1^(2*k)*coef_P1_F^2*H1^2*a13*a23*k^3+2*a1^(2*k)*co
ef_C_F*x1*C1*a13^2*coef_P1_F*H1*k^2-a1^(2*k)*coef_C_F^2*x1^2*C1^2*a11*a33*k^2-
a1^(2*k)*coef_C_F^2*x1^2*C1^2*a13*a23*k-2*a1^(2*k)*coef_C_F*x1*C1*a13*a23*coef_P1_F*H1*k-
2*a1^(2*k)*coef_C_F*x1*C1*a13^2*coef_P1_F*H1-
2*a1^(2*k)*coef_C_F*x1*C1*a11*a33*coef_P1_F*H1*k^2+a1^(2*k)*coef_C_F^2*x1^2*C1^2*a13*a23*
k^3+2*a1^(2*k)*coef_C_F*x1*C1*a12*a33*coef_P1_F*H1*k+2*a1^(2*k)*coef_C_F*x1*C1*a11*a33*co
ef_P1_F*H1+a1^(2*k)*coef_C_F^2*x1^2*C1^2*a12*a33*k-a1^(2*k)*coef_C_F^2*x1^2*C1^2*a13^2-
4*coef_C_F*a1^(k+1)*x1*a13^2*coef_P1_F*H1*k+4*coef_C_F*a1^(k+1)*x1*a13^2*coef_P1_F*H1*k^2
+4*log(a2)*coef_C_F^2*x1^2*C1*a13^2*C2*k-4*log(a2)*coef_C_F^2*x1^2*C1*a13^2*C2*k^3-
4*log(a1)*coef_C_F^2*x1^2*C1*a13^2*C2*k+4*log(a1)*coef_C_F^2*x1^2*C1*a13^2*C2*k^3-a1^(-
2*k)*coef_P1_F^2*H2^2*a12*a33*k^3-
a2^2*coef_C_F^2*x1*a13*a33*k+a1^2*coef_C_F^2*x1^2*a12*a33*k-
a2^2*coef_C_F^2*x1^2*a12*a33*k-
a2^2*coef_C_F^2*x1^2*a11*a33*k+a2^2*coef_C_F^2*x1^2*a11*a33*k^3+a1^2*coef_C_F^2*x1*a13*a3
3*k-a1^2*coef_C_F^2*x1*a13*a33*k^3-
a1^(2*k)*coef_P1_F^2*H1^2*a13^2+a2^(2*k)*coef_P1_F^2*H1^2*a13^2+a1^(-
2*k)*coef_P1_F^2*H2^2*a13^2-a2^(-
2*k)*coef_P1_F^2*H2^2*a13^2+a1^(2*k)*coef_P1_F^2*H1^2*a13^2*k^2-a2^(-
2*k)*coef_C_F^2*x1^2*C2^2*a13^2-
4*coef_C_F^2*a2^(k+1)*x1^2*a11*C1*a33*k+4*coef_C_F^2*a2^(k+1)*x1^2*a11*C1*a33*k^2-
4*coef_C_F^2*a1^(k+1)*x1^2*a13^2*C1*k-2*coef_C_F^2*a2^(1-
k)*k^3*x1^2*a13*a23*C2+4*coef_C_F^2*a2^(1-k)*k^2*x1^2*a13^2*C2-a2^(-
2*k)*coef_P1_F^2*H2^2*a12*a33*k+a1^(2*k)*coef_P1_F^2*H1^2*a11*a33+4*coef_C_F^2*a2^(k+1)*x
1^2*a13^2*C1*k-4*coef_C_F^2*a2^(k+1)*x1^2*a13^2*C1*k^2-
2*coef_C_F*a2^(k+1)*coef_P1_F*H1*a13*a33*k+2*coef_C_F*a2^(k+1)*coef_P1_F*H1*a13*a33*k^2-
4*log(a2)*coef_C_F*x1*C1*a13^2*coef_P1_F*H2*k+4*log(a2)*coef_C_F*x1*C1*a13^2*coef_P1_F*H2
*k^3+4*log(a2)*coef_C_F*x1*C2*a13^2*coef_P1_F*H1*k-
4*log(a2)*coef_C_F*x1*C2*a13^2*coef_P1_F*H1*k^3+2*coef_C_F*a2^(k+1)*coef_P1_F*H1*a12*x1*a
33*k^3+2*coef_C_F^2*a2^(k+1)*x1^2*a12*k^3*C1*a33-
4*coef_C_F*a2^(k+1)*x1*a11*coef_P1_F*H1*a33*k+4*coef_C_F*a2^(k+1)*x1*a11*coef_P1_F*H1*a33
*k^2-4*log(a2)*coef_P1_F^2*H1*a13^2*H2*k)/a33/k/(k^2-1));

Ut1_FF = 0.5*(-L*pi*(a2^(2*k)*coef_P1_F^2*H1^2*k*a22*a33-
2*a1^(2*k)*coef_C_F*x1*C1*a12*coef_P1_F*H1*a33+2*a1^(2*k)*coef_C_F*x1*C1*a12*coef_P1_F*H1
*a33*k^2-a1^(-2*k)*coef_C_F^2*x1^2*k^3*C2^2*a22*a33+2*coef_C_F*a2^(1-
k)*coef_P1_F*H2*a13*a23*x1-2*coef_C_F^2*a2^(1-k)*x1^2*C2*a13*a23+4*coef_C_F^2*a2^(1-
k)*x1^2*k^2*C2*a23^2+2*coef_C_F*a2^(1-
```

```
k)*a33*coef_P1_F*H2*k^2*a23+a1^(2*k)*coef_P1_F^2*H1^2*k*a23^2+a1^(2*k)*coef_P1_F^2*H1^2*k
^3*a22*a33-4*coef_C_F^2*a2^(1-k)*a33*x1^2*k^2*C2*a22-2*coef_C_F^2*a2^(1-
k)*a33*x1*k*C2*a23-2*coef_C_F*a2^(1-k)*coef_P1_F*H2*a12*a33*x1-2*coef_C_F^2*a2^(1-
k)*a33*x1*k^2*C2*a23+2*coef_C_F^2*a2^(1-k)*x1^2*a13*a23*k^2*C2-
a2^(2*k)*coef_C_F^2*x1^2*C1^2*a12*a33*k^2-a1^(2*k)*coef_P1_F^2*H1^2*k^3*a23^2-
a1^(2*k)*coef_P1_F^2*H1^2*k*a22*a33+a2^(2*k)*coef_C_F^2*x1^2*C1^2*a12*a33+2*a2^(2*k)*coef
_C_F*x1*C1*a12*coef_P1_F*H1*a33-2*a2^(2*k)*coef_C_F*x1*C1*a12*coef_P1_F*H1*a33*k^2+a1^(-
2*k)*coef_C_F^2*x1^2*k*C2^2*a22*a33+a2^2*coef_C_F^2*x1^2*a22*a33-
a2^2*coef_C_F^2*x1^2*a22*a33*k^2-a2^2*coef_C_F^2*x1^2*a23^2-2*coef_C_F*a2^(1-
k)*x1*a13*a23*coef_P1_F*H2*k^2+4*log(a1)*coef_C_F*x1*k^2*C2*a22*coef_P1_F*H1*a33-
4*log(a1)*coef_C_F*x1*k^4*C2*a22*coef_P1_F*H1*a33+4*log(a2)*coef_P1_F^2*H1*k^2*a22*H2*a33
+a2^2*coef_C_F^2*x1^2*a23^2*k^2+a2^2*coef_C_F^2*x1^2*a12*a33-
a2^2*coef_C_F^2*x1^2*a12*a33*k^2+2*coef_C_F*a2^(1-
k)*x1*a12*a33*coef_P1_F*H2*k^2+4*coef_C_F*a2^(1-k)*a33*coef_P1_F*H2*k^2*a22*x1-
2*coef_C_F^2*a2^(1-k)*x1^2*a12*a33*k^2*C2+4*coef_C_F*a2^(1-k)*a33*coef_P1_F*H2*k*a22*x1-
a1^2*coef_C_F^2*x1^2*a12*a33+a1^2*coef_C_F^2*x1^2*a12*a33*k^2+4*coef_C_F*a2^(k+1)*a33*coe
f_P1_F*H1*k*a22*x1+2*coef_C_F*a2^(k+1)*a33*coef_P1_F*H1*k*a23-
4*coef_C_F*a2^(k+1)*coef_P1_F*H1*k*a23^2*x1+4*coef_C_F^2*a2^(k+1)*a33*x1^2*k*C1*a22-
a2^2*coef_C_F^2*x1^2*a13*a23+a2^2*coef_C_F^2*x1^2*a13*a23*k^2-
a1^2*coef_C_F^2*x1^2*a23^2*k^2+4*log(a2)*coef_C_F^2*x1^2*k^4*C1*a22*C2*a33+a1^(2*k)*coef_
P1_F^2*H1^2*a23*a13-
4*coef_C_F^2*a2^(k+1)*a33*x1^2*k^2*C1*a22+2*coef_C_F^2*a2^(k+1)*a33*x1*k*C1*a23+a1^2*coef
_C_F^2*x1^2*a23^2+2*coef_C_F*a2^(k+1)*coef_P1_F*H1*a12*a33*x1+2*coef_C_F^2*a2^(k+1)*x1^2*
C1*a12*a33-2*coef_C_F^2*a2^(k+1)*a33*x1*k^2*C1*a23-
4*coef_C_F*a2^(k+1)*a33*coef_P1_F*H1*k^2*a22*x1+4*coef_C_F^2*a2^(1-k)*x1^2*k*C2*a23^2-
4*coef_C_F*a2^(1-k)*coef_P1_F*H2*k*a23^2*x1-
4*log(a2)*coef_P1_F^2*H1*k^4*a22*H2*a33+4*log(a2)*coef_C_F^2*x1^2*k^2*C1*a23^2*C2-
a2^(2*k)*coef_P1_F^2*H1^2*a23*a13-4*log(a2)*coef_C_F^2*x1^2*k^4*C1*a23^2*C2-
4*log(a2)*coef_C_F*x1*k^2*C2*a22*coef_P1_F*H1*a33+4*log(a2)*coef_P1_F^2*H1*k^4*a23^2*H2+4
*log(a2)*coef_C_F*x1*k^4*C2*a22*coef_P1_F*H1*a33-
2*coef_C_F*a2^(k+1)*a33*coef_P1_F*H1*k^2*a23-
2*coef_C_F^2*a2^(k+1)*x1^2*a12*a33*k^2*C1+4*coef_C_F*a2^(k+1)*coef_P1_F*H1*k^2*a23^2*x1+4
*coef_C_F^2*a2^(k+1)*x1^2*k^2*C1*a23^2-
2*coef_C_F*a2^(k+1)*x1*a12*a33*coef_P1_F*H1*k^2+2*coef_C_F*a2^(k+1)*x1*a13*a23*coef_P1_F*
H1*k^2-
2*a2^(2*k)*coef_C_F*x1*C1*a23*a13*coef_P1_F*H1+2*coef_C_F^2*a2^(k+1)*x1^2*a13*a23*k^2*C1+
2*coef_C_F^2*a2^(1-k)*x1^2*C2*a12*a33+2*coef_C_F*a2^(1-
k)*a33*coef_P1_F*H2*k*a23+a2^(2*k)*coef_P1_F^2*H1^2*k^3*a23^2-4*coef_C_F^2*a2^(1-
k)*a33*x1^2*k*C2*a22-4*coef_C_F*a2^(1-k)*coef_P1_F*H2*k^2*a23^2*x1-
4*log(a1)*coef_C_F*x1*k^2*C1*a22*coef_P1_F*H2*a33+4*log(a1)*coef_C_F*x1*k^4*C1*a22*coef_P
1_F*H2*a33-
4*log(a2)*coef_P1_F^2*H1*k^2*a23^2*H2+2*a1^(2*k)*coef_C_F*x1*C1*a23*a13*coef_P1_F*H1-
a1^(2*k)*coef_C_F^2*x1^2*k*C1^2*a22*a33+a1^(2*k)*coef_C_F^2*x1^2*k^3*C1^2*a22*a33-a1^(-
2*k)*coef_P1_F^2*H2^2*a12*a33+a1^(-
2*k)*coef_P1_F^2*H2^2*a12*a33*k^2+a2^(2*k)*coef_P1_F^2*H1^2*a12*a33+2*a2^(2*k)*coef_C_F*x
1*C1*a23*a13*coef_P1_F*H1*k^2-4*coef_C_F^2*a2^(k+1)*x1^2*k*C1*a23^2-
a1^(2*k)*coef_C_F^2*x1^2*C1^2*a12*a33+a1^(2*k)*coef_C_F^2*x1^2*C1^2*a12*a33*k^2+a1^(-
2*k)*coef_P1_F^2*H2^2*k*a22*a33-a2^(-2*k)*coef_P1_F^2*H2^2*k*a22*a33+a2^(-
2*k)*coef_P1_F^2*H2^2*a13*a23*k^2-a1^(-2*k)*coef_C_F^2*x1^2*C2^2*a12*a33+a1^(-
2*k)*coef_C_F^2*x1^2*C2^2*a12*a33*k^2-a2^(2*k)*coef_P1_F^2*H1^2*a12*a33*k^2+2*a2^(-
2*k)*coef_C_F*x1*k*C2*a22*coef_P1_F*H2*a33-2*a2^(-
2*k)*coef_C_F*x1*k^3*C2*a22*coef_P1_F*H2*a33+a2^(-
2*k)*coef_P1_F^2*H2^2*k^3*a22*a33+4*log(a1)*coef_C_F^2*x1^2*k^2*C1*a22*C2*a33+4*log(a2)*c
oef_C_F*x1*k^2*C1*a22*coef_P1_F*H2*a33-4*log(a2)*coef_C_F*x1*k^4*C1*a22*coef_P1_F*H2*a33-
a2^(-2*k)*coef_P1_F^2*H2^2*a13*a23-2*a1^(2*k)*coef_C_F*x1*C1*a23*a13*coef_P1_F*H1*k^2-
a2^(2*k)*coef_C_F^2*x1^2*C1^2*a23*a13+a2^(2*k)*coef_C_F^2*x1^2*C1^2*a23*a13*k^2-a1^(-
2*k)*coef_P1_F^2*H2^2*k^3*a22*a33+2*a2^(2*k)*coef_C_F*x1*k*C1*a22*coef_P1_F*H1*a33-
2*a2^(2*k)*coef_C_F*x1*k^3*C1*a22*coef_P1_F*H1*a33+a2^(2*k)*coef_P1_F^2*H1^2*a23*a13*k^2-
4*log(a1)*coef_C_F*x1*k^2*C2*a23^2*coef_P1_F*H1+4*log(a1)*coef_C_F*x1*k^4*C2*a23^2*coef_P
```

```
1_F*H1-a1^(-2*k)*coef_P1_F^2*H2^2*k*a23^2-
4*log(a1)*coef_C_F^2*x1^2*k^4*C1*a22*C2*a33+a1^2*coef_C_F^2*x1^2*a13*a23-
a1^2*coef_C_F^2*x1^2*a13*a23*k^2+4*log(a1)*coef_C_F*x1*k^2*C1*a23^2*coef_P1_F*H2-
4*log(a1)*coef_C_F*x1*k^4*C1*a23^2*coef_P1_F*H2+a2^(-2*k)*coef_C_F^2*x1^2*C2^2*a12*a33-
4*log(a1)*coef_P1_F^2*H1*k^4*a23^2*H2-
2*coef_C_F^2*a2^(k+1)*x1^2*C1*a13*a23+a1^(2*k)*coef_C_F^2*x1^2*C1^2*a23*a13-
a1^(2*k)*coef_C_F^2*x1^2*C1^2*a23*a13*k^2+a1^(-
2*k)*coef_P1_F^2*H2^2*k^3*a23^2+4*log(a1)*coef_P1_F^2*H1*k^2*a23^2*H2+a1^(2*k)*coef_C_F^2
*x1^2*k*C1^2*a23^2-
a1^(2*k)*coef_C_F^2*x1^2*k^3*C1^2*a23^2+2*a1^(2*k)*coef_C_F*x1*k*C1*a23^2*coef_P1_F*H1-
a2^(-2*k)*coef_C_F^2*x1^2*C2^2*a12*a33*k^2-2*a1^(-
2*k)*coef_C_F*x1*k*C2*a22*coef_P1_F*H2*a33+2*a1^(-
2*k)*coef_C_F*x1*k^3*C2*a22*coef_P1_F*H2*a33-
2*a1^(2*k)*coef_C_F*x1*k^3*C1*a23^2*coef_P1_F*H1+a1^(-2*k)*coef_P1_F^2*H2^2*a13*a23-
2*a1^(2*k)*coef_C_F*x1*k*C1*a22*coef_P1_F*H1*a33+2*a1^(2*k)*coef_C_F*x1*k^3*C1*a22*coef_P
1_F*H1*a33-4*log(a2)*coef_C_F^2*x1^2*k^2*C1*a22*C2*a33-a2^(-
2*k)*coef_P1_F^2*H2^2*k^3*a23^2+4*coef_C_F^2*a1^(1-k)*a33*x1^2*k*C2*a22-
4*log(a1)*coef_C_F^2*x1^2*k^2*C1*a23^2*C2+4*log(a1)*coef_C_F^2*x1^2*k^4*C1*a23^2*C2+4*log
(a2)*coef_C_F*x1*k^2*C2*a23^2*coef_P1_F*H1-
2*a2^(2*k)*coef_C_F*x1*k*C1*a23^2*coef_P1_F*H1+2*a2^(2*k)*coef_C_F*x1*k^3*C1*a23^2*coef_P
1_F*H1-a1^(-2*k)*coef_P1_F^2*H2^2*a13*a23*k^2-2*coef_C_F*a1^(1-
k)*a33*coef_P1_F*H2*k*a23+2*a1^(-2*k)*coef_C_F*x1*k*C2*a23^2*coef_P1_F*H2-2*a1^(-
2*k)*coef_C_F*x1*k^3*C2*a23^2*coef_P1_F*H2-2*coef_C_F*a1^(1-
k)*coef_P1_F*H2*a13*a23*x1+2*coef_C_F^2*a1^(1-k)*x1^2*C2*a13*a23-
4*log(a2)*coef_C_F*x1*k^4*C2*a23^2*coef_P1_F*H1+2*a2^(-
2*k)*coef_C_F*x1*C2*a13*a23*coef_P1_F*H2-2*a2^(-
2*k)*coef_C_F*x1*C2*a13*a23*coef_P1_F*H2*k^2+4*coef_C_F*a1^(1-
k)*coef_P1_F*H2*k^2*a23^2*x1+4*coef_C_F^2*a1^(1-
k)*a33*x1^2*k^2*C2*a22+2*coef_C_F^2*a1^(1-k)*a33*x1*k*C2*a23+2*coef_C_F*a1^(1-
k)*coef_P1_F*H2*a12*a33*x1+2*coef_C_F*a1^(1-k)*x1*a13*a23*coef_P1_F*H2*k^2-
4*coef_C_F^2*a1^(1-k)*x1^2*k^2*C2*a23^2-2*coef_C_F*a1^(1-
k)*a33*coef_P1_F*H2*k^2*a23+2*coef_C_F^2*a1^(1-k)*a33*x1*k^2*C2*a23-2*coef_C_F^2*a1^(1-
k)*x1^2*a13*a23*k^2*C2+2*coef_C_F^2*a1^(1-k)*x1^2*a12*a33*k^2*C2-
a1^(2*k)*coef_P1_F^2*H1^2*a23*a13*k^2+2*coef_C_F^2*a1^(k+1)*x1^2*C1*a13*a23+2*coef_C_F*a1
^(k+1)*coef_P1_F*H1*a13*a23*x1+a2^(-2*k)*coef_P1_F^2*H2^2*k*a23^2-
a1^2*coef_C_F^2*x1^2*a22*a33-4*coef_C_F*a1^(1-k)*a33*coef_P1_F*H2*k*a22*x1-
4*coef_C_F^2*a1^(1-k)*x1^2*k*C2*a23^2+4*coef_C_F*a1^(1-k)*coef_P1_F*H2*k*a23^2*x1-
2*coef_C_F*a1^(1-k)*x1*a12*a33*coef_P1_F*H2*k^2+a1^2*coef_C_F^2*x1^2*a22*a33*k^2-
4*coef_C_F*a1^(k+1)*a33*coef_P1_F*H1*k*a22*x1-
2*coef_C_F*a1^(k+1)*a33*coef_P1_F*H1*k*a23+4*coef_C_F*a1^(k+1)*coef_P1_F*H1*k*a23^2*x1-
4*coef_C_F^2*a1^(k+1)*a33*x1^2*k*C1*a22+2*coef_C_F^2*a1^(k+1)*a33*x1*k^2*C1*a23+4*coef_C_
F*a1^(k+1)*a33*coef_P1_F*H1*k^2*a22*x1+2*coef_C_F*a1^(k+1)*a33*coef_P1_F*H1*k^2*a23+2*coe
f_C_F^2*a1^(k+1)*x1^2*a12*a33*k^2*C1+4*coef_C_F^2*a1^(k+1)*a33*x1^2*k^2*C1*a22-
2*coef_C_F^2*a1^(k+1)*a33*x1*k*C1*a23-2*coef_C_F*a1^(k+1)*coef_P1_F*H1*a12*a33*x1-
2*coef_C_F^2*a1^(k+1)*x1^2*C1*a12*a33+a2^(-
2*k)*coef_C_F^2*x1^2*k^3*C2^2*a22*a33+a2^(2*k)*coef_C_F^2*x1^2*k*C1^2*a22*a33-
a2^(2*k)*coef_C_F^2*x1^2*k^3*C1^2*a22*a33+4*log(a1)*coef_P1_F^2*H1*k^4*a22*H2*a33-
4*coef_C_F*a1^(1-k)*a33*coef_P1_F*H2*k^2*a22*x1-a2^(-2*k)*coef_C_F^2*x1^2*k*C2^2*a22*a33-
a2^(-2*k)*coef_C_F^2*x1^2*k^3*C2^2*a23^2-2*coef_C_F^2*a1^(1-k)*x1^2*C2*a12*a33-
a2^(2*k)*coef_P1_F^2*H1^2*k*a23^2-
2*coef_C_F^2*a1^(k+1)*x1^2*a13*a23*k^2*C1+4*coef_C_F^2*a1^(k+1)*x1^2*k*C1*a23^2-2*a1^(-
2*k)*coef_C_F*x1*C2*a13*a23*coef_P1_F*H2+a2^(-2*k)*coef_P1_F^2*H2^2*a12*a33-
4*coef_C_F*a1^(k+1)*coef_P1_F*H1*k^2*a23^2*x1-
4*coef_C_F^2*a1^(k+1)*x1^2*k^2*C1*a23^2+2*coef_C_F*a1^(k+1)*x1*a12*a33*coef_P1_F*H1*k^2-
2*coef_C_F*a1^(k+1)*x1*a13*a23*coef_P1_F*H1*k^2-
2*coef_C_F*a2^(k+1)*coef_P1_F*H1*a13*a23*x1+2*a1^(-
2*k)*coef_C_F*x1*C2*a13*a23*coef_P1_F*H2*k^2-a1^(-2*k)*coef_C_F^2*x1^2*k*C2^2*a23^2+a1^(-
2*k)*coef_C_F^2*x1^2*k^3*C2^2*a23^2+2*a1^(-2*k)*coef_C_F*x1*C2*a12*coef_P1_F*H2*a33-
2*a1^(-2*k)*coef_C_F*x1*C2*a12*coef_P1_F*H2*a33*k^2-
```

```
4*log(a1)*coef_P1_F^2*H1*k^2*a22*H2*a33+a1^(2*k)*coef_P1_F^2*H1^2*a12*a33*k^2-a2^(-
2*k)*coef_C_F^2*x1^2*C2^2*a13*a23+a2^(-2*k)*coef_C_F^2*x1^2*C2^2*a13*a23*k^2-a2^(-
2*k)*coef_P1_F^2*H2^2*a12*a33*k^2-2*a2^(-2*k)*coef_C_F*x1*C2*a12*coef_P1_F*H2*a33+2*a2^(-
2*k)*coef_C_F*x1*C2*a12*coef_P1_F*H2*a33*k^2+a2^(-2*k)*coef_C_F^2*x1^2*k*C2^2*a23^2+a1^(-
2*k)*coef_C_F^2*x1^2*C2^2*a13*a23-a1^(-
2*k)*coef_C_F^2*x1^2*C2^2*a13*a23*k^2+a1^2*coef_C_F^2*x1*a23*a33*k^2-
a2^(2*k)*coef_P1_F^2*H1^2*k^3*a22*a33-2*a2^(-
2*k)*coef_C_F*x1*k*C2*a23^2*coef_P1_F*H2+2*a2^(-
2*k)*coef_C_F*x1*k^3*C2*a23^2*coef_P1_F*H2-a2^(2*k)*coef_C_F^2*x1^2*k*C1^2*a23^2-
a1^2*coef_C_F^2*x1*a23*a33+a2^2*coef_C_F^2*x1*a23*a33-
a2^2*coef_C_F^2*x1*a23*a33*k^2+a2^(2*k)*coef_C_F^2*x1^2*k^3*C1^2*a23^2-
4*log(a2)*coef_C_F*x1*k^2*C1*a23^2*coef_P1_F*H2+4*log(a2)*coef_C_F*x1*k^4*C1*a23^2*coef_P
1_F*H2-a1^(2*k)*coef_P1_F^2*H1^2*a12*a33)/a33/(k^2-1));

Uz1_FF = 0.5*(coef_C_F*L*pi*(2*a1^(k+1)*coef_C_F*a13*x1*C1*k-2*a2^(1-
k)*a13*coef_P1_F*H2*k-2*a1^(k+1)*a13*coef_P1_F*H1-2*a1^(k+1)*coef_C_F*a13*x1*C1+2*a2^(1-
k)*coef_P1_F*H2*k^2*a23+2*a2^(k+1)*coef_C_F*x1*k*C1*a23-
2*a2^(k+1)*coef_C_F*x1*k^2*C1*a23+2*a2^(k+1)*coef_P1_F*H1*k*a23-
2*a2^(k+1)*coef_P1_F*H1*k^2*a23+2*a2^(k+1)*coef_C_F*a13*x1*C1-
2*a2^(k+1)*coef_C_F*a13*x1*C1*k-2*a2^(k+1)*a13*coef_P1_F*H1*k-2*a1^(1-
k)*coef_C_F*a13*x1*C2+2*a1^(1-k)*a13*coef_P1_F*H2*k-2*a1^(1-
k)*coef_C_F*a13*x1*C2*k+2*a1^(1-k)*coef_C_F*x1*k*C2*a23+2*a1^(1-
k)*coef_C_F*x1*k^2*C2*a23-2*a1^(1-k)*coef_P1_F*H2*k*a23-2*a1^(1-k)*coef_P1_F*H2*k^2*a23-
2*a1^(k+1)*coef_C_F*x1*k*C1*a23+2*a1^(k+1)*coef_C_F*x1*k^2*C1*a23-
2*a1^(k+1)*coef_P1_F*H1*k*a23+2*a1^(k+1)*coef_P1_F*H1*k^2*a23-
a2^2*coef_C_F*a33+a2^2*coef_C_F*a33*k^2+2*a2^(1-k)*coef_C_F*a13*x1*C2+2*a2^(1-
k)*coef_C_F*a13*x1*C2*k+a2^2*coef_C_F*a13*x1-
a2^2*coef_C_F*a13*x1*k^2+a2^2*coef_C_F*x1*a23-a2^2*coef_C_F*x1*a23*k^2-2*a2^(1-
k)*coef_C_F*x1*k*C2*a23-2*a2^(1-k)*coef_C_F*x1*k^2*C2*a23+2*a2^(1-k)*coef_P1_F*H2*k*a23-
a1^2*coef_C_F*a33*k^2+a1^2*coef_C_F*a33+2*a2^(k+1)*a13*coef_P1_F*H1+2*a1^(1-
k)*a13*coef_P1_F*H2-2*a2^(1-k)*a13*coef_P1_F*H2-
a1^2*coef_C_F*a13*x1+a1^2*coef_C_F*a13*x1*k^2-
a1^2*coef_C_F*x1*a23+a1^2*coef_C_F*x1*a23*k^2+2*a1^(k+1)*a13*coef_P1_F*H1*k)/(k^2-1));

Ur2_FF = 0.5*(-L*coef_P1_F*a1^2*(a0^2*nu+a1^2*nu*coef_F1_F-a0^2*nu*coef_F1_F-
2*a0^2*log(a0)*nu+2*a0^2*log(a1)*nu-a1^2*nu-
4*a0^2*a1^2*log(a0)*coef_P1_F*pi+a0^4*pi*nu*coef_P1_F+4*a0^2*a1^2*log(a1)*coef_P1_F*pi+a1
^4*coef_P1_F*nu*pi-
2*a0^2*coef_P1_F*a1^2*nu*pi+2*a0^2*log(a0)*nu*coef_F1_F+a0^4*pi*coef_P1_F-
a1^4*coef_P1_F*pi-2*a0^2*log(a1)*nu*coef_F1_F)/E/(a1^2-a0^2)^2);

Ut2_FF = 0.5*(-L*coef_P1_F*a1^2*(a0^2*nu+a1^2*nu*coef_F1_F-
a0^2*nu*coef_F1_F+2*a0^2*log(a0)*nu-2*a0^2*log(a1)*nu-
a1^2*nu+4*a0^2*a1^2*log(a0)*coef_P1_F*pi+a0^4*pi*nu*coef_P1_F-
4*a0^2*a1^2*log(a1)*coef_P1_F*pi+a1^4*coef_P1_F*nu*pi-2*a0^2*coef_P1_F*a1^2*nu*pi-
2*a0^2*log(a0)*nu*coef_F1_F+a0^4*pi*coef_P1_F-
a1^4*coef_P1_F*pi+2*a0^2*log(a1)*nu*coef_F1_F)/E/(a1^2-a0^2)^2);

Uz2_FF = 0.5*(-(-1+2*coef_F1_F-2*nu*pi*coef_P1_F*a1^2-
coef_F1_F^2+2*coef_F1_F*nu*pi*coef_P1_F*a1^2)*L/pi/E/(a1^2-a0^2));

Ur1_PF = (L*pi*(a2^(-2*k)*coef_P1_F*H2^2*a13^2*coef_P1_P*k^2+a2^(-
2*k)*coef_P1_F*H2^2*a11*a33*coef_P1_P+a2^(-2*k)*coef_C_F*x1^2*C2^2*a12*a33*k^3*coef_C_P-
a2^(-2*k)*coef_C_P*x1*C2*a12*a33*coef_P1_F*H2*k^3-a2^(-
2*k)*coef_C_F*x1*C2*a12*a33*coef_P1_P*H2*k^3-a2^(-
2*k)*coef_C_F*x1^2*C2^2*a13*a23*k^3*coef_C_P+a1^(-
2*k)*coef_P1_F*H2^2*a13*a23*k^3*coef_P1_P-a1^(-2*k)*coef_C_F*x1^2*C2^2*a11*a33*coef_C_P-
a1^(-2*k)*coef_C_P*x1*C2*a13^2*coef_P1_F*H2+a1^(-
2*k)*coef_P1_F*H2^2*a13^2*coef_P1_P+a1^(-2*k)*coef_C_F*x1^2*C2^2*a13*a23*k^3*coef_C_P-
```

```
a1^(-2*k)*coef_C_P*x1*C2*a13*a23*coef_P1_F*H2*k^3-a1^(-
2*k)*coef_C_F*x1*C2*a13*a23*coef_P1_P*H2*k^3-a1^(-
2*k)*coef_P1_F*H2^2*a12*a33*k^3*coef_P1_P-coef_C_F*a1^(1-k)*k^2*coef_P1_P*H2*a13*a33-
2*coef_C_F*a1^(1-
k)*k*x1*a11*a33*coef_P1_P*H2+2*coef_C_F*a2^(k+1)*x1^2*C1*a12*coef_C_P*a33*k^3-
coef_C_P*a2^(k+1)*coef_P1_F*H1*a13*a33*k+coef_C_P*a2^(k+1)*coef_P1_F*H1*a13*a33*k^2+4*coe
f_C_F*a2^(k+1)*x1^2*a11*C1*coef_C_P*a33*k^2-
4*log(a1)*coef_C_F*x1^2*C1*a13^2*C2*coef_C_P*k+4*log(a1)*coef_C_F*x1^2*C1*a13^2*C2*coef_C
_P*k^3+2*coef_C_P*a2^(k+1)*x1*a13^2*coef_P1_F*H1*k-
2*coef_C_P*a2^(k+1)*x1*a13^2*coef_P1_F*H1*k^2+2*coef_C_F*a1^(k+1)*x1*C1*a13*coef_C_P*a33*
k-
2*coef_C_F*a1^(k+1)*x1*C1*a13*coef_C_P*a33*k^2+a2^(2*k)*coef_C_F*x1^2*C1^2*a12*a33*k^3*co
ef_C_P-a2^(2*k)*coef_C_F*x1*C1*a13^2*coef_P1_P*H1*k^2-
2*coef_C_F*a1^(k+1)*x1*a13^2*coef_P1_P*H1*k+2*coef_C_F*a1^(k+1)*x1*a13^2*coef_P1_P*H1*k^2
+coef_C_F*a1^(1-k)*k^3*x1*a12*a33*coef_P1_P*H2+2*coef_C_F*a1^(1-
k)*k*x1*a13^2*coef_P1_P*H2+2*coef_C_F*a1^(1-k)*k^2*x1*a13^2*coef_P1_P*H2+coef_C_F*a1^(1-
k)*k*coef_P1_P*H2*a13*a23*x1-a1^(-2*k)*coef_C_F*x1^2*C2^2*a12*a33*k^3*coef_C_P+a1^(-
2*k)*coef_C_P*x1*C2*a12*a33*coef_P1_F*H2*k^3+a1^(-
2*k)*coef_C_F*x1*C2*a12*a33*coef_P1_P*H2*k^3+a1^(2*k)*coef_C_P*x1*C1*a13*a23*coef_P1_F*H1
*k^3+a1^(2*k)*coef_C_F*x1*C1*a13*a23*coef_P1_P*H1*k^3+coef_C_P*a2^(1-
k)*k^2*coef_P1_F*H2*a13*a33+2*coef_C_P*a2^(1-k)*k^2*x1*a11*a33*coef_P1_F*H2-
2*coef_C_P*a2^(1-k)*k^2*x1*a13^2*coef_P1_F*H2-
2*log(a2)*coef_C_P*x1*C2*a11*coef_P1_F*H1*a33*k+2*log(a2)*coef_C_P*x1*C2*a11*coef_P1_F*H1
*a33*k^3+coef_C_P*a1^(k+1)*coef_P1_F*H1*a12*x1*a33*k+4*coef_C_F*a1^(k+1)*x1^2*a13^2*C1*co
ef_C_P*k^2+2*coef_C_P*a1^(k+1)*x1*a11*coef_P1_F*H1*a33*k-
2*coef_C_P*a1^(k+1)*x1*a11*coef_P1_F*H1*a33*k^2+4*log(a1)*coef_P1_F*H1*a13^2*H2*coef_P1_P
*k-4*log(a1)*coef_P1_F*H1*a13^2*H2*coef_P1_P*k^3-
coef_C_P*a1^(k+1)*coef_P1_F*H1*a13*a33*k^2+2*log(a2)*coef_C_P*x1*C1*a11*coef_P1_F*H2*a33*
k-
2*log(a2)*coef_C_P*x1*C1*a11*coef_P1_F*H2*a33*k^3+2*log(a2)*coef_C_F*x1*C1*a11*coef_P1_P*
H2*a33*k-2*coef_C_F*a2^(1-k)*k^3*coef_C_P*x1^2*a13*a23*C2+2*coef_C_F*a2^(1-
k)*k*coef_C_P*x1^2*C2*a13*a23-coef_C_F*a2^(1-k)*k*coef_P1_P*H2*a13*a23*x1-
4*coef_C_F*a2^(1-k)*k^2*coef_C_P*x1^2*a11*a33*C2-2*coef_C_F*a2^(1-
k)*k^2*coef_C_P*x1*C2*a13*a33+coef_C_F*a2^(1-
k)*k^2*coef_P1_P*H2*a13*a33+2*coef_C_F*a2^(1-
k)*k*x1*a11*a33*coef_P1_P*H2+2*log(a1)*coef_C_P*x1*C1*a11*coef_P1_F*H2*a33*k^3-
2*coef_C_F*a2^(k+1)*x1^2*C1*a13*a23*coef_C_P*k^3+coef_C_P*a1^(1-
k)*k^3*x1*a12*a33*coef_P1_F*H2-coef_C_P*a1^(1-
k)*k^3*x1*a13*a23*coef_P1_F*H2+4*coef_C_P*a1^(1-k)*k^2*coef_C_F*x1^2*a11*a33*C2-
4*coef_C_P*a1^(1-k)*k^2*coef_C_F*x1^2*a13^2*C2+2*coef_C_P*a1^(1-
k)*k^2*coef_C_F*x1*C2*a13*a33-coef_C_P*a1^(1-k)*k^2*coef_P1_F*H2*a13*a33-
2*coef_C_P*a1^(1-k)*k^2*x1*a11*a33*coef_P1_F*H2+2*coef_C_P*a1^(1-
k)*k^2*x1*a13^2*coef_P1_F*H2-2*coef_C_P*a1^(1-k)*k*coef_C_F*x1^2*C2*a13*a23-
a2^2*coef_C_F*x1^2*a12*coef_C_P*a33*k+a2^2*coef_C_F*x1^2*a12*coef_C_P*a33*k^3-
a1^2*coef_C_F*x1^2*a13*a23*coef_C_P*k+a1^2*coef_C_F*x1^2*a13*a23*coef_C_P*k^3-
2*log(a2)*coef_C_F*x1*C1*a13^2*coef_P1_P*H2*k+2*log(a2)*coef_C_F*x1*C1*a13^2*coef_P1_P*H2
*k^3+coef_C_P*a2^(k+1)*coef_P1_F*H1*a12*x1*a33*k^3+2*log(a2)*coef_C_P*x1*C2*a13^2*coef_P1
_F*H1*k-2*log(a2)*coef_C_P*x1*C2*a13^2*coef_P1_F*H1*k^3-coef_C_F*a1^(1-
k)*k*coef_P1_P*H2*a13*a33-coef_C_F*a1^(1-k)*k^3*x1*a13*a23*coef_P1_P*H2-coef_C_F*a1^(1-
k)*k*coef_P1_P*H2*a12*a33*x1+4*coef_C_F*a1^(k+1)*x1^2*a11*C1*coef_C_P*a33*k-
a2^2*coef_C_F*x1*a13*coef_C_P*a33*k+a2^2*coef_C_F*x1*a13*coef_C_P*a33*k^3-a1^(-
2*k)*coef_C_F*x1*C2*a13^2*coef_P1_P*H2-a1^(-2*k)*coef_P1_F*H2^2*a13*a23*k*coef_P1_P+a1^(-
2*k)*coef_C_P*x1*C2*a11*a33*coef_P1_F*H2+a1^(-
2*k)*coef_C_F*x1*C2*a11*a33*coef_P1_P*H2+a1^(-2*k)*coef_P1_F*H2^2*a12*a33*k*coef_P1_P-
a2^(2*k)*coef_C_F*x1^2*C1^2*a12*a33*k*coef_C_P+a2^(2*k)*coef_P1_F*H1^2*a13^2*coef_P1_P+a2
^(-2*k)*coef_C_P*x1*C2*a13*a23*coef_P1_F*H2*k^3+a2^(-
2*k)*coef_C_F*x1*C2*a13*a23*coef_P1_P*H2*k^3+2*coef_C_P*a1^(1-
k)*k^3*coef_C_F*x1^2*a13*a23*C2-2*coef_C_P*a1^(1-k)*k^3*coef_C_F*x1^2*a12*a33*C2-
2*log(a1)*coef_C_F*x1*C2*a11*coef_P1_P*H1*a33*k^3-
```

```
2*log(a2)*coef_C_F*x1*C2*a11*coef_P1_P*H1*a33*k+2*log(a2)*coef_C_F*x1*C2*a11*coef_P1_P*H1
*a33*k^3+4*log(a2)*coef_P1_F*H1*a11*H2*coef_P1_P*a33*k-
4*log(a2)*coef_P1_F*H1*a11*H2*coef_P1_P*a33*k^3-
2*log(a1)*coef_C_P*x1*C1*a11*coef_P1_F*H2*a33*k-
a2^(2*k)*coef_P1_F*H1^2*a11*a33*coef_P1_P+a2^(-2*k)*coef_P1_F*H2^2*a12*a33*k^3*coef_P1_P-
a2^(-2*k)*coef_P1_F*H2^2*a13*a23*k^3*coef_P1_P+a2^(-
2*k)*coef_C_F*x1^2*C2^2*a11*a33*coef_C_P+a2^(-
2*k)*coef_C_P*x1*C2*a13^2*coef_P1_F*H2+a2^(-2*k)*coef_C_F*x1*C2*a13^2*coef_P1_P*H2+a2^(-
2*k)*coef_P1_F*H2^2*a13*a23*k*coef_P1_P+coef_C_P*a2^(1-k)*k*coef_P1_F*H2*a13*a33-
coef_C_P*a2^(1-k)*k*coef_P1_F*H2*a13*a23*x1+coef_C_P*a2^(1-
k)*k*coef_P1_F*H2*a12*a33*x1+a1^(2*k)*coef_C_F*x1^2*C1^2*a13^2*coef_C_P*k^2+2*coef_C_P*a2
^(1-k)*k*x1*a11*a33*coef_P1_F*H2-
2*log(a1)*coef_C_P*x1*C2*a13^2*coef_P1_F*H1*k+2*log(a1)*coef_C_P*x1*C2*a13^2*coef_P1_F*H1
*k^3-
a1^(2*k)*coef_C_F*x1^2*C1^2*a12*a33*k^3*coef_C_P+a1^(2*k)*coef_C_F*x1*C1*a13^2*coef_P1_P*
H1*k^2-
a1^(2*k)*coef_C_F*x1^2*C1^2*a11*a33*coef_C_P*k^2+a1^(2*k)*coef_C_F*x1*C1*a11*a33*coef_P1_
P*H1+a1^(2*k)*coef_P1_F*H1^2*a11*a33*coef_P1_P-
a1^(2*k)*coef_C_F*x1^2*C1^2*a13*a23*k*coef_C_P-
a2^(2*k)*coef_C_F*x1*C1*a13*a23*coef_P1_P*H1*k^3+coef_C_F*a1^(k+1)*coef_P1_P*H1*a12*x1*a3
3*k+2*coef_C_F*a1^(k+1)*x1^2*C1*a12*coef_C_P*a33*k-
coef_C_F*a1^(k+1)*coef_P1_P*H1*a12*x1*a33*k^3+coef_C_P*a1^(1-
k)*k*coef_P1_F*H2*a13*a23*x1-coef_C_P*a1^(1-k)*k*coef_P1_F*H2*a12*a33*x1-
2*coef_C_P*a1^(1-k)*k*x1*a11*a33*coef_P1_F*H2+2*coef_C_P*a1^(1-
k)*k*x1*a13^2*coef_P1_F*H2+4*coef_C_P*a1^(1-k)*k*coef_C_F*x1^2*a11*a33*C2-
2*coef_C_F*a2^(k+1)*x1^2*C1*a12*coef_C_P*a33*k-
a1^(2*k)*coef_C_P*x1*C1*a12*a33*coef_P1_F*H1*k^3-
a1^(2*k)*coef_C_F*x1*C1*a12*a33*coef_P1_P*H1*k^3+a1^(2*k)*coef_P1_F*H1^2*a13*a23*k^3*coef
_P1_P-a1^(2*k)*coef_C_P*x1*C1*a11*a33*coef_P1_F*H1*k^2-
a1^(2*k)*coef_C_F*x1*C1*a11*a33*coef_P1_P*H1*k^2-
a1^(2*k)*coef_P1_F*H1^2*a11*a33*coef_P1_P*k^2+a1^(2*k)*coef_C_P*x1*C1*a13^2*coef_P1_F*H1*
k^2+a1^(2*k)*coef_C_F*x1^2*C1^2*a13*a23*k^3*coef_C_P+4*log(a2)*coef_C_F*x1^2*C1*a13^2*C2*
coef_C_P*k-4*log(a2)*coef_C_F*x1^2*C1*a13^2*C2*coef_C_P*k^3-
2*coef_C_P*a2^(k+1)*x1*a11*coef_P1_F*H1*a33*k+2*coef_C_P*a2^(k+1)*x1*a11*coef_P1_F*H1*a33
*k^2+2*coef_C_F*a1^(k+1)*x1^2*a13*a23*k^3*C1*coef_C_P-a1^(-
2*k)*coef_C_P*x1*C2*a11*a33*coef_P1_F*H2*k^2-a1^(-
2*k)*coef_C_F*x1*C2*a11*a33*coef_P1_P*H2*k^2+2*coef_C_F*a1^(k+1)*x1*a11*coef_P1_P*H1*a33*
k-2*coef_C_F*a1^(k+1)*x1*a11*coef_P1_P*H1*a33*k^2-
2*coef_C_F*a2^(k+1)*x1*a11*coef_P1_P*H1*a33*k+2*coef_C_F*a2^(k+1)*x1*a11*coef_P1_P*H1*a33
*k^2+2*coef_C_F*a2^(k+1)*x1^2*C1*a13*a23*coef_C_P*k-
2*coef_C_P*a1^(k+1)*x1*a13^2*coef_P1_F*H1*k+2*coef_C_P*a1^(k+1)*x1*a13^2*coef_P1_F*H1*k^2
-coef_C_P*a2^(k+1)*coef_P1_F*H1*a13*a23*x1*k^3-
4*coef_C_F*a2^(k+1)*x1^2*a11*C1*coef_C_P*a33*k-
a1^(2*k)*coef_C_F*x1^2*C1^2*a13^2*coef_C_P-a2^(-2*k)*coef_C_P*x1*C2*a11*a33*coef_P1_F*H2-
a2^(-2*k)*coef_C_F*x1*C2*a11*a33*coef_P1_P*H2-a2^(-
2*k)*coef_P1_F*H2^2*a12*a33*k*coef_P1_P-a2^(-
2*k)*coef_C_F*x1^2*C2^2*a12*a33*k*coef_C_P+a2^(-
2*k)*coef_C_P*x1*C2*a12*a33*coef_P1_F*H2*k+a2^(-
2*k)*coef_C_F*x1*C2*a12*a33*coef_P1_P*H2*k+a2^(-
2*k)*coef_C_F*x1^2*C2^2*a13*a23*k*coef_C_P-
4*log(a1)*coef_P1_F*H1*a11*H2*coef_P1_P*a33*k+4*log(a1)*coef_P1_F*H1*a11*H2*coef_P1_P*a33
*k^3-
4*log(a2)*coef_P1_F*H1*a13^2*H2*coef_P1_P*k+4*log(a2)*coef_P1_F*H1*a13^2*H2*coef_P1_P*k^3
-
2*coef_C_F*a2^(k+1)*x1*C1*a13*coef_C_P*a33*k+2*coef_C_F*a2^(k+1)*x1*C1*a13*coef_C_P*a33*k
^2+a1^(-2*k)*coef_C_F*x1^2*C2^2*a12*a33*k*coef_C_P-a1^(-
2*k)*coef_C_P*x1*C2*a12*a33*coef_P1_F*H2*k-a1^(-
2*k)*coef_C_F*x1*C2*a12*a33*coef_P1_P*H2*k-a1^(-
2*k)*coef_C_F*x1^2*C2^2*a13*a23*k*coef_C_P+a1^(-
```

```
2*k)*coef_C_P*x1*C2*a13*a23*coef_P1_F*H2*k+a1^(-
2*k)*coef_C_F*x1*C2*a13*a23*coef_P1_P*H2*k+2*log(a1)*coef_C_F*x1*C2*a11*coef_P1_P*H1*a33*
k-
a1^(2*k)*coef_C_P*x1*C1*a13^2*coef_P1_F*H1+a1^(2*k)*coef_C_F*x1^2*C1^2*a11*a33*coef_C_P-
a1^(2*k)*coef_C_P*x1*C1*a13*a23*coef_P1_F*H1*k-
a1^(2*k)*coef_C_F*x1*C1*a13*a23*coef_P1_P*H1*k-
a1^(2*k)*coef_P1_F*H1^2*a13*a23*k*coef_P1_P-coef_C_F*a2^(k+1)*coef_P1_P*H1*a13*a33*k-
a2^(-2*k)*coef_P1_F*H2^2*a13^2*coef_P1_P+a2^(-
2*k)*coef_C_F*x1*C2*a11*a33*coef_P1_P*H2*k^2+a2^(-
2*k)*coef_C_F*x1^2*C2^2*a13^2*coef_C_P*k^2-a2^(-
2*k)*coef_P1_F*H2^2*a11*a33*coef_P1_P*k^2-a2^(-
2*k)*coef_C_P*x1*C2*a13^2*coef_P1_F*H2*k^2-
a1^(2*k)*coef_P1_F*H1^2*a13^2*coef_P1_P+a1^(2*k)*coef_C_P*x1*C1*a11*a33*coef_P1_F*H1-
a1^(2*k)*coef_P1_F*H1^2*a12*a33*k^3*coef_P1_P+a1^(2*k)*coef_P1_F*H1^2*a13^2*coef_P1_P*k^2
-a2^(-
2*k)*coef_C_F*x1*C2*a13^2*coef_P1_P*H2*k^2+a1^(2*k)*coef_C_P*x1*C1*a12*a33*coef_P1_F*H1*k
+a1^(2*k)*coef_C_F*x1*C1*a12*a33*coef_P1_P*H1*k-
2*log(a1)*coef_C_F*x1*C1*a11*coef_P1_P*H2*a33*k+2*log(a1)*coef_C_F*x1*C1*a11*coef_P1_P*H2
*a33*k^3+coef_C_F*a2^(k+1)*coef_P1_P*H1*a13*a33*k^2-2*coef_C_P*a2^(1-
k)*k*x1*a13^2*coef_P1_F*H2-coef_C_P*a2^(1-k)*k^3*x1*a12*a33*coef_P1_F*H2+coef_C_P*a2^(1-
k)*k^3*x1*a13*a23*coef_P1_F*H2+a1^(2*k)*coef_P1_F*H1^2*a12*a33*k*coef_P1_P-
a2^2*coef_C_F*x1^2*a11*coef_C_P*a33*k+a2^2*coef_C_F*x1^2*a11*coef_C_P*a33*k^3-
2*coef_C_F*a1^(k+1)*x1^2*a12*k^3*C1*coef_C_P*a33-
coef_C_F*a2^(k+1)*coef_P1_P*H1*a12*x1*a33*k-
2*log(a1)*coef_C_P*x1*C1*a13^2*coef_P1_F*H2*k^3-
coef_C_F*a2^(k+1)*coef_P1_P*H1*a13*a23*x1*k^3+2*log(a1)*coef_C_F*x1*C1*a13^2*coef_P1_P*H2
*k-
2*log(a1)*coef_C_F*x1*C1*a13^2*coef_P1_P*H2*k^3+2*coef_C_F*a2^(k+1)*x1*a13^2*coef_P1_P*H1
*k+coef_C_P*a1^(k+1)*coef_P1_F*H1*a13*a33*k-a2^(2*k)*coef_P1_F*H1^2*a12*a33*k*coef_P1_P-
4*coef_C_F*a1^(k+1)*x1^2*a11*C1*coef_C_P*a33*k^2+2*log(a2)*coef_C_F*x1*C2*a13^2*coef_P1_P
*H1*k-
2*log(a2)*coef_C_F*x1*C2*a13^2*coef_P1_P*H1*k^3+4*coef_C_F*a2^(k+1)*x1^2*a13^2*C1*coef_C_
P*k-4*coef_C_F*a2^(k+1)*x1^2*a13^2*C1*coef_C_P*k^2-
2*coef_C_F*a1^(k+1)*x1^2*C1*a13*a23*coef_C_P*k+4*coef_C_F*a2^(1-
k)*k*coef_C_P*x1^2*a13^2*C2-2*coef_C_F*a2^(1-k)*k*coef_C_P*x1*C2*a13*a33-
2*coef_C_F*a2^(1-k)*k*coef_C_P*x1^2*C2*a12*a33-
a2^(2*k)*coef_C_F*x1^2*C1^2*a13^2*coef_C_P*k^2+a2^(2*k)*coef_C_F*x1^2*C1^2*a11*a33*coef_C
_P*k^2-
a2^(2*k)*coef_C_F*x1*C1*a11*a33*coef_P1_P*H1+a2^(2*k)*coef_C_F*x1^2*C1^2*a13*a23*k*coef_C
_P+a2^(2*k)*coef_C_F*x1^2*C1^2*a13^2*coef_C_P+a2^(2*k)*coef_C_P*x1*C1*a13^2*coef_P1_F*H1-
a2^(2*k)*coef_C_F*x1^2*C1^2*a11*a33*coef_C_P+a2^(2*k)*coef_C_P*x1*C1*a13*a23*coef_P1_F*H1
*k+a2^(2*k)*coef_C_F*x1*C1*a13*a23*coef_P1_P*H1*k+a2^2*coef_C_F*x1^2*a13^2*coef_C_P*k-
a2^2*coef_C_F*x1^2*a13^2*coef_C_P*k^3+4*log(a1)*coef_C_F*x1^2*C1*a11*C2*coef_C_P*a33*k-
4*log(a1)*coef_C_F*x1^2*C1*a11*C2*coef_C_P*a33*k^3-
coef_C_P*a2^(k+1)*coef_P1_F*H1*a12*x1*a33*k+a1^(2*k)*coef_C_F*x1^2*C1^2*a12*a33*k*coef_C_
P-a1^(2*k)*coef_C_F*x1*C1*a13^2*coef_P1_P*H1-a2^(-
2*k)*coef_C_P*x1*C2*a13*a23*coef_P1_F*H2*k-a2^(-
2*k)*coef_C_F*x1*C2*a13*a23*coef_P1_P*H2*k-coef_C_F*a1^(k+1)*coef_P1_P*H1*a13*a23*x1*k-
a2^(2*k)*coef_P1_F*H1^2*a13^2*coef_P1_P*k^2-a1^(-
2*k)*coef_C_F*x1^2*C2^2*a13^2*coef_C_P*k^2-a2^(-2*k)*coef_C_F*x1^2*C2^2*a13^2*coef_C_P-
a2^(-2*k)*coef_C_F*x1^2*C2^2*a11*a33*coef_C_P*k^2+a2^(-
2*k)*coef_C_P*x1*C2*a11*a33*coef_P1_F*H2*k^2-
2*log(a2)*coef_C_P*x1*C1*a13^2*coef_P1_F*H2*k+2*log(a2)*coef_C_P*x1*C1*a13^2*coef_P1_F*H2
*k^3+coef_C_F*a1^(k+1)*coef_P1_P*H1*a13*a33*k-coef_C_F*a1^(k+1)*coef_P1_P*H1*a13*a33*k^2-
coef_C_P*a1^(k+1)*coef_P1_F*H1*a13*a23*x1*k+a2^(2*k)*coef_C_P*x1*C1*a12*a33*coef_P1_F*H1*
k^3+a2^(2*k)*coef_C_F*x1*C1*a12*a33*coef_P1_P*H1*k^3-
a2^(2*k)*coef_P1_F*H1^2*a13*a23*k^3*coef_P1_P+2*coef_C_P*a1^(1-
k)*k*coef_C_F*x1*C2*a13*a33+2*coef_C_P*a1^(1-k)*k*coef_C_F*x1^2*C2*a12*a33-
coef_C_P*a1^(1-k)*k*coef_P1_F*H2*a13*a33-4*coef_C_P*a1^(1-
```

```
k)*k*coef_C_F*x1^2*a13^2*C2+a1^(-2*k)*coef_C_F*x1^2*C2^2*a13^2*coef_C_P+a1^(-
2*k)*coef_C_F*x1^2*C2^2*a11*a33*coef_C_P*k^2-a1^(-
2*k)*coef_P1_F*H2^2*a13^2*coef_P1_P*k^2-2*coef_C_F*a1^(1-k)*k^2*x1*a11*a33*coef_P1_P*H2-
2*log(a2)*coef_C_F*x1*C1*a11*coef_P1_P*H2*a33*k^3+a2^(2*k)*coef_C_P*x1*C1*a11*a33*coef_P1
_F*H1*k^2+a2^(2*k)*coef_C_F*x1*C1*a11*a33*coef_P1_P*H1*k^2+a2^(2*k)*coef_P1_F*H1^2*a11*a3
3*coef_P1_P*k^2-a2^(2*k)*coef_C_P*x1*C1*a13^2*coef_P1_F*H1*k^2-
a2^(2*k)*coef_C_F*x1^2*C1^2*a13*a23*k^3*coef_C_P-
a2^(2*k)*coef_C_P*x1*C1*a13*a23*coef_P1_F*H1*k^3+a2^2*coef_C_F*x1^2*a13*a23*coef_C_P*k+a2
^(2*k)*coef_P1_F*H1^2*a13*a23*k*coef_P1_P-a2^(2*k)*coef_C_P*x1*C1*a12*a33*coef_P1_F*H1*k-
a2^(2*k)*coef_C_F*x1*C1*a12*a33*coef_P1_P*H1*k+coef_C_F*a2^(1-
k)*k*coef_P1_P*H2*a13*a33+2*coef_C_F*a2^(1-
k)*k^3*coef_C_P*x1^2*a12*a33*C2+coef_C_F*a2^(k+1)*coef_P1_P*H1*a13*a23*x1*k-
coef_C_P*a1^(k+1)*x1*a12*coef_P1_F*H1*k^3*a33+coef_C_P*a1^(k+1)*x1*a13*a23*coef_P1_F*H1*k
^3+coef_C_F*a2^(k+1)*x1*a12*coef_P1_P*H1*k^3*a33+2*coef_C_F*a2^(1-
k)*k^2*x1*a11*a33*coef_P1_P*H2-
2*log(a1)*coef_C_F*x1*C2*a13^2*coef_P1_P*H1*k+2*log(a1)*coef_C_F*x1*C2*a13^2*coef_P1_P*H1
*k^3+a1^(-2*k)*coef_P1_F*H2^2*a11*a33*coef_P1_P*k^2+a1^(-
2*k)*coef_C_P*x1*C2*a13^2*coef_P1_F*H2*k^2+a1^(-
2*k)*coef_C_F*x1*C2*a13^2*coef_P1_P*H2*k^2-a1^(-
2*k)*coef_P1_F*H2^2*a11*a33*coef_P1_P+coef_C_F*a1^(k+1)*x1*a13*a23*coef_P1_P*H1*k^3+coef_
C_P*a2^(k+1)*coef_P1_F*H1*a13*a23*x1*k+2*log(a1)*coef_C_P*x1*C2*a11*coef_P1_F*H1*a33*k-
2*log(a1)*coef_C_P*x1*C2*a11*coef_P1_F*H1*a33*k^3-
4*log(a2)*coef_C_F*x1^2*C1*a11*C2*coef_C_P*a33*k+4*log(a2)*coef_C_F*x1^2*C1*a11*C2*coef_C
_P*a33*k^3+2*log(a1)*coef_C_P*x1*C1*a13^2*coef_P1_F*H2*k-
2*coef_C_F*a2^(k+1)*x1*a13^2*coef_P1_P*H1*k^2+coef_C_F*a2^(1-
k)*k^3*x1*a13*a23*coef_P1_P*H2+coef_C_F*a2^(1-k)*k*coef_P1_P*H2*a12*a33*x1-
a2^2*coef_C_F*x1^2*a13*a23*coef_C_P*k^3-coef_C_F*a2^(1-k)*k^3*x1*a12*a33*coef_P1_P*H2-
4*coef_C_F*a2^(1-k)*k*coef_C_P*x1^2*a11*a33*C2-2*coef_C_F*a2^(1-
k)*k*x1*a13^2*coef_P1_P*H2-2*coef_C_F*a2^(1-
k)*k^2*x1*a13^2*coef_P1_P*H2+4*coef_C_F*a2^(1-
k)*k^2*coef_C_P*x1^2*a13^2*C2+a2^(2*k)*coef_C_F*x1*C1*a13^2*coef_P1_P*H1-
a2^(2*k)*coef_C_P*x1*C1*a11*a33*coef_P1_F*H1+a2^(2*k)*coef_P1_F*H1^2*a12*a33*k^3*coef_P1_
P-4*coef_C_F*a1^(k+1)*x1^2*a13^2*C1*coef_C_P*k+a1^2*coef_C_F*x1^2*a11*coef_C_P*a33*k-
a1^2*coef_C_F*x1^2*a11*coef_C_P*a33*k^3-
a1^2*coef_C_F*x1^2*a13^2*coef_C_P*k+a1^2*coef_C_F*x1^2*a13^2*coef_C_P*k^3+a1^2*coef_C_F*x
1*a13*coef_C_P*a33*k-
a1^2*coef_C_F*x1*a13*coef_C_P*a33*k^3+a1^2*coef_C_F*x1^2*a12*coef_C_P*a33*k-
a1^2*coef_C_F*x1^2*a12*coef_C_P*a33*k^3)/a33/k/(k^2-1));

Ut1_PF = (-L*pi*(-
2*log(a1)*coef_C_F*x1*k^2*C1*a22*coef_P1_P*H2*a33+2*log(a1)*coef_C_F*x1*k^4*C1*a22*coef_P
1_P*H2*a33+a1^(-
2*k)*coef_C_P*x1*C2*a12*coef_P1_F*H2*a33+a2^(2*k)*coef_C_F*x1*k^3*C1*a23^2*coef_P1_P*H1+4
*log(a2)*coef_P1_F*H1*k^4*a23^2*H2*coef_P1_P+a1^(-
2*k)*coef_C_F*x1*k*C2*a23^2*coef_P1_P*H2-a1^(-2*k)*coef_C_F*x1*k^3*C2*a23^2*coef_P1_P*H2-
a2^(-2*k)*coef_P1_F*H2^2*k^3*a23^2*coef_P1_P-
a2^(2*k)*coef_C_F*x1*k*C1*a23^2*coef_P1_P*H1-
2*log(a1)*coef_C_P*x1*k^4*C2*a22*coef_P1_F*H1*a33-
4*log(a2)*coef_P1_F*H1*k^2*a23^2*H2*coef_P1_P+2*log(a2)*coef_C_F*x1*k^2*C2*a23^2*coef_P1_
P*H1-2*log(a2)*coef_C_F*x1*k^4*C2*a23^2*coef_P1_P*H1-a1^(-
2*k)*coef_C_P*x1*C2*a12*coef_P1_F*H2*a33*k^2+a1^(2*k)*coef_C_P*x1*C1*a23*a13*coef_P1_F*H1
-a1^(2*k)*coef_C_P*x1*C1*a23*a13*coef_P1_F*H1*k^2+a2^(-
2*k)*coef_C_F*x1^2*k*C2^2*a23^2*coef_C_P-a2^(-2*k)*coef_C_F*x1^2*k^3*C2^2*a23^2*coef_C_P-
2*log(a1)*coef_C_P*x1*k^2*C1*a22*coef_P1_F*H2*a33+2*log(a1)*coef_C_P*x1*k^4*C1*a22*coef_P
1_F*H2*a33-a1^(-2*k)*coef_C_F*x1*k*C2*a22*coef_P1_P*H2*a33-coef_C_P*a2^(1-
k)*coef_P1_F*H2*a12*a33*x1-2*coef_C_P*a2^(1-k)*a33*coef_C_F*x1*k*C2*a23+2*coef_C_P*a2^(1-
k)*a33*coef_P1_F*H2*k*a22*x1+2*coef_C_P*a2^(1-k)*coef_C_F*x1^2*C2*a12*a33+a1^(-
2*k)*coef_C_F*x1*k^3*C2*a22*coef_P1_P*H2*a33+2*log(a2)*coef_C_F*x1*k^2*C1*a22*coef_P1_P*H
2*a33-
```

```
2*log(a2)*coef_C_F*x1*k^4*C1*a22*coef_P1_P*H2*a33+4*log(a2)*coef_P1_F*H1*k^2*a22*H2*coef_
P1_P*a33+a1^(-2*k)*coef_C_F*x1*C2*a12*coef_P1_P*H2*a33-
a1^2*coef_C_F*x1^2*a12*coef_C_P*a33+a1^2*coef_C_F*x1^2*a12*coef_C_P*a33*k^2-
a2^2*coef_C_F*x1^2*a23^2*coef_C_P-a1^(2*k)*coef_C_F*x1*k*C1*a22*coef_P1_P*H1*a33-
4*log(a2)*coef_P1_F*H1*k^4*a22*H2*coef_P1_P*a33-
2*log(a2)*coef_C_P*x1*k^2*C1*a23^2*coef_P1_F*H2+2*log(a2)*coef_C_P*x1*k^4*C1*a23^2*coef_P
1_F*H2-a2^(-2*k)*coef_C_F*x1*k*C2*a23^2*coef_P1_P*H2+coef_C_P*a2^(1-
k)*a33*coef_P1_F*H2*k*a23+coef_C_P*a2^(1-k)*coef_P1_F*H2*a13*a23*x1+a2^(-
2*k)*coef_P1_F*H2^2*k^3*a22*coef_P1_P*a33+a1^(2*k)*coef_C_F*x1^2*C1^2*a23*a13*coef_C_P-
a1^(2*k)*coef_C_F*x1^2*C1^2*a23*a13*coef_C_P*k^2+2*log(a1)*coef_C_F*x1*k^2*C1*a23^2*coef_
P1_P*H2+a2^(-
2*k)*coef_C_F*x1*k^3*C2*a23^2*coef_P1_P*H2+a1^(2*k)*coef_C_F*x1*k*C1*a23^2*coef_P1_P*H1-
a1^(2*k)*coef_C_F*x1*k^3*C1*a23^2*coef_P1_P*H1+a1^(-
2*k)*coef_C_P*x1*k*C2*a23^2*coef_P1_F*H2-a1^(-
2*k)*coef_C_P*x1*k^3*C2*a23^2*coef_P1_F*H2+a1^(-
2*k)*coef_P1_F*H2^2*k^3*a23^2*coef_P1_P+4*coef_C_F*a1^(1-k)*a33*coef_C_P*x1^2*k*C2*a22-
coef_C_F*a1^(1-k)*coef_P1_P*H2*a13*a23*x1+2*coef_C_F*a1^(1-k)*coef_C_P*x1^2*C2*a13*a23-
coef_C_F*a1^(1-k)*a33*coef_P1_P*H2*k^2*a23+coef_C_F*a1^(1-k)*coef_P1_P*H2*a12*a33*x1-
2*log(a1)*coef_C_F*x1*k^4*C1*a23^2*coef_P1_P*H2+4*coef_C_P*a2^(1-
k)*coef_C_F*x1^2*k^2*C2*a23^2-2*coef_C_P*a2^(1-
k)*coef_P1_F*H2*k^2*a23^2*x1+coef_C_P*a2^(1-k)*x1*a12*a33*coef_P1_F*H2*k^2-
2*coef_C_P*a2^(1-k)*coef_C_F*x1^2*a12*a33*k^2*C2+coef_C_P*a2^(1-
k)*a33*coef_P1_F*H2*k^2*a23-2*coef_C_P*a2^(1-k)*a33*coef_C_F*x1*k^2*C2*a23-a2^(-
2*k)*coef_C_P*x1*C2*a12*coef_P1_F*H2*a33+a2^(-
2*k)*coef_C_P*x1*C2*a12*coef_P1_F*H2*a33*k^2-4*coef_C_F*a1^(1-
k)*coef_C_P*x1^2*k*C2*a23^2-4*coef_C_F*a1^(1-
k)*coef_C_P*x1^2*k^2*C2*a23^2+2*coef_C_F*a1^(1-k)*a33*coef_C_P*x1*k^2*C2*a23-a1^(-
2*k)*coef_P1_F*H2^2*a12*coef_P1_P*a33-2*coef_C_F*a2^(k+1)*coef_C_P*x1^2*a12*a33*k^2*C1-
coef_C_F*a2^(k+1)*x1*a12*a33*coef_P1_P*H1*k^2+coef_C_F*a2^(k+1)*x1*a13*a23*coef_P1_P*H1*k
^2+2*coef_C_F*a2^(k+1)*coef_C_P*x1^2*a13*a23*k^2*C1+coef_C_F*a2^(k+1)*coef_P1_P*H1*a12*a3
3*x1+a1^(2*k)*coef_P1_F*H1^2*a23*a13*coef_P1_P+2*coef_C_F*a2^(k+1)*a33*coef_P1_P*H1*k*a22
*x1-
2*coef_C_F*a2^(k+1)*a33*coef_C_P*x1*k^2*C1*a23+2*coef_C_F*a2^(k+1)*coef_P1_P*H1*k^2*a23^2
*x1-
a2^(2*k)*coef_C_F*x1*C1*a23*a13*coef_P1_P*H1+a2^(2*k)*coef_C_F*x1*C1*a23*a13*coef_P1_P*H1
*k^2-a1^(-2*k)*coef_P1_F*H2^2*k*a23^2*coef_P1_P+2*coef_C_P*a2^(1-
k)*a33*coef_P1_F*H2*k^2*a22*x1+a1^(2*k)*coef_C_F*x1*k^3*C1*a22*coef_P1_P*H1*a33-a1^(-
2*k)*coef_C_F*x1^2*C2^2*a12*coef_C_P*a33-a2^(-
2*k)*coef_C_F*x1^2*k*C2^2*a22*coef_C_P*a33+a2^(-
2*k)*coef_C_F*x1^2*k^3*C2^2*a22*coef_C_P*a33+a2^(2*k)*coef_P1_F*H1^2*a12*coef_P1_P*a33+a2
^2*coef_C_F*x1*a23*coef_C_P*a33-
a2^2*coef_C_F*x1*a23*coef_C_P*a33*k^2+coef_C_P*a1^(k+1)*a33*coef_P1_F*H1*k^2*a23-
2*coef_C_P*a1^(k+1)*coef_P1_F*H1*k^2*a23^2*x1+coef_C_P*a1^(k+1)*x1*a12*a33*coef_P1_F*H1*k
^2+a1^(2*k)*coef_C_F*x1^2*k*C1^2*a23^2*coef_C_P-
a1^(2*k)*coef_C_F*x1^2*k^3*C1^2*a23^2*coef_C_P+a1^(-
2*k)*coef_C_F*x1^2*C2^2*a13*a23*coef_C_P+2*coef_C_P*a1^(k+1)*coef_P1_F*H1*k*a23^2*x1+2*co
ef_C_P*a1^(k+1)*a33*coef_P1_F*H1*k^2*a22*x1-
2*coef_C_P*a1^(k+1)*a33*coef_P1_F*H1*k*a22*x1-
coef_C_P*a1^(k+1)*coef_P1_F*H1*a12*a33*x1+coef_C_P*a1^(k+1)*coef_P1_F*H1*a13*a23*x1+a1^(-
2*k)*coef_C_F*x1^2*C2^2*a12*coef_C_P*a33*k^2+a1^2*coef_C_F*x1^2*a23^2*coef_C_P-
a1^2*coef_C_F*x1^2*a22*coef_C_P*a33+a1^2*coef_C_F*x1^2*a22*coef_C_P*a33*k^2-
a2^2*coef_C_F*x1^2*a22*coef_C_P*a33*k^2-a1^(-
2*k)*coef_C_F*x1^2*C2^2*a13*a23*coef_C_P*k^2-
2*log(a2)*coef_C_F*x1*k^2*C2*a22*coef_P1_P*H1*a33+2*log(a2)*coef_C_F*x1*k^4*C2*a22*coef_P
1_P*H1*a33-
4*log(a2)*coef_C_F*x1^2*k^2*C1*a22*C2*coef_C_P*a33+4*log(a2)*coef_C_F*x1^2*k^4*C1*a22*C2*
coef_C_P*a33+2*coef_C_P*a2^(k+1)*a33*coef_P1_F*H1*k*a22*x1+a2^(2*k)*coef_C_F*x1^2*C1^2*a1
2*coef_C_P*a33-
a2^(2*k)*coef_C_F*x1^2*C1^2*a12*coef_C_P*a33*k^2+coef_C_P*a2^(k+1)*coef_P1_F*H1*a12*a33*x
```

```
1-coef_C_P*a2^(k+1)*coef_P1_F*H1*a13*a23*x1-2*coef_C_P*a2^(k+1)*coef_P1_F*H1*k*a23^2*x1-
2*coef_C_P*a2^(k+1)*a33*coef_P1_F*H1*k^2*a22*x1-
coef_C_P*a2^(k+1)*a33*coef_P1_F*H1*k^2*a23+4*log(a2)*coef_C_F*x1^2*k^2*C1*a23^2*C2*coef_C
_P-
4*log(a2)*coef_C_F*x1^2*k^4*C1*a23^2*C2*coef_C_P+2*log(a1)*coef_C_P*x1*k^2*C1*a23^2*coef_
P1_F*H2-a2^(2*k)*coef_C_F*x1^2*k*C1^2*a23^2*coef_C_P-
2*log(a1)*coef_C_F*x1*k^4*C2*a22*coef_P1_P*H1*a33+a1^(-
2*k)*coef_P1_F*H2^2*k*a22*coef_P1_P*a33+2*coef_C_F*a2^(1-
k)*a33*coef_P1_P*H2*k^2*a22*x1+coef_C_F*a2^(1-k)*x1*a12*a33*coef_P1_P*H2*k^2-
coef_C_F*a2^(1-k)*x1*a13*a23*coef_P1_P*H2*k^2-a2^(-2*k)*coef_P1_F*H2^2*a13*a23*coef_P1_P-
a2^(-2*k)*coef_C_P*x1*k^3*C2*a22*coef_P1_F*H2*a33-a2^(-
2*k)*coef_C_F*x1^2*C2^2*a13*a23*coef_C_P+a2^(-
2*k)*coef_C_F*x1^2*C2^2*a13*a23*coef_C_P*k^2+2*coef_C_F*a1^(1-
k)*coef_P1_P*H2*k^2*a23^2*x1+2*log(a1)*coef_C_F*x1*k^2*C2*a22*coef_P1_P*H1*a33+a2^(2*k)*c
oef_P1_F*H1^2*k^3*a23^2*coef_P1_P-2*coef_C_F*a1^(1-k)*a33*coef_P1_P*H2*k^2*a22*x1-
coef_C_F*a1^(1-k)*x1*a12*a33*coef_P1_P*H2*k^2+a1^(-
2*k)*coef_P1_F*H2^2*a12*coef_P1_P*a33*k^2+a2^(-2*k)*coef_C_F*x1^2*C2^2*a12*coef_C_P*a33-
a2^(-2*k)*coef_C_F*x1^2*C2^2*a12*coef_C_P*a33*k^2-
a1^(2*k)*coef_P1_F*H1^2*k*a22*coef_P1_P*a33-
2*log(a1)*coef_C_P*x1*k^4*C1*a23^2*coef_P1_F*H2-
coef_C_P*a1^(k+1)*x1*a13*a23*coef_P1_F*H1*k^2+a2^(-
2*k)*coef_C_F*x1*k*C2*a22*coef_P1_P*H2*a33-a2^(-
2*k)*coef_C_F*x1*k^3*C2*a22*coef_P1_P*H2*a33+a2^(2*k)*coef_C_F*x1^2*k^3*C1^2*a23^2*coef_C
_P+a1^(2*k)*coef_P1_F*H1^2*k^3*a22*coef_P1_P*a33+a2^(2*k)*coef_P1_F*H1^2*k*a22*coef_P1_P*
a33-a2^(2*k)*coef_P1_F*H1^2*k^3*a22*coef_P1_P*a33+2*coef_C_F*a2^(1-
k)*a33*coef_P1_P*H2*k*a22*x1-2*coef_C_F*a2^(1-k)*coef_P1_P*H2*k*a23^2*x1+coef_C_F*a2^(1-
k)*a33*coef_P1_P*H2*k*a23+a1^2*coef_C_F*x1^2*a13*a23*coef_C_P-
a1^2*coef_C_F*x1^2*a13*a23*coef_C_P*k^2-4*log(a1)*coef_P1_F*H1*k^4*a23^2*H2*coef_P1_P-
coef_C_F*a1^(k+1)*a33*coef_P1_P*H1*k*a23-
2*coef_C_F*a1^(k+1)*coef_C_P*x1^2*C1*a12*a33+2*coef_C_F*a1^(k+1)*coef_P1_P*H1*k*a23^2*x1-
coef_C_P*a1^(k+1)*a33*coef_P1_F*H1*k*a23+a2^(2*k)*coef_C_P*x1*C1*a12*coef_P1_F*H1*a33-
2*coef_C_F*a1^(k+1)*a33*coef_C_P*x1*k*C1*a23+4*coef_C_F*a1^(k+1)*a33*coef_C_P*x1^2*k^2*C1
*a22+2*coef_C_F*a1^(k+1)*coef_C_P*x1^2*a12*a33*k^2*C1+coef_C_F*a1^(k+1)*x1*a12*a33*coef_P
1_P*H1*k^2-coef_C_F*a1^(k+1)*x1*a13*a23*coef_P1_P*H1*k^2-
a1^(2*k)*coef_P1_F*H1^2*k^3*a23^2*coef_P1_P-
a2^(2*k)*coef_C_P*x1*C1*a12*coef_P1_F*H1*a33*k^2-
a2^(2*k)*coef_P1_F*H1^2*a12*coef_P1_P*a33*k^2-
4*log(a1)*coef_P1_F*H1*k^2*a22*H2*coef_P1_P*a33+4*log(a1)*coef_P1_F*H1*k^4*a22*H2*coef_P1
_P*a33+4*coef_C_F*a1^(k+1)*coef_C_P*x1^2*k*C1*a23^2+coef_C_F*a1^(k+1)*a33*coef_P1_P*H1*k^
2*a23-2*coef_C_F*a1^(k+1)*coef_C_P*x1^2*a13*a23*k^2*C1-
coef_C_F*a1^(k+1)*coef_P1_P*H1*a12*a33*x1+2*coef_C_F*a1^(k+1)*coef_C_P*x1^2*C1*a13*a23+co
ef_C_F*a1^(k+1)*coef_P1_P*H1*a13*a23*x1-4*coef_C_F*a1^(k+1)*a33*coef_C_P*x1^2*k*C1*a22-
4*coef_C_F*a1^(k+1)*coef_C_P*x1^2*k^2*C1*a23^2-
a2^2*coef_C_F*x1^2*a13*a23*coef_C_P+a2^2*coef_C_F*x1^2*a13*a23*coef_C_P*k^2+2*coef_C_F*a1
^(k+1)*a33*coef_P1_P*H1*k^2*a22*x1-
2*coef_C_F*a1^(k+1)*a33*coef_P1_P*H1*k*a22*x1+2*coef_C_F*a1^(k+1)*a33*coef_C_P*x1*k^2*C1*
a23-2*coef_C_F*a1^(k+1)*coef_P1_P*H1*k^2*a23^2*x1-
2*coef_C_F*a2^(k+1)*coef_C_P*x1^2*C1*a13*a23-
coef_C_F*a2^(k+1)*coef_P1_P*H1*a13*a23*x1+4*coef_C_F*a2^(k+1)*a33*coef_C_P*x1^2*k*C1*a22+
4*coef_C_F*a2^(k+1)*coef_C_P*x1^2*k^2*C1*a23^2-
2*coef_C_F*a2^(k+1)*a33*coef_P1_P*H1*k^2*a22*x1+coef_C_P*a2^(k+1)*a33*coef_P1_F*H1*k*a23+
2*coef_C_P*a2^(k+1)*coef_P1_F*H1*k^2*a23^2*x1-
coef_C_P*a2^(k+1)*x1*a12*a33*coef_P1_F*H1*k^2+a2^(-
2*k)*coef_P1_F*H2^2*a13*a23*coef_P1_P*k^2+2*coef_C_P*a1^(1-k)*coef_P1_F*H2*k^2*a23^2*x1-
coef_C_P*a1^(1-k)*x1*a12*a33*coef_P1_F*H2*k^2-coef_C_P*a1^(1-
k)*a33*coef_P1_F*H2*k^2*a23+coef_C_P*a1^(1-
k)*x1*a13*a23*coef_P1_F*H2*k^2+2*coef_C_P*a1^(1-k)*coef_P1_F*H2*k*a23^2*x1-
coef_C_P*a1^(1-k)*coef_P1_F*H2*a13*a23*x1+a2^(2*k)*coef_C_P*x1*k*C1*a22*coef_P1_F*H1*a33-
a2^(2*k)*coef_C_P*x1*k^3*C1*a22*coef_P1_F*H1*a33-
```

```
2*log(a1)*coef_C_P*x1*k^2*C2*a23^2*coef_P1_F*H1+2*log(a1)*coef_C_P*x1*k^4*C2*a23^2*coef_P
1_F*H1-a1^(-2*k)*coef_P1_F*H2^2*a13*a23*coef_P1_P*k^2-
a2^(2*k)*coef_C_F*x1^2*C1^2*a23*a13*coef_C_P+a2^(2*k)*coef_C_F*x1^2*C1^2*a23*a13*coef_C_P
*k^2+coef_C_P*a1^(1-k)*coef_P1_F*H2*a12*a33*x1-2*coef_C_P*a1^(1-
k)*a33*coef_P1_F*H2*k*a22*x1-coef_C_P*a1^(1-
k)*a33*coef_P1_F*H2*k*a23+coef_C_P*a2^(k+1)*x1*a13*a23*coef_P1_F*H1*k^2-a1^(-
2*k)*coef_C_F*x1*C2*a12*coef_P1_P*H2*a33*k^2-a2^(-
2*k)*coef_C_P*x1*k*C2*a23^2*coef_P1_F*H2+a2^(-2*k)*coef_C_P*x1*k^3*C2*a23^2*coef_P1_F*H2-
a1^(-2*k)*coef_C_F*x1*C2*a13*a23*coef_P1_P*H2-
a1^(2*k)*coef_C_P*x1*k*C1*a22*coef_P1_F*H1*a33+a1^(2*k)*coef_C_P*x1*k^3*C1*a22*coef_P1_F*
H1*a33+a2^(2*k)*coef_P1_F*H1^2*a23*a13*coef_P1_P*k^2-
a1^(2*k)*coef_P1_F*H1^2*a23*a13*coef_P1_P*k^2-a2^(2*k)*coef_P1_F*H1^2*k*a23^2*coef_P1_P-
4*log(a1)*coef_C_F*x1^2*k^2*C1*a23^2*C2*coef_C_P+a1^(-
2*k)*coef_C_F*x1*C2*a13*a23*coef_P1_P*H2*k^2+a1^(-
2*k)*coef_C_F*x1^2*k*C2^2*a22*coef_C_P*a33-a1^(-
2*k)*coef_C_F*x1^2*k^3*C2^2*a22*coef_C_P*a33-a2^(-
2*k)*coef_P1_F*H2^2*k*a22*coef_P1_P*a33+a2^(-
2*k)*coef_C_P*x1*C2*a13*a23*coef_P1_F*H2+a1^(2*k)*coef_P1_F*H1^2*k*a23^2*coef_P1_P+a2^2*c
oef_C_F*x1^2*a12*coef_C_P*a33-
a2^2*coef_C_F*x1^2*a12*coef_C_P*a33*k^2+4*log(a1)*coef_C_F*x1^2*k^4*C1*a23^2*C2*coef_C_P+
2*log(a1)*coef_C_P*x1*k^2*C2*a22*coef_P1_F*H1*a33-2*coef_C_F*a2^(1-
k)*coef_P1_P*H2*k^2*a23^2*x1-
2*log(a1)*coef_C_F*x1*k^2*C2*a23^2*coef_P1_P*H1+2*log(a1)*coef_C_F*x1*k^4*C2*a23^2*coef_P
1_P*H1-a1^(2*k)*coef_P1_F*H1^2*a12*coef_P1_P*a33+coef_C_F*a2^(1-
k)*coef_P1_P*H2*a13*a23*x1-a2^(-2*k)*coef_P1_F*H2^2*a12*coef_P1_P*a33*k^2-
4*coef_C_P*a2^(1-k)*a33*coef_C_F*x1^2*k*C2*a22-2*coef_C_P*a2^(1-
k)*coef_C_F*x1^2*C2*a13*a23-a1^(2*k)*coef_C_P*x1*C1*a12*coef_P1_F*H1*a33+coef_C_F*a2^(1-
k)*a33*coef_P1_P*H2*k^2*a23+a2^(-2*k)*coef_C_F*x1*C2*a12*coef_P1_P*H2*a33*k^2-
2*coef_C_F*a1^(1-k)*a33*coef_P1_P*H2*k*a22*x1-
a2^(2*k)*coef_C_P*x1*k*C1*a23^2*coef_P1_F*H1+a2^(2*k)*coef_C_P*x1*k^3*C1*a23^2*coef_P1_F*
H1+4*log(a1)*coef_P1_F*H1*k^2*a23^2*H2*coef_P1_P+a2^(-
2*k)*coef_P1_F*H2^2*a12*coef_P1_P*a33-a2^(-
2*k)*coef_C_P*x1*C2*a13*a23*coef_P1_F*H2*k^2+a1^(2*k)*coef_C_F*x1*C1*a23*a13*coef_P1_P*H1
-a1^(-2*k)*coef_C_P*x1*k*C2*a22*coef_P1_F*H2*a33+a1^(-
2*k)*coef_C_P*x1*k^3*C2*a22*coef_P1_F*H2*a33-a2^(-
2*k)*coef_C_F*x1*C2*a12*coef_P1_P*H2*a33-coef_C_P*a2^(1-k)*x1*a13*a23*coef_P1_F*H2*k^2-
4*coef_C_P*a2^(1-k)*a33*coef_C_F*x1^2*k^2*C2*a22+2*coef_C_P*a2^(1-
k)*coef_C_F*x1^2*a13*a23*k^2*C2-2*coef_C_P*a2^(1-
k)*coef_P1_F*H2*k*a23^2*x1+4*coef_C_P*a2^(1-k)*coef_C_F*x1^2*k*C2*a23^2-
2*log(a2)*coef_C_F*x1*k^2*C1*a23^2*coef_P1_P*H2+a1^2*coef_C_F*x1*a23*coef_C_P*a33*k^2-
a1^(2*k)*coef_C_F*x1*C1*a23*a13*coef_P1_P*H1*k^2+2*log(a2)*coef_C_F*x1*k^4*C1*a23^2*coef_
P1_P*H2-a2^(2*k)*coef_C_P*x1*C1*a23*a13*coef_P1_F*H1+2*coef_C_F*a1^(1-
k)*coef_P1_P*H2*k*a23^2*x1-coef_C_F*a1^(1-k)*a33*coef_P1_P*H2*k*a23-2*coef_C_F*a1^(1-
k)*coef_C_P*x1^2*C2*a12*a33+coef_C_F*a2^(k+1)*a33*coef_P1_P*H1*k*a23+2*coef_C_F*a2^(k+1)*
coef_C_P*x1^2*C1*a12*a33-2*coef_C_F*a2^(k+1)*coef_P1_P*H1*k*a23^2*x1-
4*coef_C_F*a2^(k+1)*coef_C_P*x1^2*k*C1*a23^2+2*coef_C_F*a2^(k+1)*a33*coef_C_P*x1*k*C1*a23
-4*coef_C_F*a2^(k+1)*a33*coef_C_P*x1^2*k^2*C1*a22-
coef_C_F*a2^(k+1)*a33*coef_P1_P*H1*k^2*a23+2*log(a2)*coef_C_P*x1*k^2*C2*a23^2*coef_P1_F*H
1-
2*log(a2)*coef_C_P*x1*k^4*C2*a23^2*coef_P1_F*H1+2*log(a2)*coef_C_P*x1*k^2*C1*a22*coef_P1_
F*H2*a33-
2*log(a2)*coef_C_P*x1*k^4*C1*a22*coef_P1_F*H2*a33+a1^(2*k)*coef_C_P*x1*k*C1*a23^2*coef_P1
_F*H1-a1^(2*k)*coef_C_P*x1*k^3*C1*a23^2*coef_P1_F*H1-a1^(-
2*k)*coef_C_F*x1^2*k*C2^2*a23^2*coef_C_P+a1^(-
2*k)*coef_C_F*x1^2*k^3*C2^2*a23^2*coef_C_P+4*log(a1)*coef_C_F*x1^2*k^2*C1*a22*C2*coef_C_P
*a33-a1^(2*k)*coef_C_F*x1^2*C1^2*a12*coef_C_P*a33-
a1^2*coef_C_F*x1^2*a23^2*coef_C_P*k^2+a1^(2*k)*coef_P1_F*H1^2*a12*coef_P1_P*a33*k^2-
a1^(2*k)*coef_C_F*x1^2*k*C1^2*a22*coef_C_P*a33+a1^(2*k)*coef_C_F*x1^2*k^3*C1^2*a22*coef_C
_P*a33-
```

```
2*log(a2)*coef_C_P*x1*k^2*C2*a22*coef_P1_F*H1*a33+2*log(a2)*coef_C_P*x1*k^4*C2*a22*coef_P
1_F*H1*a33-
a1^(2*k)*coef_C_F*x1*C1*a12*coef_P1_P*H1*a33+a1^(2*k)*coef_C_F*x1*C1*a12*coef_P1_P*H1*a33
*k^2-a2^(2*k)*coef_P1_F*H1^2*a23*a13*coef_P1_P-a1^(-
2*k)*coef_C_P*x1*C2*a13*a23*coef_P1_F*H2+a1^(-
2*k)*coef_C_P*x1*C2*a13*a23*coef_P1_F*H2*k^2+a2^(-
2*k)*coef_P1_F*H2^2*k*a23^2*coef_P1_P+a1^(2*k)*coef_C_P*x1*C1*a12*coef_P1_F*H1*a33*k^2+a2
^(-2*k)*coef_C_P*x1*k*C2*a22*coef_P1_F*H2*a33-coef_C_F*a2^(1-
k)*coef_P1_P*H2*a12*a33*x1+2*coef_C_F*a1^(1-
k)*coef_C_P*x1^2*a12*a33*k^2*C2+coef_C_F*a1^(1-
k)*x1*a13*a23*coef_P1_P*H2*k^2+a2^2*coef_C_F*x1^2*a22*coef_C_P*a33+4*coef_C_F*a1^(1-
k)*a33*coef_C_P*x1^2*k^2*C2*a22-2*coef_C_F*a1^(1-
k)*coef_C_P*x1^2*a13*a23*k^2*C2+2*coef_C_F*a1^(1-k)*a33*coef_C_P*x1*k*C2*a23-a1^(-
2*k)*coef_P1_F*H2^2*k^3*a22*coef_P1_P*a33-2*coef_C_P*a1^(1-
k)*a33*coef_P1_F*H2*k^2*a22*x1+a1^(-
2*k)*coef_P1_F*H2^2*a13*a23*coef_P1_P+a2^2*coef_C_F*x1^2*a23^2*coef_C_P*k^2+a2^(2*k)*coef
_C_P*x1*C1*a23*a13*coef_P1_F*H1*k^2+a2^(-2*k)*coef_C_F*x1*C2*a13*a23*coef_P1_P*H2-a2^(-
2*k)*coef_C_F*x1*C2*a13*a23*coef_P1_P*H2*k^2-
4*log(a1)*coef_C_F*x1^2*k^4*C1*a22*C2*coef_C_P*a33+a2^(2*k)*coef_C_F*x1*k*C1*a22*coef_P1_
P*H1*a33-a1^2*coef_C_F*x1*a23*coef_C_P*a33+a2^(2*k)*coef_C_F*x1*C1*a12*coef_P1_P*H1*a33-
a2^(2*k)*coef_C_F*x1*C1*a12*coef_P1_P*H1*a33*k^2-
a2^(2*k)*coef_C_F*x1*k^3*C1*a22*coef_P1_P*H1*a33+a1^(2*k)*coef_C_F*x1^2*C1^2*a12*coef_C_P
*a33*k^2+a2^(2*k)*coef_C_F*x1^2*k*C1^2*a22*coef_C_P*a33-
a2^(2*k)*coef_C_F*x1^2*k^3*C1^2*a22*coef_C_P*a33)/a33/(k^2-1));

Uz1_PF = (L*pi*(2*a2^(1-
k)*coef_C_P*coef_C_F*a13*x1*C2*k+a2^(k+1)*coef_C_F*coef_P1_P*H1*k*a23-
a2^(k+1)*coef_C_F*coef_P1_P*H1*k^2*a23-
2*a2^(k+1)*coef_C_P*coef_C_F*x1*k^2*C1*a23+2*a2^(k+1)*coef_C_P*coef_C_F*x1*k*C1*a23-
a1^(1-k)*coef_C_F*coef_P1_P*H2*k*a23-a1^(1-k)*coef_C_F*coef_P1_P*H2*k^2*a23-
a2^(k+1)*coef_C_P*coef_P1_F*H1*k^2*a23+2*a2^(1-k)*coef_C_P*coef_C_F*a13*x1*C2-
a2^2*coef_C_F*a33*coef_C_P+a2^2*coef_C_F*a33*coef_C_P*k^2-a2^(1-
k)*coef_C_F*a13*coef_P1_P*H2-a2^(1-k)*coef_C_F*a13*coef_P1_P*H2*k-
2*a2^(k+1)*coef_C_P*coef_C_F*a13*x1*C1*k+a2^(k+1)*coef_C_P*a13*coef_P1_F*H1+a2^(k+1)*coef
_C_P*coef_P1_F*H1*k*a23+2*a1^(1-k)*coef_C_P*coef_C_F*x1*k*C2*a23+2*a1^(1-
k)*coef_C_P*coef_C_F*x1*k^2*C2*a23-
a2^(k+1)*coef_C_P*a13*coef_P1_F*H1*k+a2^(k+1)*coef_C_F*a13*coef_P1_P*H1+a1^(1-
k)*coef_C_P*a13*coef_P1_F*H2*k+a1^(1-k)*coef_C_F*a13*coef_P1_P*H2+a1^(1-
k)*coef_C_F*a13*coef_P1_P*H2*k-
a1^(k+1)*coef_C_F*a13*coef_P1_P*H1+a1^(k+1)*coef_C_F*a13*coef_P1_P*H1*k+a2^(1-
k)*coef_C_F*coef_P1_P*H2*k*a23+a2^(1-k)*coef_C_F*coef_P1_P*H2*k^2*a23+a2^(1-
k)*coef_C_P*coef_P1_F*H2*k*a23-2*a1^(1-k)*coef_C_P*coef_C_F*a13*x1*C2-2*a1^(1-
k)*coef_C_P*coef_C_F*a13*x1*C2*k+2*a2^(k+1)*coef_C_P*coef_C_F*a13*x1*C1-
a2^(k+1)*coef_C_F*a13*coef_P1_P*H1*k-
2*a1^(k+1)*coef_C_P*coef_C_F*a13*x1*C1+2*a1^(k+1)*coef_C_P*coef_C_F*a13*x1*C1*k+a1^(1-
k)*coef_C_P*a13*coef_P1_F*H2+a2^(1-k)*coef_C_P*coef_P1_F*H2*k^2*a23-
a1^(k+1)*coef_C_F*coef_P1_P*H1*k*a23+a1^(k+1)*coef_C_F*coef_P1_P*H1*k^2*a23-a2^(1-
k)*coef_C_P*a13*coef_P1_F*H2-a2^(1-k)*coef_C_P*a13*coef_P1_F*H2*k-a1^(1-
k)*coef_C_P*coef_P1_F*H2*k*a23-a1^(1-k)*coef_C_P*coef_P1_F*H2*k^2*a23-
a1^(k+1)*coef_C_P*a13*coef_P1_F*H1-
a1^(k+1)*coef_C_P*coef_P1_F*H1*k*a23+a1^(k+1)*coef_C_P*coef_P1_F*H1*k^2*a23-2*a2^(1-
k)*coef_C_P*coef_C_F*x1*k*C2*a23-2*a2^(1-
k)*coef_C_P*coef_C_F*x1*k^2*C2*a23+a1^(k+1)*coef_C_P*a13*coef_P1_F*H1*k-
2*a1^(k+1)*coef_C_P*coef_C_F*x1*k*C1*a23+2*a1^(k+1)*coef_C_P*coef_C_F*x1*k^2*C1*a23-
a1^2*coef_C_F*a13*x1*coef_C_P+a1^2*coef_C_F*a13*x1*coef_C_P*k^2+a1^2*coef_C_F*x1*a23*coef
_C_P*k^2+a2^2*coef_C_F*x1*a23*coef_C_P-a2^2*coef_C_F*x1*a23*coef_C_P*k^2-
a1^2*coef_C_F*x1*a23*coef_C_P+a2^2*coef_C_F*a13*x1*coef_C_P-
a2^2*coef_C_F*a13*x1*coef_C_P*k^2+a1^2*coef_C_F*a33*coef_C_P-
a1^2*coef_C_F*a33*coef_C_P*k^2)/(k^2-1));
```

```
Ur2_PF = (-
1/2*L*(a0^2*coef_P1_P*a1^2*nu+4*a1^4*a0^2*pi*coef_P1_F+2*a1^2*a0^4*pi*nu*coef_P1_F*coef_P
1_P+8*a0^2*a1^4*log(a1)*coef_P1_F*pi*coef_P1_P-2*a0^2*a1^2*log(a0)*nu*coef_F1_F-
2*a0^4*a1^2*log(a0)*coef_P1_F*nu*pi+2*a0^2*a1^2*log(a0)*coef_P1_P*nu*coef_F1_F+2*a0^4*a1^
2*log(a1)*coef_P1_F*nu*pi-
8*a0^2*a1^4*log(a0)*coef_P1_F*pi*coef_P1_P+4*a0^2*a1^4*log(a0)*pi*coef_P1_F+a0^4*nu*coef_
F1_F-4*a0^2*a1^4*log(a1)*pi*coef_P1_F-
2*a1^6*coef_P1_F*pi*coef_P1_P+2*a0^2*a1^2*log(a0)*coef_P1_F*nu*coef_F1_P-
a1^4*a0^2*pi*nu*coef_P1_F-2*a0^2*a1^2*log(a1)*coef_P1_P*nu*coef_F1_F-a1^4*coef_P1_P*nu-
2*a0^2*a1^2*log(a1)*coef_P1_F*nu*coef_F1_P+2*a0^2*a1^2*log(a1)*coef_P1_P*nu-
4*a0^4*a1^2*log(a1)*coef_P1_F*pi-4*a0^2*coef_P1_F*a1^4*nu*pi*coef_P1_P-
4*a1^2*a0^4*pi*coef_P1_F-
2*a0^2*a1^2*log(a1)*nu+2*a1^2*a0^4*pi*coef_P1_F*coef_P1_P+2*a0^2*a1^2*log(a0)*nu+2*a1^6*c
oef_P1_F*nu*pi*coef_P1_P-a0^2*coef_P1_P*a1^2*nu*coef_F1_F-a0^4*nu-
a0^2*coef_P1_F*a1^2*nu*coef_F1_P+a1^2*a0^2*nu-
a1^2*a0^2*nu*coef_F1_F+a1^2*a0^4*pi*nu*coef_P1_F+4*a0^4*a1^2*log(a0)*coef_P1_F*pi+2*a0^2*
a1^2*log(a1)*nu*coef_F1_F-
2*a0^2*a1^2*log(a0)*coef_P1_P*nu+a1^4*coef_P1_P*nu*coef_F1_F+a1^4*coef_P1_F*nu*coef_F1_P)
/E/(a1^2-a0^2)^2);

Ut2_PF = (-
1/2*L*(a0^2*coef_P1_P*a1^2*nu+4*a1^4*a0^2*pi*coef_P1_F+2*a1^2*a0^4*pi*nu*coef_P1_F*coef_P
1_P-
8*a0^2*a1^4*log(a1)*coef_P1_F*pi*coef_P1_P+2*a0^2*a1^2*log(a0)*nu*coef_F1_F+2*a0^4*a1^2*l
og(a0)*coef_P1_F*nu*pi-2*a0^2*a1^2*log(a0)*coef_P1_P*nu*coef_F1_F-
2*a0^4*a1^2*log(a1)*coef_P1_F*nu*pi+8*a0^2*a1^4*log(a0)*coef_P1_F*pi*coef_P1_P-
4*a0^2*a1^4*log(a0)*pi*coef_P1_F+a0^4*nu*coef_F1_F+4*a0^2*a1^4*log(a1)*pi*coef_P1_F-
2*a1^6*coef_P1_F*pi*coef_P1_P-2*a0^2*a1^2*log(a0)*coef_P1_F*nu*coef_F1_P-
a1^4*a0^2*pi*nu*coef_P1_F+2*a0^2*a1^2*log(a1)*coef_P1_P*nu*coef_F1_F-
a1^4*coef_P1_P*nu+2*a0^2*a1^2*log(a1)*coef_P1_F*nu*coef_F1_P-
2*a0^2*a1^2*log(a1)*coef_P1_P*nu+4*a0^4*a1^2*log(a1)*coef_P1_F*pi-
4*a0^2*coef_P1_F*a1^4*nu*pi*coef_P1_P-
4*a1^2*a0^4*pi*coef_P1_F+2*a0^2*a1^2*log(a1)*nu+2*a1^2*a0^4*pi*coef_P1_F*coef_P1_P-
2*a0^2*a1^2*log(a0)*nu+2*a1^6*coef_P1_F*nu*pi*coef_P1_P-a0^2*coef_P1_P*a1^2*nu*coef_F1_F-
a0^4*nu-a0^2*coef_P1_F*a1^2*nu*coef_F1_P+a1^2*a0^2*nu-
a1^2*a0^2*nu*coef_F1_F+a1^2*a0^4*pi*nu*coef_P1_F-4*a0^4*a1^2*log(a0)*coef_P1_F*pi-
2*a0^2*a1^2*log(a1)*nu*coef_F1_F+2*a0^2*a1^2*log(a0)*coef_P1_P*nu+a1^4*coef_P1_P*nu*coef_
F1_F+a1^4*coef_P1_F*nu*coef_F1_P)/E/(a1^2-a0^2)^2);

Uz2_PF = (-(coef_F1_P-pi*a0^2+nu*pi*a0^2-nu*pi*coef_P1_P*a1^2-
coef_F1_F*coef_F1_P+coef_F1_F*pi*a0^2-
coef_F1_F*nu*pi*a0^2+coef_F1_P*nu*pi*coef_P1_F*a1^2+coef_F1_F*nu*pi*coef_P1_P*a1^2-
pi^2*a0^2*nu*coef_P1_F*a1^2)*L/pi/E/(a1^2-a0^2));

U = [Ur1_PP+Ut1_PP+Uz1_PP+Ur2_PP+Ut2_PP+Uz2_PP;
     Ur1_PF+Ut1_PF+Uz1_PF+Ur2_PF+Ut2_PF+Uz2_PF;
     Ur1_FF+Ut1_FF+Uz1_FF+Ur2_FF+Ut2_FF+Uz2_FF];
```

# Vita

# Amir Lotfi Gaskarimahalle

## Education

**Doctor of Philosophy,** Mechanical Engineering- *Pennsylvania State University*, 2009.

**Ph.D. Minor in Computational Science** (High Performance Computing), *PSU*, 2009.

**Master of Science,** Mechanical Engineering- *Sharif University of Technology*, 2004.

**Bachelor of Science,** Mechanical Engineering, *Sharif University of Technology*, 2002.

## Work Experience

**Mechatronics Research Lab (MRL), PSU,** *Research Assistant* **Jan 05 – Aug 09**

Electrochemical Engines: Li-ion and Li-$FePo_4$ Batteries (Supervisors C.Y. Wang, C. Rahn)
Vibration control of Fluidic Flexible Matrix Composites (Supervisors: K.W. Wang, C. Bakis, C. Rahn)
Vibration control of continuous systems (e.g. cables, beams, webs): Input shaping controllers (Sup: C. Rahn)

**United Technologies - Otis Elevator Company** **Summer 08**

*Internship*: Dynamics modeling of elevator safety system (Supervisor: R. Roberts)

**Center of Excellence in Design, Robotics and Automation (CEDRA),** Sharif U. of T. **Sep 01 - Jul 04**

*Research Assistant*: Design, modeling and control of mobile robots and under-water remotely operated vehicles

**Research Center of Advanced Industrial Systems** **2002-03**

*Modeling and Automation Engineer*: Simulation of a computer aided manufacturing system.

**Mega Motors Co.**, Iran, **Sep 99 - May 02**

*Internship*: motor and gearbox assembly and machining lines, Quality control, Safety measures

## Awards and Honors

- **Silver Medal** and certificate, International competition of RoboCup, Rescue Robot Division, Padova, Italy, 2003.
- **Entrepreneurship Award** for design and fabrication of a novel rescue mobile robot, 2003.
- **Ranked 10th** in the 7th Olympiad of Mechanical Eng, Iran, 2002 and **Ranked 8th** in Iranian university entrance exam, 1998.
- **Member** of American Society of Mechanical Engineering

## Journal Publication

1. **A. Lotfi-Gaskarimahalle**, L. H. Scarborough III, C. D. Rahn, E. C. Smith, "Fluidic Composite Tuned Vibration Absorbers," Submitted to ASME Journal of Vibration and Acoustics, 2009.
2. **A. Lotfi-Gaskarimahalle**, L. H. Scarborough III, C. D. Rahn, E. C. Smith, "Passive and Switched Stiffness Vibration Controllers Using Fluidic Flexible Matrix Composites," Submitted to ASME Journal of Vibration and Acoustics, 2009.
3. Y. Shan, M. Philen, **A. Lotfi**, Suyi Li, C. E. Bakis, C. D. Rahn, K.W. Wang, "Variable Stiffness Structures Utilizing Fluidic Flexible Matrix Composites," Journal of Intelligent Material Systems and Structures, In press, 2008.
4. D. Trivedi, **A. Lotfi**, C.D. Rahn, "Geometrically Exact Dynamic Models for Soft Robotic Manipulators," IEEE Transactions on Robotics, Vol. 24, No. 4, 2008.
5. **A. Lotfi-Gaskarimahalle**, C.D. Rahn, "Two Dimensional Input Shaping In One Dimensional Continua," ASME Journal of Vibration and Acoustics, 2006.
6. A. Meghdari, S.H. Mahboobi, **A.L. Gaskarimahalle**, "Dynamics Modeling of CEDRA Rescue Robot on Uneven Terrain," Scientia Iranica, Vol. 13, No. 3, pp.272-283, 2006.
7. A. Meghdari, R. Karimi, H. N. Pishkenari, **A. L. Gaskarimahalle**, S. H. Mahboobi, "An Effective Approach for Dynamic Analysis of Rovers", Robotica, Vol. 23, pp. 771-780, 2005.
8. A. Meghdari, H. N. Pishkenari, **A. L. Gaskarimahalle**, S. H. Mahboobi, R. Karimi, " A Novel Approach for Optimal Design of a Rover Mechanism ", Journal of Intelligent and Robotic Systems - Theory and Applications, Vol. 44, No. 4, pp 291-312, 2005.